

EVALUATION OF STRUCTURAL ANALYSIS METHODS USED
FOR THE DESIGN OF TBM SEGMENTAL LININGS

A THESIS SUBMITTED TO
THE GRADUATE SCHOOL OF NATURAL AND APPLIED SCIENCES
OF
MIDDLE EAST TECHNICAL UNIVERSITY

BY

AHMET GÜRAY ÇİMENTEPE

IN PARTIAL FULFILMENT OF THE REQUIREMENTS
FOR
THE DEGREE OF MASTER OF SCIENCE
IN
CIVIL ENGINEERING

DECEMBER 2010

Approval of the thesis:

**EVALUATION OF STRUCTURAL ANALYSIS METHODS USED
FOR THE DESIGN OF TBM SEGMENTAL LININGS**

submitted by **AHMET GÜRAY ÇİMENTEPE** in partial fulfillment of the requirements for the degree of **Master of Science in Civil Engineering Department, Middle East Technical University** by,

Prof. Dr. Canan Özgen
Dean, Graduate School of **Natural and Applied Sciences** _____

Prof. Dr. Güney Özcebe
Head of Department, **Civil Engineering** _____

Assist. Prof. Dr. Alp Caner
Supervisor, **Civil Engineering Dept., METU** _____

Examining Committee Members:

Prof. Dr. Çetin Yılmaz
Civil Engineering Dept., METU _____

Assist. Prof. Dr. Alp Caner
Civil Engineering Dept., METU _____

Prof. Dr. Mehmet Utku
Civil Engineering Dept., METU _____

Assoc. Prof. Dr. Erdem Canbay
Civil Engineering Dept., METU _____

Harun Tulu Tunçay, M.Sc.
Project Coordinator, YÜKSEL PROJE _____

Date: _____

I hereby declare that all information in this document has been obtained and presented in accordance with academic rules and ethical conduct. I also declare that, as required by these rules and conduct, I have fully cited and referenced all material and results that are not original to this work.

Name, Last Name : Ahmet Gray imentepe

Signature :

ABSTRACT

EVALUATION OF STRUCTURAL ANALYSIS METHODS USED FOR THE DESIGN OF TBM SEGMENTAL LININGS

Çimentepe, Ahmet Güray
M.Sc., Department of Civil Engineering
Supervisor : Assist. Prof. Dr. Alp Caner

December 2010, 157 pages

Contrary to the linings of conventionally driven tunnels, the linings of tunnels bored by tunnel boring machines (TBMs) consist of precast concrete segments which are articulated or coupled at the longitudinal and circumferential joints. There are several analytical and numerical structural analysis methods proposed for the design of TBM segmental linings. In this thesis study, different calculation methods including elastic equation method and two dimensional (2D) and three dimensional (3D) beam – spring methods are compared and discussed. This study shows that in addition to the characteristics of concrete segments, the mechanical and geometrical properties of longitudinal and circumferential joints have significant effects on the structural behavior of segmental lining.

Keywords: TBM, Segmental Lining, Structural Analysis, Elastic Equation Method, Beam – Spring Method

ÖZ

TBM İÇ KAPLAMA SEGMANLARININ TASARIMINDA KULLANILAN YAPISAL ANALİZ METOTLARININ DEĞERLENDİRİLMESİ

Çimentepe, Ahmet Güray
Yüksek Lisans, İnşaat Mühendisliği Bölümü
Tez Yöneticisi : Yrd. Doç. Dr. Alp Caner

Aralık 2010, 157 sayfa

Klasik metotlarla açılan tünellerin iç kaplamalarının aksine, tünel açma makinalarıyla (TBM) inşa edilen tünellerin iç kaplamaları boyuna ve dairesel yöndeki düğüm noktalarında kenetlenmiş ya da bağlanmış prekast betonarme segmanlardan oluşmaktadır. TBM iç kaplama segmanlarının tasarımı için önerilen birçok analitik ve nümerik yapısal analiz metodu bulunmaktadır. Bu tez çalışmasında, elastik denklem metodu ile iki boyutlu ve üç boyutlu çubuk – yay metotlarını içeren farklı hesaplama yöntemleri incelenmiştir. Bu çalışma, betonarme segmanların niteliklerine ilaveten, boyuna ve dairesel yöndeki düğüm noktalarının mekanik ve geometrik özelliklerinin de segmanların yapısal davranışında önemli etkileri olduğunu göstermiştir.

Anahtar Kelimeler: TBM, İç Kaplama Segmanı, Yapısal Analiz, Elastik Denklem Metodu, Çubuk – Yay Modeli

to my beloved wife, Buğçe

ACKNOWLEDGEMENTS

I would like to express my deepest gratitude to my supervisor Dr. Alp Caner for his endless supervision, trust, guidance and encouragement during and beyond this work. Without his vision and support, I could never complete this work.

I also would like to acknowledge the valuable comments and contributions of my Supervising Committee Members.

Deepest thanks are dedicated to mom, dad and my brother. They were always near me with their endless support.

And finally, words are not enough to express the role played by my wife, Buğçe Doğan Çimentepe, to whom I owe most of beauty in my life. I proudly dedicate this work to her so as to express my appreciation for her role.

TABLE OF CONTENTS

| | |
|--|------|
| ABSTRACT..... | iv |
| ÖZ..... | v |
| ACKNOWLEDGEMENTS..... | vii |
| TABLE OF CONTENTS..... | viii |
| LIST OF TABLES..... | xi |
| LIST OF FIGURES..... | xiii |
| LIST OF ABBREVIATIONS..... | xvii |
| CHAPTERS | |
| 1. INTRODUCTION..... | 1 |
| 1.1. Foreword..... | 1 |
| 1.2. Scope and Objective of the Study..... | 2 |
| 1.3. Thesis Overview..... | 3 |
| 2. OVERVIEW OF TUNNELING..... | 4 |
| 2.1. Brief History of Tunneling..... | 4 |
| 2.2. Classification of Tunnels..... | 6 |
| 2.2.1. Type of Function..... | 6 |
| 2.2.2. Type of Construction Technique..... | 8 |
| 2.3. Essentials of Mechanized Shield Tunneling | 11 |
| 2.3.1. Structure and Dimensions of Tunnel Shields..... | 12 |
| 2.3.2. Operations of Shield Machines..... | 14 |
| 2.3.3. Classification of Tunnel Boring Machines (TBMs)..... | 19 |
| 2.3.3.1. Rock Tunneling Machines..... | 21 |
| 2.3.3.2. Soft Ground Tunneling Machines..... | 24 |
| 2.3.4. Selection of TBM..... | 27 |
| 2.3.5. Conventional Tunneling versus Mechanized Shield Tunneling..... | 28 |

| | |
|--|----|
| 2.4. Segmental Tunnel Linings..... | 30 |
| 2.4.1. Geometry of Rings and Segments..... | 31 |
| 2.4.2. Types of Rings and Segments..... | 35 |
| 2.4.3. Segmental Lining Materials..... | 38 |
| 2.4.4. Contact Surfaces..... | 39 |
| 2.4.4.1. Longitudinal (Segment) Joints | 40 |
| 2.4.4.2. Circumferential (Ring) Joints..... | 42 |
| 2.4.5. Connectors..... | 45 |
| 2.4.6. Waterproofing System | 48 |
| 2.4.7. Ring Assembly..... | 49 |
| 3. LITERATURE REVIEW..... | 52 |
| 3.1. Analysis Types..... | 52 |
| 3.1.1. Elastic Equation Method | 53 |
| 3.1.2. Schultze and Duddeck Method..... | 56 |
| 3.1.3. Muir Wood Method..... | 57 |
| 3.1.4. Beam – Spring Method..... | 58 |
| 3.1.5. Finite Element Method..... | 61 |
| 3.2. Theoretical Approaches on Beam – Spring Method..... | 62 |
| 3.3. 2D and 3D Analysis of TBM Segmental Linings..... | 72 |
| 4. TBM SEGMENTAL LINING DESIGN..... | 75 |
| 4.1. Design Procedure..... | 76 |
| 4.1.1. Design for the Ultimate Limit States..... | 76 |
| 4.1.2. Design for the Serviceability Limit States..... | 77 |
| 4.1.3. Design Stages..... | 77 |
| 4.2. Loading Conditions | 79 |
| 4.2.1. Primary Loads..... | 81 |
| 4.2.2. Secondary Loads..... | 88 |
| 4.2.3. Special Loads..... | 90 |
| 4.3. Structural Calculation Procedure..... | 92 |
| 4.3.1. Critical Sections..... | 92 |

| | |
|--|-----|
| 4.3.2. Computation of Member Forces..... | 93 |
| 4.3.3. Safety of Section..... | 93 |
| 4.3.4. Limit State Design Method..... | 94 |
| 4.3.5. Allowable Stress Design Method..... | 94 |
| 4.3.6. Safety of Joints..... | 95 |
| 5. METHODS OF ANALYSES..... | 96 |
| 5.1. The Geometry of the Problem..... | 97 |
| 5.2. Geotechnical and Material Parameters..... | 100 |
| 5.3. Analytical Analysis with Elastic Equation Method..... | 101 |
| 5.4. Numerical Analyses..... | 102 |
| 5.4.1. 2D Structural Models..... | 106 |
| 5.4.2. 3D Structural Model..... | 110 |
| 5.5. Loading Conditions..... | 112 |
| 5.6. Flowchart of Calculation..... | 114 |
| 6. RESULTS AND DISCUSSION..... | 123 |
| 6.1. Evaluation of Analysis Methods..... | 123 |
| 6.2. The Effect of Soil Stiffness on Beam – Spring Analysis..... | 129 |
| 6.3. The Effect of Surcharge Load on Beam – Spring Analysis.... | 131 |
| 6.4. The Effect of Mesh Coarseness on Beam – Spring Analysis.. | 132 |
| 6.5. The Effect of Shear Spring Constant on Beam – Spring Analysis..... | 134 |
| 6.6. The Effect of Segment Layout on Beam – Spring Analysis... | 135 |
| 7. CONCLUSION..... | 137 |
| REFERENCES..... | 139 |
| APPENDICES | |
| APPENDIX A. Working Sheets for the Analysis with Elastic Equation Method..... | 145 |
| APPENDIX B. Shear Spring Constants for 2D and 3D BSMs..... | 150 |

LIST OF TABLES

TABLES

| | |
|--|-----|
| Table 2.1. Comparison of major criteria for conventional tunneling and TBM tunneling..... | 28 |
| Table 2.2. Ranges for the dimensions of segmental linings..... | 35 |
| Table 3.1. Equations of member forces for Elastic Equation Method..... | 55 |
| Table 4.1. Limit states for the design of segmental lining | 76 |
| Table 4.2. Classification of the loads for shield tunneling..... | 80 |
| Table 5.1. Geotechnical parameters of the soil layers..... | 100 |
| Table 5.2. General features of beam - spring models..... | 105 |
| Table 5.3. Summary of load conditions..... | 113 |
| Table 5.4. Combination of loads..... | 114 |
| Table 5.5. Soil stiffness for transition zones..... | 116 |
| Table 5.6 Summary of load conditions for Case 3..... | 119 |
| Table 5.7 Summary of analysis cases..... | 122 |
| Table 6.1. Analysis results obtained from elastic equation method and 2D beam – spring methods..... | 124 |
| Table 6.2. Analysis results obtained from elastic equation method and 2D & 3D beam – spring methods..... | 127 |
| Table 6.3. Analysis results obtained from 2D & 3D beam – spring methods for the section passing though a soil transiton zone... | 130 |
| Table 6.4. Analysis results obtained from 2D & 3D beam – spring methods for the tunnel section subjected to surcharge load..... | 131 |
| Table 6.5. Analysis results obtained from 2D & 3D beam – spring methods for different mesh coarseness..... | 133 |
| Table 6.6. Analysis results obtained from 3D beam – spring methods for three different shear spring constants..... | 134 |

| | |
|--|-----|
| Table 6.7. Analysis results obtained from 3D beam – spring methods for four different segmental configurations..... | 136 |
|--|-----|

LIST OF FIGURES

FIGURES

| | | |
|--------------|--|----|
| Figure 2.1. | System groups of a tunnel boring machine..... | 15 |
| Figure 2.2. | Boring cycle of a TBM: a) Phase of advance, b) Installation of segmental lining..... | 17 |
| Figure 2.3. | Shield tail with grouting of the ground-lining gap | 19 |
| Figure 2.4. | Classification of tunnel boring machines (TBMs)..... | 20 |
| Figure 2.5. | Rock tunneling machines: a) unshielded TBM, b) single shielded TBM, c) double shielded TBM..... | 23 |
| Figure 2.6. | Shield tunneling with a) mechanical support, b) compressed air, c) slurry support, d) earth pressure balance..... | 26 |
| Figure 2.7. | Ranges of diameters of different TBM types..... | 27 |
| Figure 2.8. | Elements constituting a typical segmental ring..... | 32 |
| Figure 2.9. | Segmental lining for a railway tunnel: a) ring position 1; b) ring position 2; c) developed view..... | 33 |
| Figure 2.10. | The cross-section of a typical TBM tunnel..... | 34 |
| Figure 2.11. | Conicity of segmental rings: a) type of rings; b) relationship between conicity and minimum radius of curvature of the tunnel..... | 36 |
| Figure 2.12. | Segment types..... | 37 |
| Figure 2.13. | Typical reinforcement cage for segmental linings..... | 39 |
| Figure 2.14. | Longitudinal joints with a) two flat surfaces, b) two convex surfaces, c) convex / concave surfaces..... | 41 |
| Figure 2.15. | Circumferential joint with flat surfaces..... | 43 |
| Figure 2.16. | Circumferential joint with tongue-and-groove system..... | 44 |
| Figure 2.17. | Circumferential joint with cam-and-pocket system..... | 45 |
| Figure 2.18. | Section of a typical housing for a single bolt..... | 46 |

| | | |
|--------------|---|-----|
| Figure 2.19. | Section of a typical room for a single dowel..... | 47 |
| Figure 2.20. | Installation of segments and transmission of thrust forces into the segmental linings..... | 50 |
| Figure 3.1. | Load condition of Elastic Equation Method..... | 54 |
| Figure 3.2. | Bedded ring model without crown bedding..... | 57 |
| Figure 3.3. | Plain strain continuum model..... | 58 |
| Figure 3.4. | Model of Beam – Spring Method..... | 59 |
| Figure 3.5. | 3D Beam – Spring Model..... | 60 |
| Figure 3.6. | Finite element method for tunnel engineering..... | 62 |
| Figure 3.7. | Structural design models for TBM segmental linings..... | 63 |
| Figure 3.8. | a) Rotational spring model, b) Stress distribution at the segment joint..... | 68 |
| Figure 3.9. | Stress and deformation in mortised portions..... | 69 |
| Figure 3.10. | Forces acting on the ring joints and joint displacements..... | 71 |
| Figure 4.1. | Flowchart of shield tunnel lining design..... | 79 |
| Figure 4.2. | Notations of bending moment, axial force and shear force.. | 81 |
| Figure 4.3. | Section of tunnel and surrounding ground..... | 82 |
| Figure 4.4. | Calculation of loosening ground load..... | 84 |
| Figure 4.5. | Ground pressures acting on lining..... | 86 |
| Figure 4.6. | Hydrostatic pressure..... | 86 |
| Figure 4.7. | Interaction diagram..... | 94 |
| Figure 5.1. | Tunnel cross-section..... | 98 |
| Figure 5.2. | Geometry of the problem..... | 99 |
| Figure 5.3. | Typical 2D beam – spring model composed of 50 members..... | 102 |
| Figure 5.4. | Typical 3D beam – spring model composed of 50 members..... | 103 |
| Figure 5.5. | Ground spring constants..... | 104 |
| Figure 5.6. | Configuration of segment joints in 2D models..... | 107 |

| | | |
|--------------|--|-----|
| Figure 5.7. | The relationship between the M/N ratio and joint rotational stiffness k_{θ} (for reference purpose only)..... | 108 |
| Figure 5.8. | The iteration process for the computation of joint rotational stiffness..... | 110 |
| Figure 5.9. | Configuration of segment joints in 3D models..... | 111 |
| Figure 5.10. | Shear spring constant..... | 112 |
| Figure 5.11. | Soil profile of the tunnel route..... | 115 |
| Figure 5.12. | Theoretical and computational models of the rotational spring constant..... | 117 |
| Figure 5.13 | Longitudinal profile of the tunnel under surcharge..... | 118 |
| Figure 5.14. | Segment configurations for 4 different layouts..... | 121 |
| Figure A.1. | Input sheet for the analysis with Elastic Equation Method... | 146 |
| Figure A.2. | Load conditions sheet 1 for the analysis with Elastic Equation Method..... | 147 |
| Figure A.3. | Load conditions sheet 2 for the analysis with Elastic Equation Method..... | 148 |
| Figure A.4. | Member forces sheet for the analysis with Elastic Equation Method..... | 149 |
| Figure B.1. | Rotational Stiffness vs. M/N diagram for 2D BSM in Case 1..... | 150 |
| Figure B.2. | Rotational Stiffness vs. M/N diagram for 3D BSM in Case 1..... | 150 |
| Figure B.3. | Rotational Stiffness vs. M/N diagram for 2D BSM consisting of 50 beam elements in Case 4..... | 151 |
| Figure B.4. | Rotational Stiffness vs. M/N diagram for 2D BSM consisting of 150 beam elements in Case 4..... | 151 |
| Figure B.5. | Rotational Stiffness vs. M/N diagram for 2D BSM consisting of 250 beam elements in Case 4..... | 152 |
| Figure B.6. | Rotational Stiffness vs. M/N diagram for 3D BSM consisting of 50 beam elements in Case 4..... | 152 |

| | |
|---|-----|
| Figure B.7. Rotational Stiffness vs. M/N diagram for 3D BSM consisting of 150 beam elements in Case 4..... | 153 |
| Figure B.8. Rotational Stiffness vs. M/N diagram for 3D BSM consisting of 250 beam elements in Case 4..... | 153 |
| Figure B.9. Rotational Stiffness vs. M/N diagram for 3D BSM (Ks=15000 kN/m) in Case 5..... | 154 |
| Figure B.10. Rotational Stiffness vs. M/N diagram for 3D BSM (Ks=20000 kN/m) in Case 5..... | 154 |
| Figure B.11. Rotational Stiffness vs. M/N diagram for 3D BSM (Ks=25000 kN/m) in Case 5..... | 155 |
| Figure B.12. Rotational Stiffness vs. M/N diagram for 3D BSM (Layout 1) in Case 6..... | 155 |
| Figure B.13. Rotational Stiffness vs. M/N diagram for 3D BSM (Layout 2) in Case 6..... | 156 |
| Figure B.14. Rotational Stiffness vs. M/N diagram for 3D BSM (Layout 3) in Case 6..... | 156 |
| Figure B.15. Rotational Stiffness vs. M/N diagram for 3D BSM (Layout 4) in Case 6..... | 157 |

LIST OF ABBREVIATIONS

| | |
|-------|---|
| ACI | American Concrete Institute |
| AFTES | French Tunnelling and Underground Engineering Association |
| BSM | Beam – Spring Model |
| DAUB | German Committee for Underground Construction |
| DIN | Deutsche Industrie-Norm |
| FEM | Finite Element Method |
| ITA | International Tunneling Association |
| JIS | Japanese Industrial Standard |
| JSCE | Japan Society of Civil Engineers |
| NATM | New Austrian Tunneling Method |
| SIG | Italian Tunnelling Association |
| SLS | Serviceability Limit State |
| SNIP | Standard and Russian Construction Norms and Regulations |
| TBM | Tunnel Boring Machine |
| ULS | Ultimate Limit State |
| 2D | Two Dimensional |
| 3D | Three Dimensional |

CHAPTER 1

INTRODUCTION

1.1. Foreword

Rapid world-wide urbanization have recently accelerated subterranean and tunnel construction [1]. Tunnels provide transportation routes for rapid transit, railroad and vehicular traffic, conveying both fresh water and waste, and transferring water for hydroelectric power generation. Moreover, they are utilized as conduits, canals, passageways for pedestrians, and used for mining, industrial cooling, storage, and military works [2]. As the demands on passenger and goods transportation increase with social and industrial development, the necessity and importance of tunnels have been extensively discovered.

Tunnels are built in several different underground environments, including soil, rock, mixed soil and rock, with extended variations in the groundwater conditions, in-situ states of stress, and geological structures. Alternative construction techniques, including hand excavation, drill-and-blast methods, cut and cover, and various mechanical tunneling equipments, are used to construct tunnels [2]. Especially in urban regions, the mechanized tunneling has consistently increased due to the ascending number of tunnels constructed for subways, railway underpasses, and urban highways. However, tunneling in urban areas generally brings to minds high-level risks, which may result in potential damage to structures and people [3]. In such a complex and risky type of structure; not only the construction phase, but also the design stage is of vital importance.

Enhanced demands and potential risks have led to development in the art and technique of tunneling especially in design and analysis methods. Accordingly, extensive improvements in the scientific background of tunneling, mainly by the scientific advances made in tunnel mechanics, have been developed [1]. Several structural design models including various analytical closed form solutions and bedded beam-spring approaches have been improved. Closed form solutions, restricted to a number of simplifications, are arguably cheaper and quicker to use. These simplified two-dimensional models have been used mostly in Austria and Germany. On the other hand, bedded Beam - Spring Models (BSMs) which represent the lining as a string of interconnected pin-ended structural beams, and the ground as a series of radial springs are the most common structural analysis tools used in shield tunneling design. Two-dimensional (2D) and three-dimensional (3D) applications of BSMs have been used worldwide, especially in Germany, Belgium, France, Japan, and United States [4]. Detailed researches on these structural models which predict the behavior of tunnel during and after the excavation are necessary for the proper design of segmental tunnel linings.

1.2. Scope and Objective of the Study

In a tunnel design, the same cross-section is used even the loads or soil conditions change along the route. In this study, the most commonly applied structural analysis methods used in the design of shield tunneling are investigated. Shield tunneling is a typical structural system selected for railroad tunnels. The scope of this thesis covers the evaluation of different structural analysis methods used for the design of segmental tunnel linings. "Elastic Equation Method" proposed by Japanese Standard for Shield Tunneling has been selected as an analytical approach. Furthermore, several BSM approaches have been selected as numerical methods. Then, both analytical and numerical methods have been examined for different mesh coarseness, loading conditions, soil stiffness, ring joint stiffness, and

segment configurations for the analysis of shield tunneling especially for tunnels excavated and shielded by Tunnel Boring Machines (TBMs).

The aim of this study is to compare and evaluate commonly used structural analysis methods for the design of segmental tunnel linings under certain situations. Strength and weaknesses of the methods will also be identified.

1.3. Thesis Overview

This thesis study has seven chapters. Chapter 1 (Introduction) generally presents the main subject, the objective and scope of the study. In Chapter 2 (Overview of Tunneling), brief history of tunneling, types and geometry of tunnels, and general knowledge on mechanized shield tunneling and TBM segmental linings are introduced. Chapter 3 (Literature Review) describes the theoretical background of structural analysis methods used in the design of TBM segmental linings and gives a summary of previous studies. Chapter 4 (TBM Segmental Lining Design) briefly indicates the design procedure, loading conditions, and structural calculation procedure used in the design of segmental tunnel linings. In Chapter 5 (Methods of Analyses), studies having done throughout this project are detailed. In Chapter 6 (Results and Discussion), comparison and evaluation of analysis results are made. Chapter 7 (Conclusion) summarizes the thesis study and gives the recommendations for further studies.

CHAPTER 2

OVERVIEW OF TUNNELING

In this chapter, a compendious overview of tunneling history, tunnel types (especially mechanized tunneling), tunnel geometry, principles of mechanized shield tunneling, tunnel boring machines, and segmental tunnel linings is provided.

2.1. Brief History of Tunneling

The history of tunneling extends up to the prehistoric era. Throughout the ages, mankind used tunnels for many purposes such as defense, assault, production, storage, communication, and transportation. The areas of usage for first tunnels were communication, mining operations and military purposes.

The oldest tunnel was constructed for the aim of communication nearly 4000 years ago. It was built to underpass the bed of the River Euphrates and to link the royal palace to the Temple of Jove in ancient Babylon. This tunnel has a length of 1 km with cross-section dimensions of 3.6 m by 4.5 m. Its walls consist of brickwork laid into bituminous mortar and a vaulted arch covers above the section. These details and scope of the work, which require broad experience and skill, show that this tunnel was not the first tunnel constructed by the Babylonians. Salt mine in Hallstatt and flint mines in France and Portugal are the earliest examples of prehistoric tunnels used for mining operations [5].

Tunnels for water conveyance were mostly built by Romans. Advanced surveying techniques to drive tunnels from both portals towards the middle of tunnel were firstly utilized by Greeks about 500 B.C. This was a great development which reduced excavation time and labor need. Also, tunnels built by Romans can be distinguished with their long service life due to the Roman philosophy that a civil engineering work had to last forever [6].

With the utilization of gunpowder in tunneling during the Renaissance era, conventional methods such as shovels, picks, and water have been replaced by blasting. Ventilation systems have also been improved in order to clean the smoke immediately after blasting [6].

Marc Isambard Brunel, inventor of shield tunneling, tried his system in great Thames Tunnel. Brunel's first shield was rectangular and tunnel was lined with brickwork. After great difficulties involving five serious floods, the double track tunnel was completed in 1842. Then, James Henry Greathead improved first cylindrical shield and employed this shield in London in 1869 for the construction of Tower Tunnel underneath Thames River. He also used cast iron lining segments for the first time [1, 7].

Inventions by Brunel and Greathead became the model for further developments in shield and mechanized tunneling. In the last century, air-compressed, slurry, and earth-pressure balance shields have been developed and these advances enabled the daily peak advance of 25 cm obtained by Brunel to be increased to 25-30 m [1].

A very quick overview in the history of tunneling has been discussed by emphasizing the milestones in tunnel construction. Advances in tunneling are still proceeding progressively by introducing and perfecting modern free face and shield methods that permit the large scale use of high capacity mechanical equipment [1].

2.2. Classification of Tunnels

Tunnels can be classified according to their functions, the method of construction, the geological situation, and the hosting medium, etc. Especially, functionality and the excavation method are the common criteria for the categorization of tunnels. General information about the certain types of tunnels in terms of their functionality and construction technique is given in the proceeding sections.

2.2.1. Type of Function

Direct transportation of passengers and goods through the certain obstacles is the main purpose of tunnels. Obstacles to be underpassed can be a mountain, river, industrial, or dense urban areas, etc. The purpose of overcoming these obstacles may be to carry road, railway, or pedestrian, to convey water, gas, sewage, or to provide indoor transportation for industrial plants [1].

The classification according to these purposes can be summarized as follows:

a) Highway Tunnels: Highway tunnels are only a part of larger highway systems. Providing a crossing under an obstacle, which is the main function of these tunnels, has a great importance in linking up remote areas as under an estuary or through a mountain range. Highway tunnels are designed in accordance with their traffic capacity, lane widths and clearances, gradients and traffic composition. Moreover, their special construction characteristics include geometrical configuration, road construction, lighting, ventilation, traffic control, fire precautions, and general facilities for cleaning and maintenance [8].

Depending on the shape, i.e. rectangular, circular or horseshoe; cut-and-cover, blasting, New Austrian Tunneling Method (NATM), or mechanized

shield tunneling with TBMs can be used as an excavation method for highway tunnels [8]. Also, highway tunnels more than 3 km long require vertical shafts for ventilation, otherwise just horizontal ventilation is permissible.

b) Railway Tunnels: Tunnels, essential features of railway systems, are mostly used to provide a track with a limited gradient. An acceptable gradient governs the longitudinal profile of all railway tunnels. Generally, a gradient less than 1% is preferred but steeper gradients may have to be adopted in many cases. Another principal geometrical factor is curvature, which is governed by speed of trains [5].

Mountain ranges, hills, and subaqueous crossings are the typical situations for main line railways. Every kind of ground such as shattered rock, squeezing rock, silt, clay, etc. is liable to be encountered. In modern railway tunnels, NATM with sprayed concrete, steel arch ribs, and in situ concrete applications is the most usual excavation method. Apart from NATM, shield tunneling with segmental concrete or even cast iron linings is also preferred depending on the project characteristics [5].

c) Metro Tunnels: Metro tunnels are special types of railway systems adapted to cities and their immediate environs. The most distinctive feature of a metro system is the rapid transportation of numerous people on an exclusive right of way without any interruption by other types of traffic. Differently from railway tunnels, metro tunnels are used for shorter and more frequent journeys, and they may have a steeper gradient due to the fact that no heavy good trains are used in metro lines [8].

Metro systems are preferred to meet the needs of cities where centers are closely built up that surface railways or elevated railways are quite impracticable. Cut-and-cover under existing streets and boring with TBM

under streets and buildings are widely used excavation methods of metro tunnels [8]. These types of tunnels require ventilation systems.

d) Pedestrian Tunnels: Since the pedestrians can descend and ascend steps or quite steep gradients, and turn sharp corners, pedestrian subways are the least demanding and the most primitive type of tunnels. Therefore, the absolute limitations on this type of underground structures are very few. On the other hand, pedestrian subways should be as shallow as possible, because long descends and ascends may discourage the users anyhow. In the construction of shallow subways, cut-and-cover method is preferred. However, boring is better to perform excavation for connecting passages in metro stations at deeper level [5].

e) Conveyance Tunnels: Conveyance tunnels are built to convey water or sewage in many fields for various purposes. Fresh water supplies for cities, canals, irrigation, discharge tunnels for hydroelectric power, and dam bypass tunnels can be certain examples for conveyance tunnels. Smoothness and watertightness are the basic characteristics required for this type of tunnels. Smoothness depends on the velocity of water and the length of the tunnel. Besides, watertightness is dependent on internal and external pressure [5].

Segmental linings meet the requirements for watertightness and smoothness better than other tunneling methods. Hence, shield tunneling is generally performed for the excavation of large-scale conveyance tunnels. If boring with TBM is not feasible, conventional methods are also applicable.

2.2.2. Type of Construction Technique

In this section, three common construction methods used in tunneling are mentioned briefly. These methods taken into consideration are cut-and-cover, New Austrian Tunneling Method (NATM), and Mechanized Shield Tunneling. Apart from these methods, there are some other techniques

including drilling and blasting, earth boring, pipe jacking, immersed tube, and floating tunnels used for special cases.

a) Cut-and-Cover: Cut-and-cover is an alternative tunnel construction technique where a trench of the required depth and width can be excavated from the surface. This method can simply be summarized that a trench is excavated, the tunnel structure is constructed, then the trench is backfilled, and finally the surface is restored. Due to the support of soft ground and maintenance of surface and underground facilities, most projects become much more complex.

Cut-and-cover is a practical and an economical technique for tunnel constructions in shallow depth and in loose ground. This method offers more feasible solutions than tunneling up to depths of 10 m in open trenches. However, incidental costs may change the situation completely. These costs including provision of alternative facilities for traffic using the surface, safeguards against subsidence, protection or diversion of services and drainage systems, social costs of disruption, and loss of amenity may usually be unavoidable in urban areas. Therefore, the choice between cut-and-cover and boring should be made by performing a detailed cost – benefit analysis [8].

Cut-and-cover tunnels are commonly implemented in subaqueous tunnels to form a transition between an open cut approach and the main tunnel, at the portals of mountain tunnels, in urban conditions where the route must be covered in, and the surface restored.

b) New Austrian Tunneling Method (NATM): NATM, introduced by Rabcewicz (1969), is an observational method and requires application of a thin layer of shotcrete with or without rockbolts, wire mesh fabric, and lattice girder; and monitoring and observing the convergence of the opening. The

shotcrete thickness is optimized with respect to the admissible deformations. Consecutive shotcrete applications are necessary until the convergence has stopped or it is within the acceptable range [6].

In NATM construction technique, tunnel is sequentially excavated and supported. The primary support is provided by the shotcrete in combination with or without steel mesh, lattice girders, and rockbolts. Cast in-situ concrete lining is installed as secondary lining which is designed separately [9].

Especially in soft ground or weak rock, partial face excavation is performed. By this way, several headings with small cross-sections are chosen to minimize ground loading on it. This enables to support headings succesively. When the top heading has advenced far enough, bench excavation begins, with ramps left in place for access to the top of the heading [10].

NATM method is commonly performed in large railway, highway, and water conveyance tunnels. Its primary advantage is the economy because of matching the amount of support installed to the requirements of the ground loading rather than having to install worst case support throughout the tunnel [10].

c) Shield Tunneling: Particularly, tunneling with a shield is well adapted for softer soils and weaker rocks which need continuous radial support. The shield is a rigid steel cylindrical tube providing facilities at its front for the excavation of ground material and at its rear for the erection of the prefabricated lining. It has to be designed to be able to take all ground and working loads with relatively small deformations. The front of shield is equipped with cutters that perform excavation. Jacks installed in the shield are used to push the shield away from the installed lining into the ground. The tunnel advance ranges from 0.8 m to 2.0 m depending on the length of segments. Then, segmental lining is placed and the gap between the lining

and ground is filled with grout. This cycle continues up to end of tunnel construction [1, 9].

Shield-driven tunnels may have single or double linings. When the functions of double layer in terms of resistance to external pressures, watertightness or aesthetic appearance can not be provided by single layer, double layers are performed. The earliest lining type for shield tunneling was made of bricks. However, cast-iron segments, structural steel segments, and reinforced concrete segmental linings have recently been in use. These modern lining segments have an ability to resist larger pressures and to provide better watertightness [1].

Tunnels having different sizes with diameters ranging from 0.10 m up to 19 m can be excavated by different types of mechanized shields and with different processes. Broader knowledge on working principle, excavation, support and installation procedures, components, and classification of shield tunneling will be provided in the proceeding chapter.

2.3. Essentials of Mechanized Shield Tunneling

According to the French Association of Tunnels and Underground Space (AFTES), “*the mechanized tunneling techniques*” (as opposed to the so-called “conventional” techniques) are all the tunneling techniques in which excavation is performed mechanically by means of teeth, picks, or discs. Within the mechanized tunneling techniques, all categories of tunneling machines range from the simplest one (backhoe digger) to the most complicated one (shield TBM) [11]. However, this thesis study covers only tunneling operations with TBMs that allow full-face excavation.

The tunnel shield is a moving metal casing, which is driven in advance of the permanent lining, to support the ground surrounding the tunnel-bore and to afford protection for construction of the permanent lining without any

temporary support. Actually, the shield is a rigid steel cylinder open at both ends, providing facilities at its front for the excavation of the ground material and at its rear for the erection of the prefabricated lining. Thus, the shield is always forced ahead by steps keeping pace with the progress of excavation and erection work to the extent that the excavated hole should be well supported until the permanent lining is constructed.

A full cycle of shield tunneling involves the following steps:

- excavation and temporary support of the front face at a suitable depth
- advancing the shield, taking support on the previously erected lining
- placing another course or ring of the permanent lining.

This cycle is repeated up to the completion of tunnel construction [1].

2.3.1. Structure and Dimensions of Tunnel Shields

The skin is the principle element of the shield. It is constructed of steel plates and bent to the shape of the tunnel section. Cylindrical skin is slightly larger than the outer diameter of tunnel for the proper placing of segmental linings.

The skin may be divided into three main parts differing in their inner rigidity and arrangement in accordance with their purpose.

1. *The front part of the skin*, where excavation is performed is heavily reinforced, generally with steel castings to form the cutting edge, its inner rigidity being increased by stiffening rings. Its main aim is to perform the smoothest possible advance and steerability of the shield skin by cutting the face, and to provide pressure distribution as uniform as possible induced ahead.

Its secondary duty is to give an adequate shelter to the workmen engaged in the excavation, through affording a certain support for the front face.

2. *The trunk (or intermediate) part* is formed for the housing of pushing machinery (hydraulic jacks, high-pressure pump installations, etc.).

3. *The tail part* of the shield is designed for the erection of segmental linings.

In addition to these parts, some important complementary elements are integrated in the interior of the shield mostly in combination with its stiffening elements, such as working platforms, or front-support jacks [1].

After the determination of structural elements, shape and dimensions of the main shield should be emphasized. Typically, a circular shape is selected for shields, because this shape shows the best resistance to outside pressures. Moreover, this is the most suitable shape that allows forming bolted joints between the consecutive rings easily and exactly. If shields of oval or rectangular shape are used, a greater pushing force will be required for the advance as compared to circular tunnels. In addition to advantages mentioned above, a bigger arching action will take place above circular shields leading to a decrease in rock pressure and in frictional resistance.

The clearance requirements of tunnel definitely determine the diameter of the shield. In this sense, all operations (excavation, mucking, transport, erection) must be performed and all mechanical equipment (jacks, pressure pumps, platforms and conduits, erectors, loading machines, etc.) must be installed within the limited inner space of the shield. A reasonable economical selection that meets the requirements mentioned above must be made.

The choice of a suitable shield length is a major problem in the design of shield machines. The length is mainly determined by the dimensions of the jacks and the lining segments. The operating conditions of the shield are mostly affected by the relative length, i.e. by the shield diameter compared with shield length (L/D). This ratio affects the steerability, mobility, and the

steadiness of its direction. The shorter the shield, the more difficult it is to keep it in the correct line and the easier it is to change of its direction on curves. On the other hand, the longer the relative length of the shield, the easier it is to keep it in its original direction, but the more difficult to bring it back from an accidental incorrect direction. The ratio of relative length ranges between 0.4 and 1.4. However, according to the present considerations, this ratio should not exceed 0.70 – 0.75 [1].

According to Richardson and Mayo [12], the approximate steel weight of a tunnel shield can be obtained by the following formula:

$$W = 15 \cdot (D - 10) \quad (2.1)$$

where, W : the weight of shield in tons,
 D : the external diameter in feet.

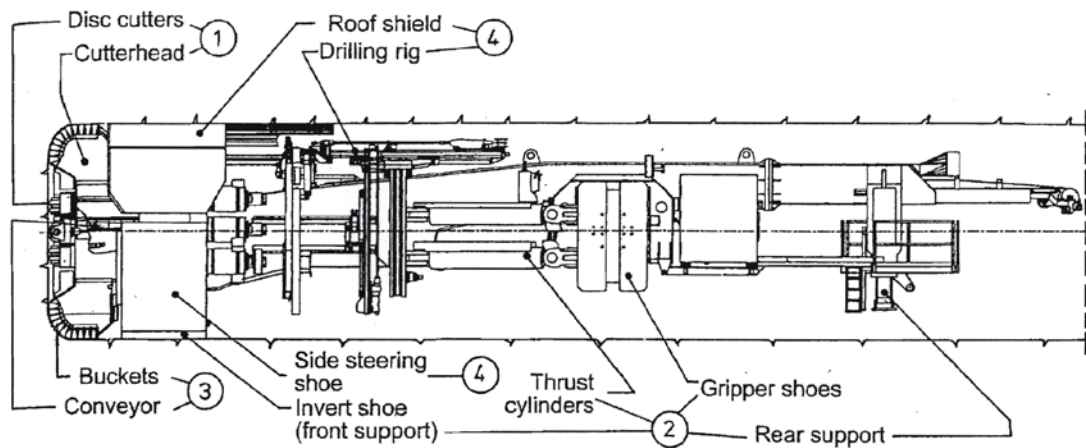
2.3.2. Operation of Shield Machines

The main components of a TBM are: 1) cutterhead, 2) cutterhead carrier with the cutterhead drive motors, 3) the machine frame, and 4) clamping and driving equipments. The necessary control and ancillary functions are connected to this basic construction on one or more trailers.

The operation systems of shield machines can be divided into four groups;

- Boring (Excavation) System
- Thrust and Clamping System
- Muck Removal System
- Support System

These system groups and their main parts are given in Figure 2.1.



System groups of a tunnel boring machine

- ① Boring system
- ② Thrust and clamping system
- ③ Muck removal system
- ④ Support system

Figure 2.1. System groups of a tunnel boring machine [13]

a) Boring (Excavation) System: The boring system which determines the performance of a TBM is the most critical part. It consists of various excavation tools which are mounted on a cutterhead. The range of application of these excavation machines depends on the surrounding ground [14].

For easily to moderately removable soils, cutting wheels equipped with drag picks or steel pins are used. A small cutting wheel in the center of the main cutting wheel is frequently arranged in cohesive soils. By this way, centric cutter rotates independently from the main cutting wheel and avoids adhesion by means of an increased circumferential speed.

In hardly excavatable soils and easily excavatable rocks, cutterheads equipped with cutter discs and drag picks are used. On the other hand, in

hardly excavatable rock, cutterheads solely equipped with discs are used [15].

The discs are arranged in an order so that they contact the entire cutting face in concentric tracks when the cutterhead turns. The separation of the cutting tracks and the discs are selected according to the ground type and the ease of cutting. This selection also designates the size of the broken pieces of ground.

The rotating cutterhead pushes the discs with high pressure against the face. Therefore, the discs make a slicing movement across the face. As the pressure at the cutting edge of the disc cutters exceeds the compressive strength of the rock, it locally grinds the rock. As a result, the cutting edge of the disc pushes rolling into the rock, until the advance force and the hardness of the rock come to equilibrium. Through this net penetration, the cutter disc creates a locally high stress, which causes long flat pieces of rock breaking off [13].

b) Thrust and Clamping System: The thrust and clamping system is an element which affects the performance of a TBM. It is responsible for the advance and the boring progress. The cutterhead with its drive unit is thrust forward with the required pressure by hydraulic cylinders which are illustrated in Figure 2.2a. The maximum stroke is governed by the length of the piston of the thrust cylinder. Today, TBMs achieve a stroke value of up to 2.0 m.

After a bore stroke has been bored, the boring process is interrupted so that the machine can be moved with the help of the clamping system. The shield TBM is stabilized during this process by the clamping at the back and the shield surfaces around the cutterhead.

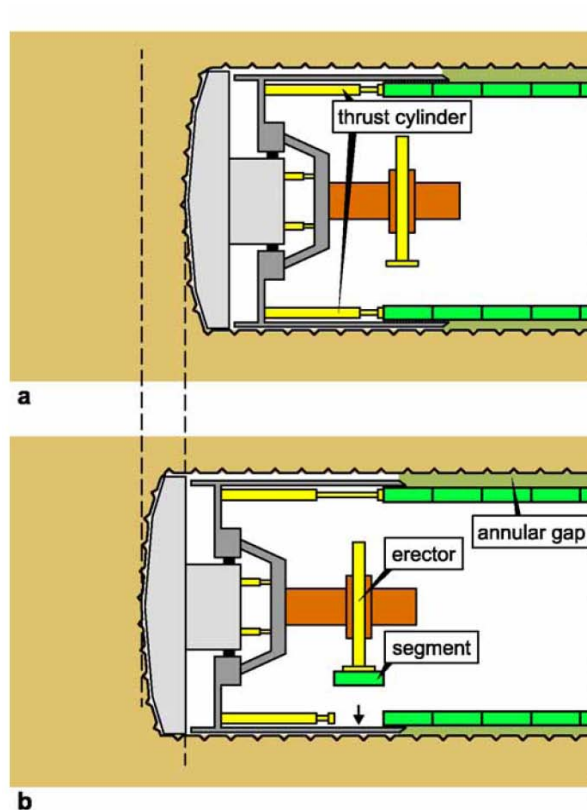


Figure 2.2. Boring cycle of a TBM: a) Phase of advance, b) Installation of segmental lining [14]

The thrust system limits the possible thrust and must resist the moments caused by the rotation of the cutterhead. The limits on the applied clamping forces are determined by the condition of segmental lining, because TBMs except for double shielded ones can not be braced radially against the tunnel walls but they are braced axially against the lining. For that reason, the segmental lining, not the rock strength, is decisive for shield TBMs [13].

c) Muck Removal System: One of the major problems of efficient tunnel driving is the effective muck haulage. It is performed in two steps in case of shield tunneling. The first step is the removal of soil from the shield body and the second is its conveyance to the ventilation or working shaft. Firstly, the

muck is collected at the face by cutter buckets and delivered to the conveyor down transfer chutes. Then, the muck is transported from the completed tunnel section to the access shafts or to the tunnel portals [1, 13].

A powerful system should be selected in order to ensure the carrying away of the muck throughout the entire tunnel. Moreover, the system equipments must make the smallest possible demand on space, since the removal system should not interfere with the supply of the TBM and necessary support measures. For this purpose, a rail system or a conveyor system is suitable according to local conditions. Furthermore, large dump trucks can alternatively be used for certain conditions [13].

d) Support System: In shield tunneling, the shield provides the temporary support of the rock around the shield. The shield casing begins directly behind the circumferential discs and also encloses the area where the support elements are installed. Reinforced concrete segments, which are mostly used for the support, are installed singly by the erector and form an immediate support. A shield TBM can be equipped with compressed air, hydraulic or earth pressure support and then it can be used under the water table [13].

Segmental lining elements are erected with a hydraulically-operated erector arm which can be mounted either directly on the axis of the shield tail or on a travelling working platform following closely behind the shield [1]. This stage is illustrated in Figure 2.2b.

Figure 2.2a shows that the shield tail, the rearmost part of the shield, overlaps the last segment and keeps the ground from deforming or falling into the excavated tunnel.

As shown in Figure 2.3, any possible loosening of the ground is prevented by grouting the annular gap. Also, a connection between ground and lining is provided. In order not to hinder the advance or interrupt it for a longer period, the rear carriage must contain all the equipment necessary for a rapid installation.

Moreover, a sealing is installed between shield tail and segmental ring in order to prevent the continuous grouting to flow into the shield. During tunnel advance, this sealing is sliding over the linings [4, 13].

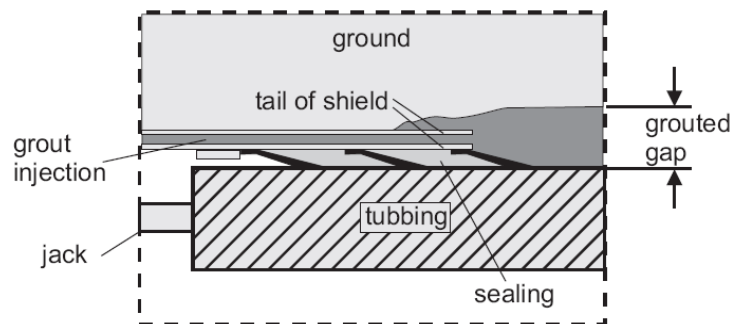


Figure 2.3. Shield tail with grouting of the ground-lining gap [4]

2.3.3. Classification of Tunneling Boring Machines

In the scope of this thesis, it is necessary to have a general overview of TBMs. In this section, the most widely-used types are emphasized.

The problem with the classification of tunneling machines is that there is no unitary definition and classification for tunneling machines accepted globally. However, the term Tunnel Boring Machine (TBM) is now universally adopted for all the machines that have a full-face cutting wheel for excavating a tunnel [3].

French Tunneling and Underground Engineering Association (AFTES), German Committee for Underground Construction (DAUB), Japan Society of Civil Engineers (JSCE), and Italian Tunneling Association (SIG) are all leading national tunneling associations and have their own classification system for tunneling machines based on different criteria. However, the classification to be considered in this study is based on what have been developed by International Tunneling Association (ITA) Working Group 14 “Mechanized Excavation”. TBMs are subdivided according to both the support typology that the machine is able to supply and the type of ground that it is able to operate in.

Like in the ITA and AFTES classifications, the term TBM also refers to all tunneling machines allowing full-face excavation in this study.

Figure 2.4 illustrates the classification scheme adopted in this study and the TBM types given in this classification are explained in terms of general characteristics, application field, and working principle in the following chapter.

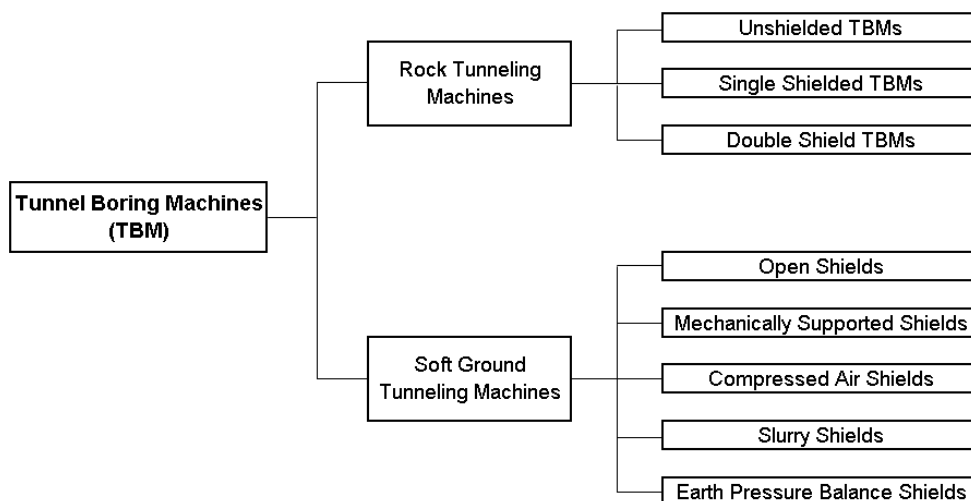


Figure 2.4. Classification of tunnel boring machines (TBMs)

2.3.3.1. Rock Tunneling Machines

Unshielded TBMs are typical rock machines used when rocks with good to very good conditions are excavated and they need to be associated with primary support system as for excavation using conventional method (rock bolts, shotcrete, steel arches, etc.). As shown in Figure 2.5a, a cutterhead is pushed against the excavation face by a series of thrust jacks, but the jacking forces are not transferred to the tunnel lining. “Grippers” which apply a force at the tunnel walls to clamp the machine to the rock mass are used. The cutters penetrate into the rock, creating intense tensile and shear stresses and then crushing it locally. The muck is collected by special buckets in the cutterhead and removed by primary mucking system. Although the machine is not equipped with a circular shield, a small safety crown-shield is provided at the back of the cutterhead.

The working cycle of unshielded TBMs includes: 1) gripping to stabilize the machine; 2) excavating for a length equivalent to the effective stroke of the thrust jacks; 3) regripping; 4) new excavation [16].

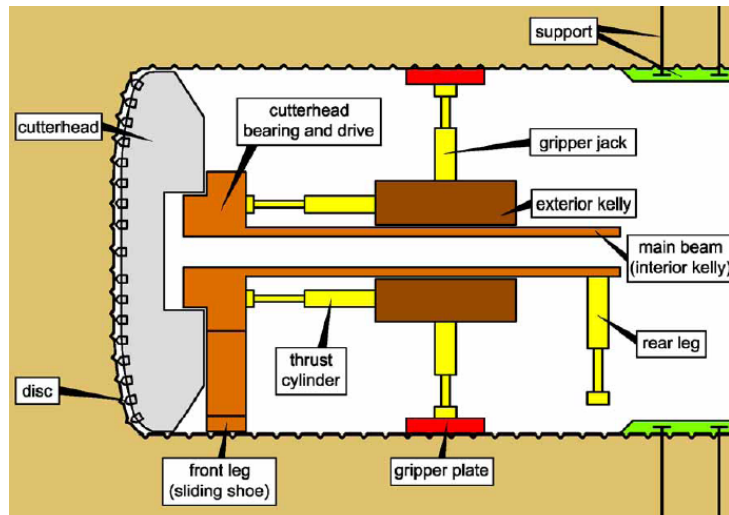
Single Shielded TBMs are typical ground or weak rock machines used when it is necessary to support the tunnel very soon with precast lining. The excavation procedure is the same with unshielded machines. As seen in Figure 2.5b, the support to the advancing thrust is provided by the precast segments constituting the tunnel lining. This machine is equipped with a full round protective shield immediately behind the cutterhead.

The working cycle of single shielded TBMs includes: 1) excavating for a length equivalent to the effective stroke of the thrust jacks; 2) assembling of segmental linings and retraction of the jacks; 3) new excavation [3, 16].

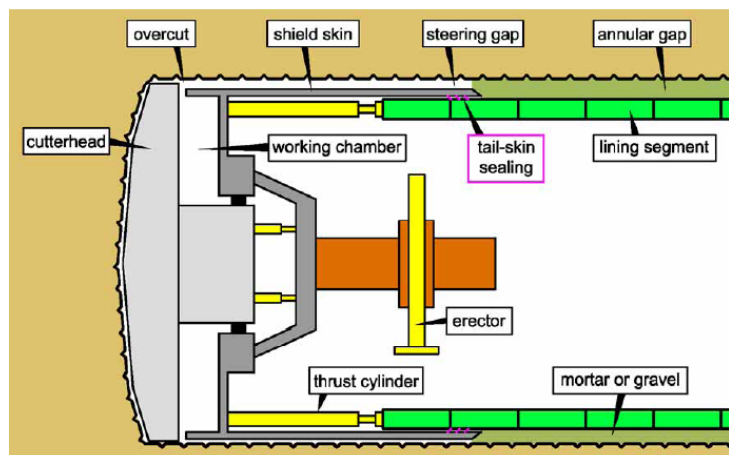
Double Shielded TBMs are very flexible and useful machines especially in mixed rock conditions. They are similar to single shielded TBMs, but offer the

possibility of a continuous work cycle owing to double thrust system. This machine is more versatile than the single shield, since it can move forward even without installing the tunnel lining or install segmental linings during excavation depending on the ground stability conditions [3, 16].

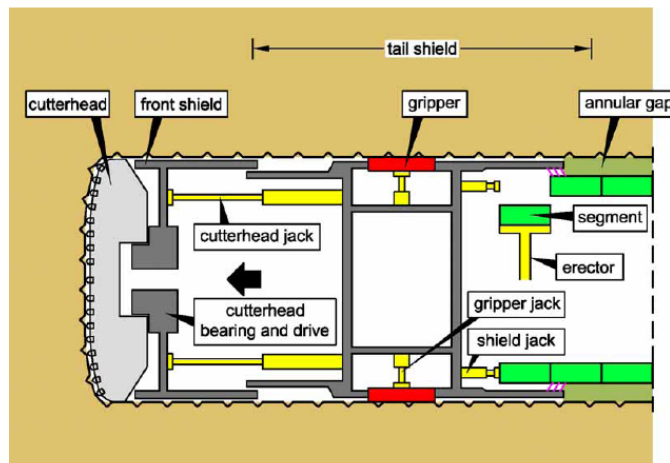
Figure 2.5c demonstrates the double thrust system which consists of a series of longitudinal jacks and a series of grippers positioned inside the front part of the shield. Longitudinal jacks use the tunnel walls to brace against the thrust jacks. Also, advance without installing segmental linings is performed by these longitudinal jacks.



a



b



c

Figure 2.5. Rock tunneling machines: a) Unshielded TBM, b) Single shielded TBM, c) Double shielded TBM [14]

2.3.3.2. Soft Ground Tunneling Machines

Open Shield is a tunneling machine in which face excavation is accomplished using a partial section cutterhead. There are hand shields and partly mechanized shields at the base of the excavating head. Excavation is performed by using a roadheader or using a bucket attached to shield, and using an automatic unloading and mucking system.

Open shields are used for rock masses whose characteristics vary from poor to very bad, cohesive or self-supporting ground in general [16].

Mechanically Supported Close Shield is a TBM in which the cutterhead plays the dual role of acting as the cutterhead and the supporting the face. As shown in Figure 2.6a, steel plates may be installed in between the free spaces of the cutting arms, to slide along the cutting face while rotating the boring machine. The debris is extracted through adjustable openings or buckets and conveyed to the primary mucking system.

This method is suitable for soft rocks, cohesive or partially cohesive ground, and self supporting ground above the ground water table [4, 16].

Compressed Air Closed Shield is used to support the face by compressed air at a suitable level to balance the hydrostatic pressure of the ground. A typical working scheme is given in Figure 2.6b. The debris is extracted from the pressurized excavation chamber using a ball-valve-type rotary hopper and then conveyed to the primary mucking system.

This method is applied to grounds with medium-low permeability under the ground water table to avoid water influx [4, 16].

Slurry Shields stabilize the tunnel face by applying pressurized bentonite slurry as illustrated in Figure 2.6c. The soil is mixed into the slurry during the

operation and at the end, the soil is removed from the slurry in a separation plant. The separation plant is generally located on the surface. A chamber with air pressure is connected to the slurry in order to control the slurry pressure.

This type of TBM is preferred in soft soils with limited self-supporting capacity. In other words, slurry shields are commonly suitable for excavation in ground composed of sand and gravels with silts under the ground water table [3, 16].

Earth Pressure Balance Shields are most commonly used TBMs in soft grounds. As illustrated in Figure 2.6d, face support is provided by the excavated earth which is kept under pressure inside the excavation chamber by the thrust jacks. Excavation debris is removed from the excavation chamber by a screw conveyor which enables the pressure control by variation of its rotation speed.

This method is mainly used in soft ground with the presence of ground water and with limited or no self-supporting capacity. In other words, typical application fields are silts or clays with sand. Furthermore, excavation in rock is possible with the use of disc cutters [3, 16].

Apart from these, there are special types of tunnel boring machines including hydroshields, mixshields, double tube shields, flexible section shields, etc. used in particular cases.

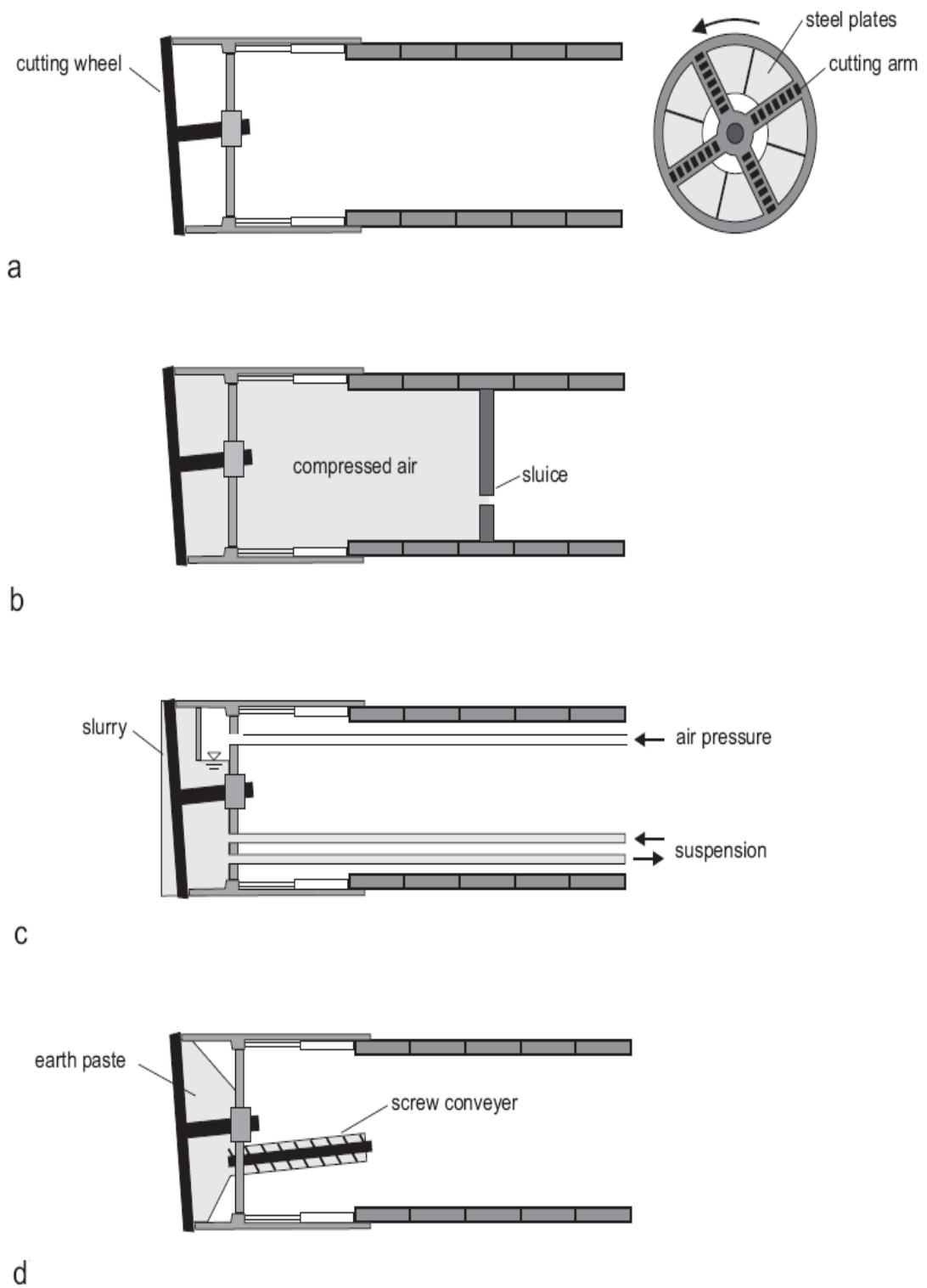


Figure 2.6. Shield tunneling with a) mechanical support, b) compressed air, c) slurry support, d) earth pressure balance [4]

2.3.4. Selection of TBM

One of the most important strategic decisions in mechanized shield tunneling is the selection of the most appropriate TBM type. The selected machine should be able to deal the best with the ground conditions expected [17].

The type and configuration of TBM are decided depending on the size of the tunnel and the geological conditions of the rock. Geological factors affecting the TBM selection are: grain size distribution, type of predominant mineral (quartz contents), soil strength, overburden, heterogeneity, and piezometric pressure [18].

Developing TBM technology allows machines having various diameters. Ranges of diameters for TBMs manufactured by Herrenknecht AG for utility tunnels (UT) and traffic tunnels (TT) are given in Figure 2.7.

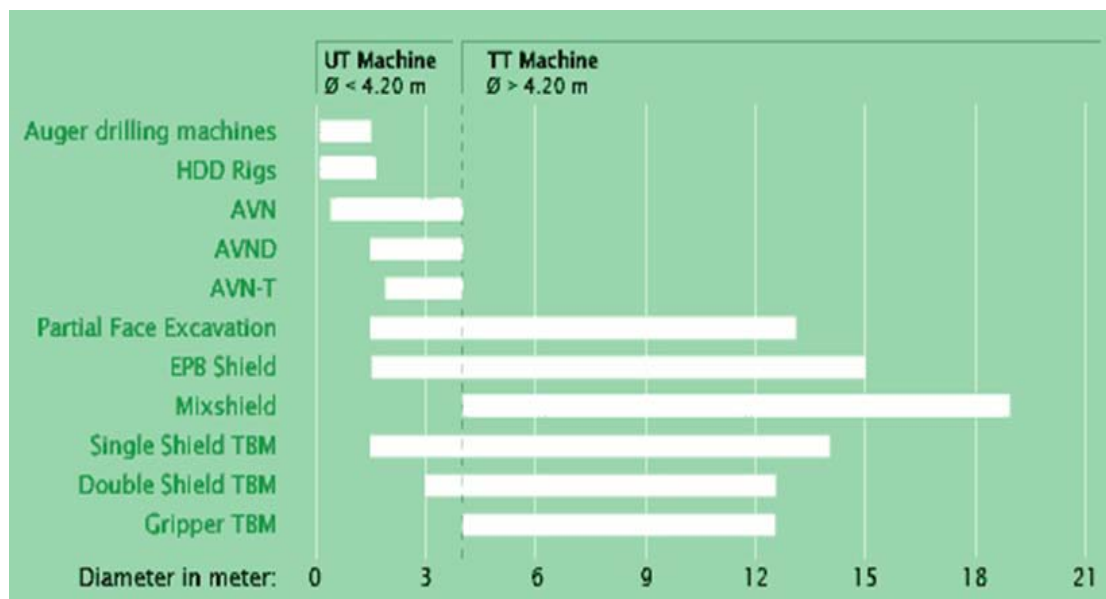


Figure 2.7. Ranges of diameters for different TBM types [19]

2.3.5. Conventional Tunneling versus TBM Tunneling

Tunnel projects which would have been excavated by the conventional method in the past will gradually be mined by the safety TBM technique [17]. Since TBM tunneling may not be feasible for certain cases, especially in short tunnels, a comprehensive comparison of methods should be made for each tunnel project. Main differences between conventional tunneling and TBM tunneling are listed in Table 2.1.

Table 2.1. Comparison of major criteria for conventional tunneling and TBM tunneling [20]

| Phase | Assessment Criteria | Conventional Tunneling | TBM Tunneling |
|--------------------|--|------------------------|-----------------|
| Construction Phase | 1. Supporting agent in face zone | variable | safer |
| | 2. Lining thickness | variable | constant |
| | 3. Safety of the tunneling crews | lower | higher |
| | 4. Working and health protection | lower | higher |
| | 5. Degree of mechanization | limited | high |
| | 6. Degree of standartization | conditional | high |
| | 7. Danger of break | higher | lower |
| | 8. Construction time for short tunnel | shorter | longer |
| | 9. Construction time for long tunnel | longer | shorter |
| | 10. Construction cost for short tunnel | lower | higher |
| | 11. Construction cost for long tunnel | higher | lower |
| Operational Phase | 12. Tunnel cross-section | variable | constant |
| | 13. Cross-section form | as desired | mostly circular |
| | 14. Degree of utilization of the drive-related tunnel cross-sections | mostly higher | mostly lower |

Comparison between conventional tunneling measures and mechanical drives in terms of constructional engineering and operational terms show that

TBM tunneling is more practical in most cases. In addition to these differences, primary advantages of TBM tunneling can be listed as follows [3, 21]:

- After leaving the TBM tail and grouting, the segmental ring can take the final loads. No hardening time is necessary.
- The constant quality of the concrete can be easily tested in the segment factory.
- Ring erection is done by the help of machines in short time (20 to 40 minutes per ring) with a high quality.
- When leaving the TBM tail, the segmental ring is pre-stressed by the grouting.
- Resulting from high normal forces, the longitudinal joints are overloaded and can take bending moments.
- Each ring is positioned with a high precision in the shield tail.
- The ground is stabilized instantly by the ring and grouting.
- Water flow into the tunnel is prevented by installing a lining which is immediately impermeable.

Furthermore, the advantages of an environmental nature and those concerning safety in the working environment have also great importance [3]:

- absence of direct contact between the workers in the tunnel and the excavated ground and groundwater.
- assembling the support in a single area of the tunnel where there is an intense use of mechanization in a clean, tidy, and protected work environment.

Finally, TBM tunneling may also have some disadvantages as listed below:

- mechanical failure of equipments may lead to very expensive processes to fix the problems.
- delay in operations may occur due to damage in the cutterhead resulting from unexpected soil conditions.
- unexpected forces by hydraulic pistons may result in cracks and damages in segments and also it is difficult to replace segments.
- compensation of deviation in tunnel route requires an effortful treatment.
- the construction of connection tunnels and turnout tunnels necessitates complicated operations.

2.4. Segmental Tunnel Linings

Lining is a structural element to ensure the security of tunnel space by resisting the earth and water pressures. As a main function, lining should satisfy the principles and requirements for safety, serviceability, and durability. In order to provide this function, different lining types are available.

Main types of linings frequently used in tunnels are:

- pipe linings (pipe jacking)
- in-situ lining
- segmental lining

The lining is generally a ring structure composed of prefabricated segments (segmental lining) but it is constructed in some cases with cast-in-place concrete or pipe linings if required [17].

Segmental linings can be composed of cast iron segments, structural steel segments, steel fiber reinforced concrete segments or reinforced concrete segments. Type of segments is selected according to conditions of project and availability of materials. Rings made from a number of segments are

installed within the protection of the shield tail. The lining segments are pre-cast and transported to the place where they will be positioned [7].

Reinforced concrete segmental lining, which is the focus of this report, is the most commonly used segmental lining type all over the world. Reinforced concrete lining with segments may have a single- or a double-layer lining construction. If a smooth internal surface is required due to esthetical or operational reasons, an interior lining of shotcrete or mixed-in-place concrete can be installed subsequently. In a single-layer lining construction, the segments form the final lining and must fulfill all requirements, resulting from construction conditions, hosting medium, groundwater conditions, and utilization [14, 22].

These construction and environmental requirements which should be satisfied by precast reinforced concrete segmental linings can be listed as follows [17]:

- the need for an immediate support (mainly for an excavation in an instable ground);
- the need to control carefully the ground movements induced by the tunnel excavation;
- to avoid the drainage of the groundwater and therefore to build a waterproof tunnel;
- provide the counterbalance for the TBM advance;
- to avoid the installation of a secondary lining.

2.4.1. Geometry of Rings and Segments

One ring of segments consists of four to nine segments and the wedge-shaped keystone (key segment), which is the last segment to be installed in a ring. The segments adjacent to the keystone are referred to as counter segments. Other segments are designated as regular or ordinary segments.

The main elements of a ring and their connections (longitudinal and circumferential joints) are illustrated in Figure 2.8.

More segments per ring need more sealing gaskets and need more time for erection. In addition, more segments per ring also allow a lower reinforcement as the ring has more hinges and less rigidity [21].

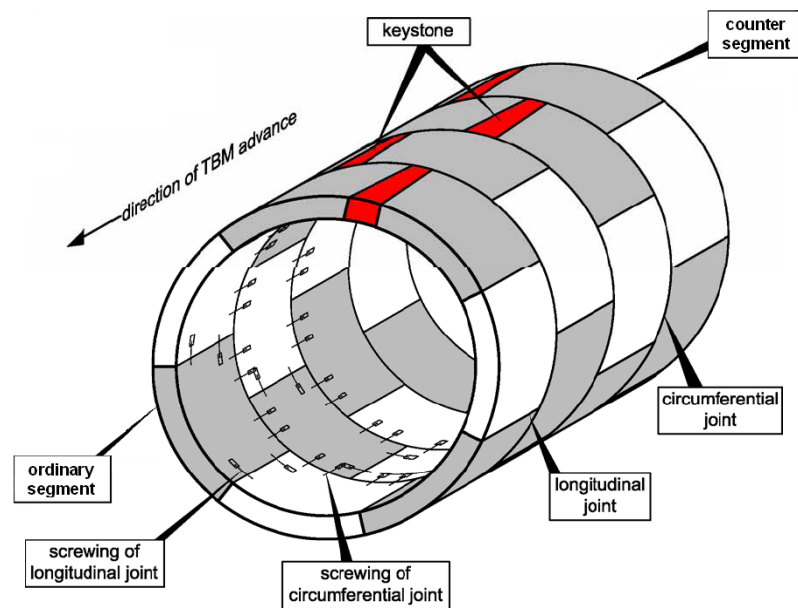


Figure 2.8. Elements constituting a typical segmental ring (not to scale) [14]

As shown in Figure 2.8, the longitudinal joints of adjacent rings are arranged in a staggered way in order to avoid problems regarding crossing joints. This staggered geometry increases the stiffness of the segmental lining, since an opening of the longitudinal joint due to a rotation of two adjacent segments is hindered by the overlapping segment of the neighboring ring [14].

As an example, the segmental lining designed for a railway tunnel is given in Figure 2.9. It consists of five regular segments (A1 to A5), two counter

segments (B and C), and the keystone (K). This figure shows schematically the arrangement of segments and allows the staggered geometry of segments to be understood more clearly.

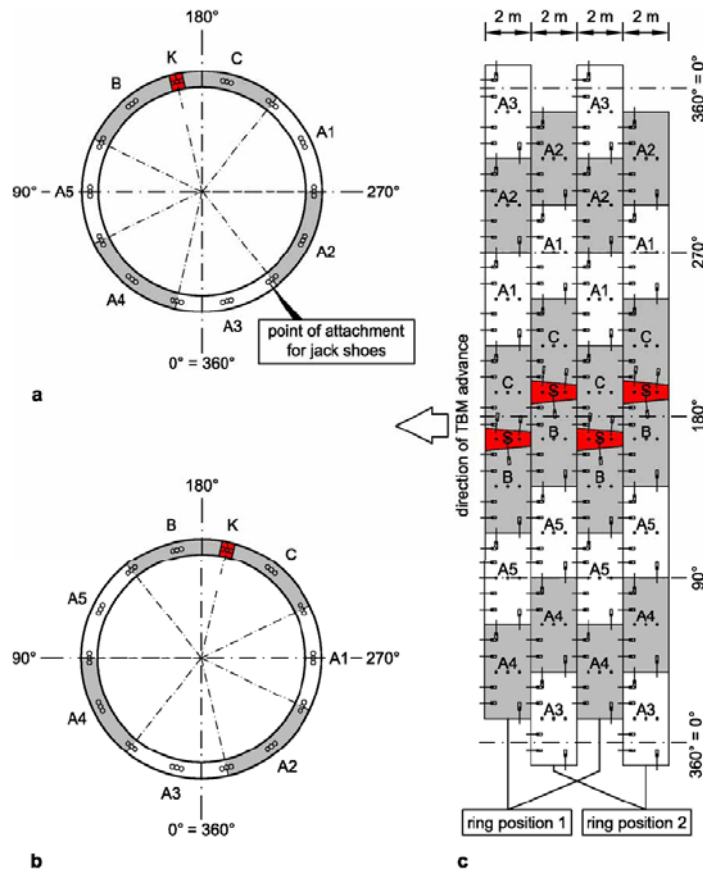


Figure 2.9. Segmental lining for a railway tunnel: a) ring position 1; b) ring position 2; c) developed view (not to scale) [14]

Depending on the necessity of project, rings having a diameter of up to 19 m can be built by means of developments in mechanized tunneling. Rings with larger diameters increase the number of segments, in order to keep the capacity of erector in reasonable limits. Ordinarily, the width of rings in longitudinal direction ranges between 1500 mm and 2000 mm. This also

depends on the weight of segments and the lifting capacity of the erector. The thickness of segments is selected so as to provide enough resistance to external loads. Generally, a thickness range of 20 cm to 40 cm is adequate for an ordinary segment. Accordingly, the cross-section of a typical TBM tunnel is shown in Figure 2.10.

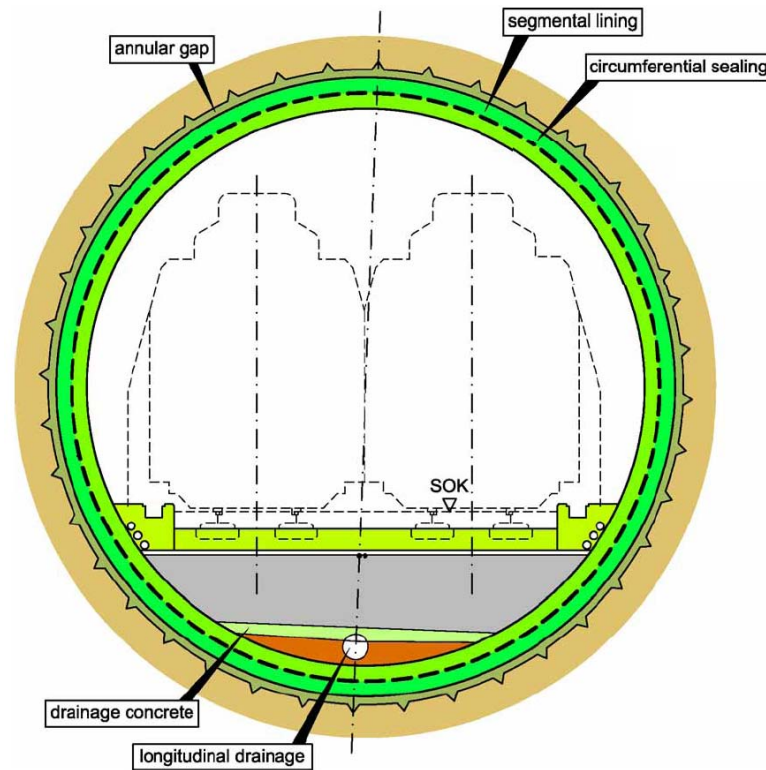


Figure 2.10. The cross-section of a typical TBM tunnel

In addition to given dimensions of an ordinary TBM tunnel, ranges for the dimensions of a segmental lining are given in Table 2.2. These values have been obtained as a result of wide experiences. The geometrical pre-dimensioning of a ring can be estimated with these ranges. Then, the pre-dimensioning stage should be confirmed in the subsequent, more detailed design stages.

Table 2.2. Ranges for the dimensions of segmental linings [21]

| Ring Size | Segment Thickness | Segment Width | Segment Numbers per Ring |
|---------------------------------|-------------------|---------------|--------------------------|
| Small Diameter Rings (2 to 5m) | 15 to 25cm | 75 to 150cm | 4 to 5 segments, 1 key |
| Medium Diameter Rings (5 to 8m) | 20 to 40cm | 125 to 200cm | 5 to 6 segments, 1 key |
| Large Diameter Rings (D>8m) | 30 to 75 cm | 150 to 225cm | 6 to 9 segments, 1 key |

2.4.2. Types of Rings and Segments

The segmental ring follows the track of the TBM in a spatial curve generally. In order to drive the TBM in curves and in gradient changes, left-hand rings and right-hand rings which are conically shaped on the corresponding side are mounted. The conical universal ring, which is conical on both sides, can also be applied. This ring can be adjusted in all directions by a corresponding rotation of segments [14]. However, the parallel rings may only be used for straight tunnels. In other words, the parallel rings are provided to obtain a “tube” with a straight axis [3]. Ring types are illustrated in Figure 2.11a.

The only difference between these types is the versatility during the assembling stage, but the function of the ring is not affected. Using of the conical universal ring systematically in both straight and curved parts of the tunnel is the current tendency in mechanized tunneling. This selection enables the horizontal and vertical trend of the alignment to be followed without the use of any other special elements and to correct any deviations made by the TBM during advancement [3].

In order to have a straight tunnel axis with conical universal ring, each ring should be turned by 180° in reference to the previous one. Using right ring and left ring always enables to have the key segment on the top. By this way, the ring is constructed from bottom to upwards [3].

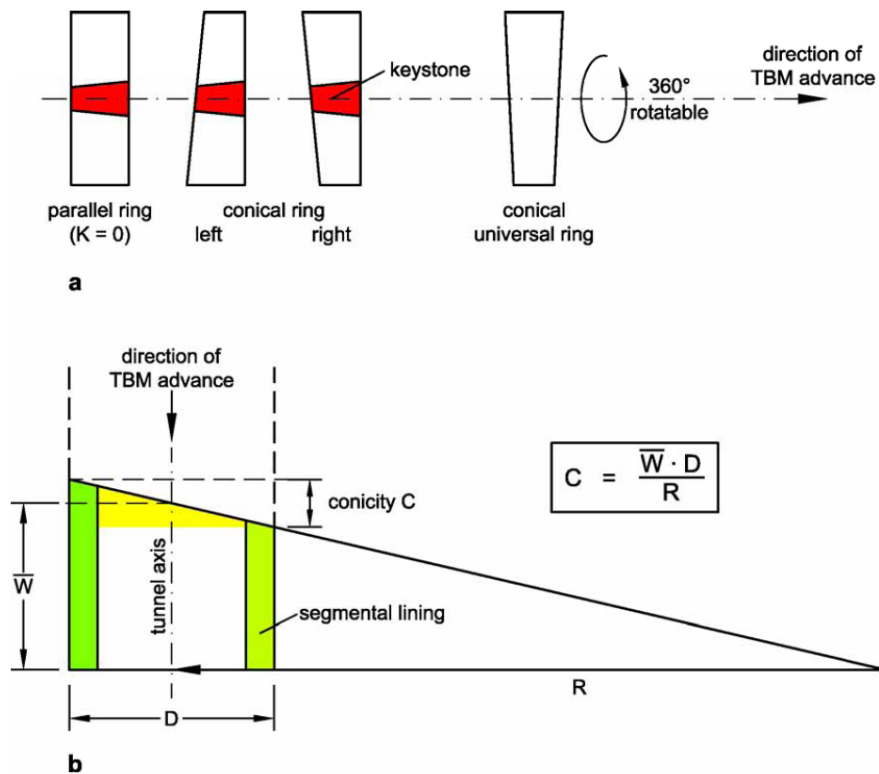


Figure 2.11. Conicity of segmental rings: a) type of rings; b) relationship between conicity and minimum radius of curvature of the tunnel [14]

The relation between the conicity (C) of the ring and the minimum radius of curvature (R) of the tunnel is determined by the formula given in the Figure 2.11b. Accordingly, C is directly proportional to the average ring width (W) and inversely proportional to the radius R. For parallel rings ($R \rightarrow \infty$), the conicity is $C = 0$.

It is necessary to understand the assembly process of the ring inside the tail of the shield in order to choose the type of segment. The assembly process involving the construction of the ring starts from the first segment, and finishes up with the key segment, whose presence is always foreseen and is placed at the opposite side of the ring that has the counter segment [3] (see Figure 2.9).

The key segment has a shape of trapezoid with the largest side facing the front of excavation. It is mostly smaller than all the other elements. For the installation of key segment, two counter segments with inclined sides to correspond with the shape of the key segment are necessary [3].

For the remaining part, segments may have any specific geometrical shapes that are demonstrated in Figure 2.12. Apart from the honeycomb shape, the others are all quadrilateral. All ring types can be built with segments having suitable shapes shown below.

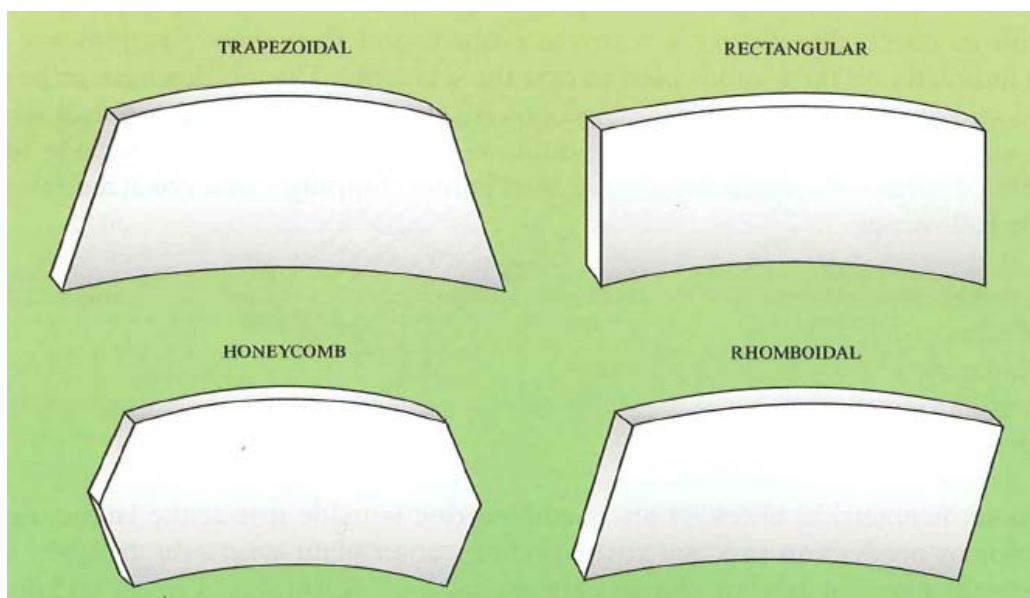


Figure 2.12. Segment types [17]

2.4.3. Segmental Lining Materials

The main constituent materials of a segmental lining are concrete and reinforcing steel. The Japanese Industrial Standard (JIS), Deutsche Industrie-Norm (DIN), American Concrete Institute (ACI) Standard and Russian Construction Norms and Regulations (SNIP) are the most widely used standards in the design of lining concrete.

For the concrete of segmental linings, strength grade of at least C 35 is demanded. Most segments are produced with quality C 40/50. Higher grades are also available but not necessary in general. Depending on the dimensions of the segments, and the support conditions, early strengths ranging from 15 to 25 MPa may become necessary. Concrete used in the production of segments should have several important properties, such as workability, watertightness, high impact resistance, high flexural tensile strength, and high resistance against aggressiveness of ground and groundwater [21]. In addition to this, concrete making materials, cement, aggregates, admixtures, and water should also comply with applicable standards.

The reinforcement of a lining segment consists of the load bearing reinforcement in circumferential and longitudinal direction, the tensile splitting reinforcement adjacent to the longitudinal and circumferential joints, the boundary reinforcement as well as the reinforcement for block outs and built-in units. Generally, shear reinforcement is not required in segmental linings, because the segments are loaded mainly by normal thrusts. However, it can be installed in the form of stirrups or additional, ladder-shaped or S-shaped rebars if needed.

The minimum yield strength of reinforcement to be used in segments should be 420 N/mm^2 . Also, the reinforcement should be carried out with bars of not more than 20 mm in diameter. If larger diameters are used, only small

imperfections of bending radii can lead to difficulties with fitting the reinforcement cages into the formwork. As a result, the installation of reinforcement becomes more complicated. Furthermore, the required concrete cover is ensured by means of reinforcement bar spacers which are generally attached to the reinforcement bars [14].

The various reinforcements of the segment are combined to a reinforcement cage, which can be placed into the formwork completely (see Figure 2.13). For this, the several rebars are welded together at single points. If required, a mounting reinforcement has to be installed to fix the position of single bars.



Figure 2.13. Typical reinforcement cage for segmental linings

2.4.4. Contact Surfaces

The proportion of joints in the tunnel tube is relatively high due to the segmental building of the individual rings and the ring-wise production of the lining. These are the longitudinal joints between the segments and the circumferential joints between the adjacent rings. Longitudinal and

circumferential joints provide the transmission of axial forces, shear forces, and moments between rings and segments.

2.4.4.1. Longitudinal (Segment) Joints

The longitudinal joints transfer axial forces, bending moment due to eccentric axial forces, and shear forces from external and also sometimes internal loading. From a statical point of view, the longitudinal joints are hinges with restricted bearing capacity for bending moments (torsion springs). Bending moments are transferred by eccentric forces acting in ring direction. Shear forces are transferred by the friction which exists between the contact surfaces of the joint.

There are three types of widely used longitudinal joints. These are:

- two flat surfaces
- two convex surfaces
- convex / concave surfaces

With longitudinal joints having two flat surfaces as shown in Figure 2.14a, the free rotation of the segments is hindered by the geometry. Therefore, in addition to the axial compression load in the longitudinal joint, bending moments can also be transferred, which reduces the bending loading on the segment [14].

Due to their small stiffness against torsion, joints with two convex surfaces shown schematically in Figure 2.14b are suitable especially in case of high compressive forces in connection with large angles of torsion between two adjacent segments [13].

Longitudinal joints with convex / concave surfaces according to Figure 2.14c normally have a high rotation capability. Therefore, this type of joint leads to a better stability of the ring during assembly [13].

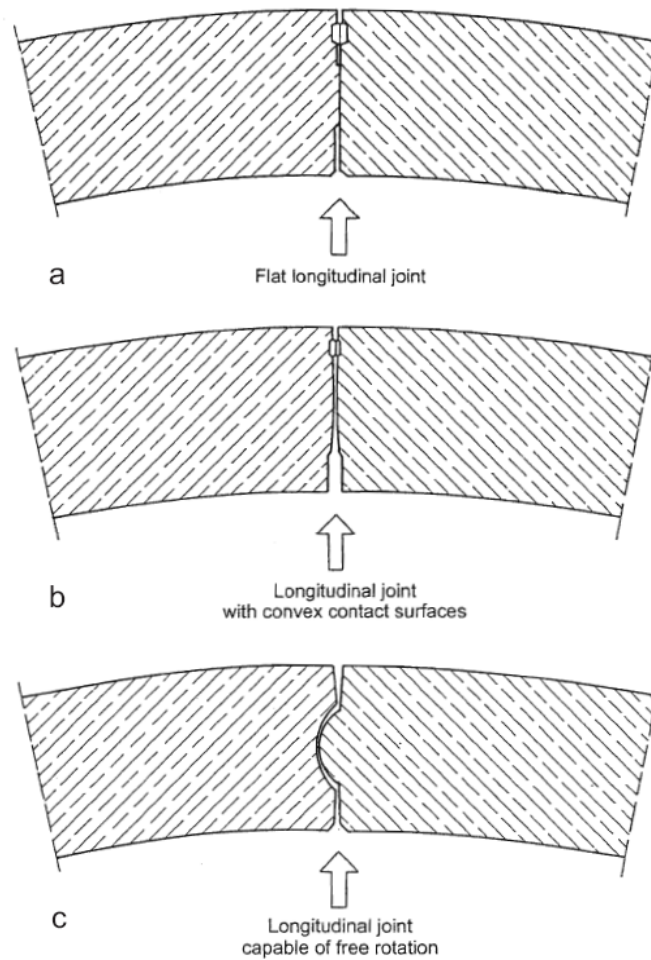


Figure 2.14. Longitudinal joints with a) two flat surfaces, b) two convex surfaces, c) convex / concave surfaces [13]

In addition to these types, longitudinal joints with tongue and groove can be mentioned as a possibility. However, it is not recommended for longitudinal joints because the tongue cannot be reinforced and the concrete spalls off if the play in the joint is only slightly exceeded.

A special form of tongue and groove joints has the one sided groove with insert. This type is only used for smaller keystones in order to avoid them falling out [13].

2.4.4.2. Circumferential (Ring) Joints

The ring joint level is positioned orthogonally to the tunnel's longitudinal axis. The thrust forces applied during construction are transferred through the circumferential joints. Due to adjacent rings having different deformation patterns, coupling forces (transverse forces) are created in the ring joints when the deformation is hindered [13]. In the circumferential joints, load transmission pads consisting of hardboard (timber sandwich layers) or "Kaubit" (caoutchouc and bitumen) are arranged to compensate for mounting tolerances and to assure the load transfer at predetermined surfaces [14].

The most common forms of ring joints can be listed as follows:

- flat ring joints
- tongue-and-groove systems
- cam-and-pocket systems

The flat ring joints shown in Figure 2.15 are the simplest form of ring joints. Each ring joints of this type supports itself without interacting with adjacent rings, or at least not intentionally. The coupling is only through friction. Transverse load transfer through joint is not intended. However, this can be implemented for small coupling forces with a durable bolted connection (see Figure 2.15).

To simplify the installation of the ring and to establish a force transmitting connection of adjacent rings during machine tunneling in the ground, the circumferential joints are equipped with tongue-and-groove systems or cam-and-pocket systems. The coupling avoids large relative displacements between adjacent rings and leads to an increase of the flexural stiffness of the segmental lining [14].

The relative displacements of adjacent rings are very small during the TBM tunneling in rock. Therefore, remarkable coupling forces do not occur.

Accordingly, circumferential joints with flat surfaces are usually carried out for segmental linings in rock.

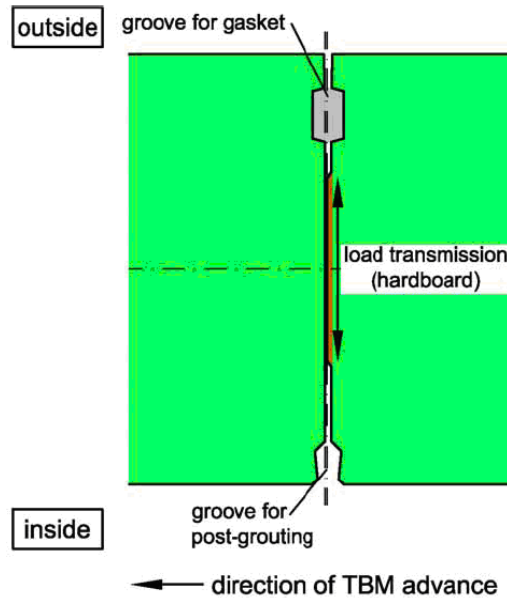


Figure 2.15. Circumferential joint with flat surfaces [14]

In a tongue-and-groove system as shown in Figure 2.16, the tongue is mostly wider than half of the segment's width and has a height of 10 to 30 mm. This flat tothing can not be reinforced for bearing the coupling forces, if the required concrete cover is obeyed. The usually inevitable assembly inaccuracies and the resulting constraints often lead to damages during machine tunneling in soil. To minimize this damage, the groove is made larger than the tongue. The available play usually reaches upto a few millimeters and is quickly eaten up by manufacturing and installation tolerances [14].

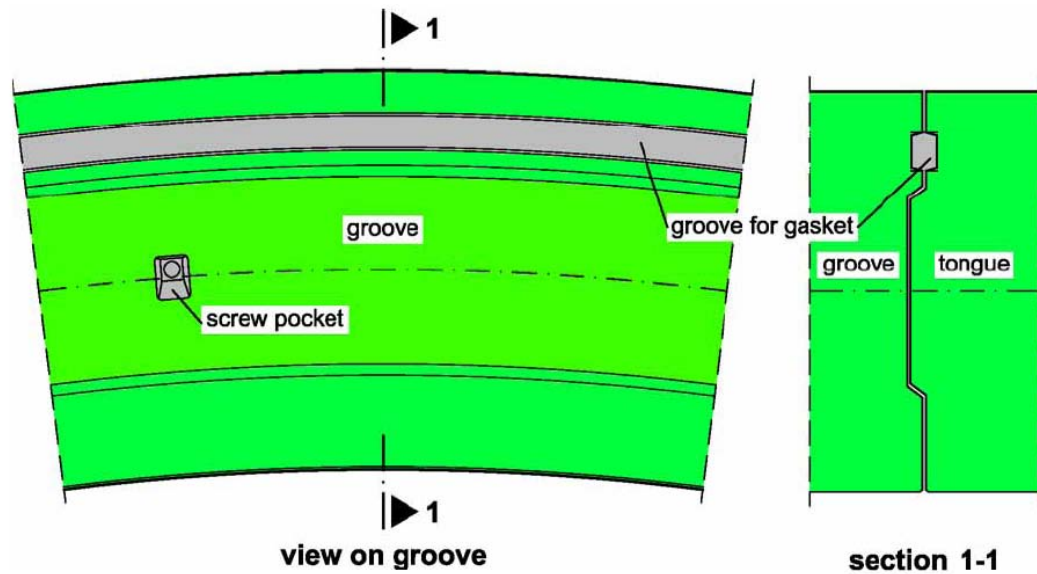


Figure 2.16. Circumferential joint with tongue-and-groove system [14]

In a cam-and-pocket system as shown in Figure 2.17, the constraints due to assembly inaccuracies are limited to the cam-and-pocket area. In case of a deep toothing with a correspondingly high cam, the cam can also be adequately reinforced. Also, the height of the cam should be selected so that a failure would occur at the cam and not shear off the edge of the pocket, then the waterproofing is preserved.

Using a tongue-and-groove system or a cam-and-pocket system, the coupling forces are transferred through load transmission pads (coupling pads) consisting of "Kaubit" instead of direct contact of concrete.

In addition to these types, convex – concave designs of the ring joint are also known. However, the edge surfaces of concave faces are at risk of damage during assembly.

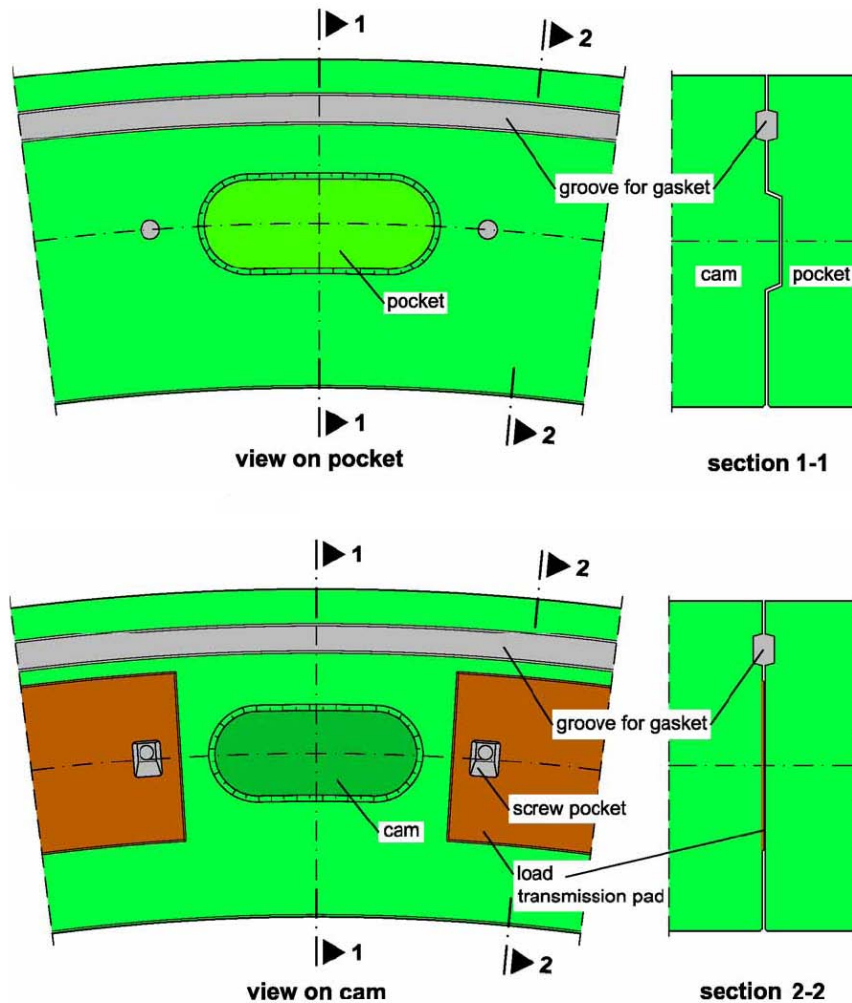


Figure 2.17. Circumferential joint with cam-and-pocket system [14]

2.4.5. Connectors

Connectors are used to hold segments and rings together until the grout material hardens and the segment or ring is fixed in its final position. For the connections between segments and rings, two types of connectors are used in general:

a) Joints with bolts: the segment is first placed in position and then the bolts are inserted and tightened. This type requires effort in the construction

of the mould because it is necessary to create “pockets” and “grooves” into which the bolts are inserted. Also, more staff is required to insert the bolts. This type is mostly used both between rings and between segments, within a ring [3].

The bolts are metallic while the embedded threads are generally plastic. Figure 2.18 shows the typical housing of a straight bolt.

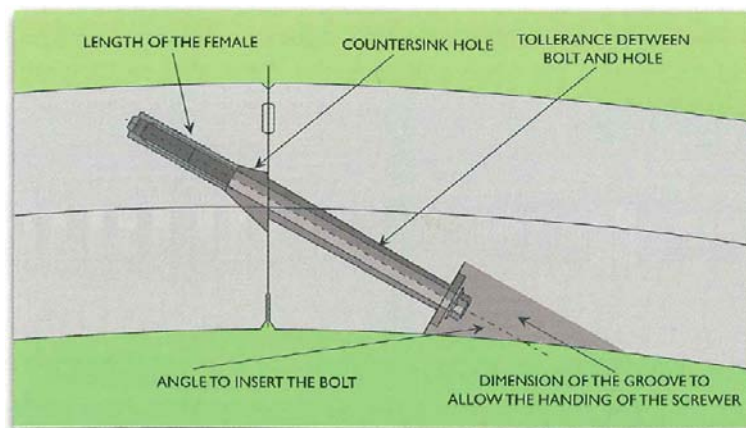


Figure 2.18. Section of a typical housing for a single bolt [3]

Bolts with curved elements also exist, but not common. However, the details about the geometry of straight elements are fundamentally valid in this case.

b) Joints with dowels: the connectors, which are completely covered and hidden, are inserted into the segment during the assemblage and are mortise-inserted into the segment of the last assembled ring.

Since the insertion is automatically performed by the erector when the segment is positioned, this type of connector requires less work for construction of the mould and less manpower in the tunnel [3].

The dowels and nuts are made of plastic and sometimes have the core in steel. Figure 2.19 shows the typical housing of a pin for the variety with a nut and without a nut, in which the pin is directly forced into a hole cut out of the concrete.

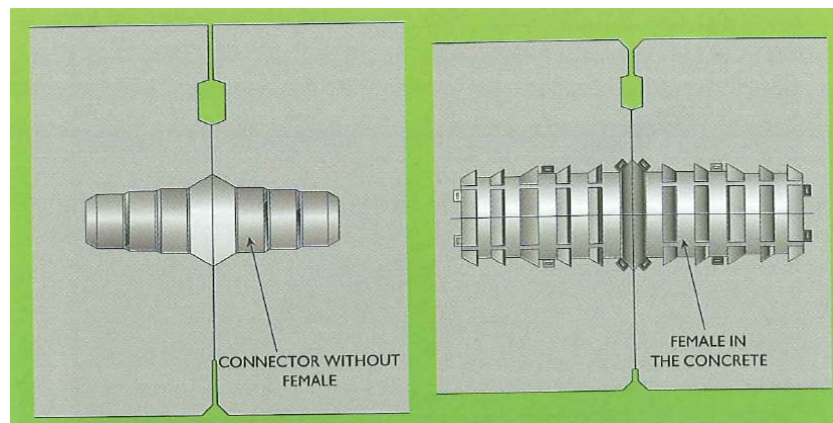


Figure 2.19. Section of a typical room for a single dowel [3]

The connection with dowels can be used only for rhomboidal and/or trapezoidal segments to avoid early crawling of the gaskets during the ring assembly [3].

Differently from dowels, screwings of bolts are released and bolts are removed as soon as the restoring forces of the gaskets can be transmitted by the annular gap grouting into the rock mass and an influence of the jacking forces does not exist anymore. For this purpose, the bolts should be removed after the gap grouting has set. However, in the area of portals and cross cuts, the screwing of bolts are permanent because the shearing bond between the annular gap grouting, the segmental lining and the rock mass may not be sufficient to carry the restoring forces of the gaskets. Furthermore, corrosion-resistant screws should be used in these regions [14].

2.4.6. Waterproofing System

Waterproofing of a ring is generally provided by the following equally important factors [3]:

- an optimal quality of the concrete and of the segment, resulting from the high level strength of the concrete used together with an accurate prefabrication process,
- provision of care when moving the individual segments to avoid the formation of cracks,
- choice and positioning of gaskets,
- proper assembly of ring, aligning the segments, and avoiding any possible damage,
- filling the annular gap with suitable material.

The sealing elements always work in pairs because they are placed in special grooves embedded on each side of all the segments close to the extrados and they come into contact when the segments are assembled to form a ring. There are mainly two types of gaskets:

a) Compression Gaskets: watertightness is ensured by the compression of gaskets. The compressive stress is ensured by the connectors (for both ring and segments) in the short term and by stresses acting in the ring in the long term [3].

b) Compression and Swelling Gaskets: working principle is basically the same with compression gaskets. In addition to compression, this type of gasket physically swells in the presence of water and develops a very high-pressure sealing capacity [3]. All of gaskets have nearly similar geometries and are only different in terms of their width, height, and hardness of rubber (EPDM) from which gasket is made.

2.4.7. Ring Assembly

Ring assembly process starts with the supply of the segments at the portal and finishes with the exit of the ring from the tail of the TBM. The segments are transported by wagons that move either on wheels or tracks. Wagons carry the segments into the back-up where they are lifted by a system known as “segment feeder” which takes them to the erector positioned inside the shield. For straight tunnels, the arrival order is arranged according to assembling order of segments. In order to prevent any confusion about ordering, the segments are marked with letters and/or numbers that determine the assembling sequence [3].

Before the installation of a new segmental ring, the previously mounted ring should be inspected. Fractured or cracked segments should be dismantled and replaced by new and sound segments. The tail-skin should be clean and dry also at the invert.

Ordinarily, the first segment is attached to invert of the ring mounted before. When positioned correctly by the erector, the segment is pushed against the previously mounted ring by the thrust cylinders as shown in Figure 2.20. Subsequently, the screwings in the circumferential joints are fixed. After all screws are fixed and prestressed respectively, the erector can be retracted from the segment.

Then, the following segments are alternatively installed to left or right of the first segment. The longitudinal joints should be completely closed. If the installation is not done properly, longitudinal joints are compressed by the annular grout after the ring assembly is completed. This may lead to damages to the segments on the outside of the ring.

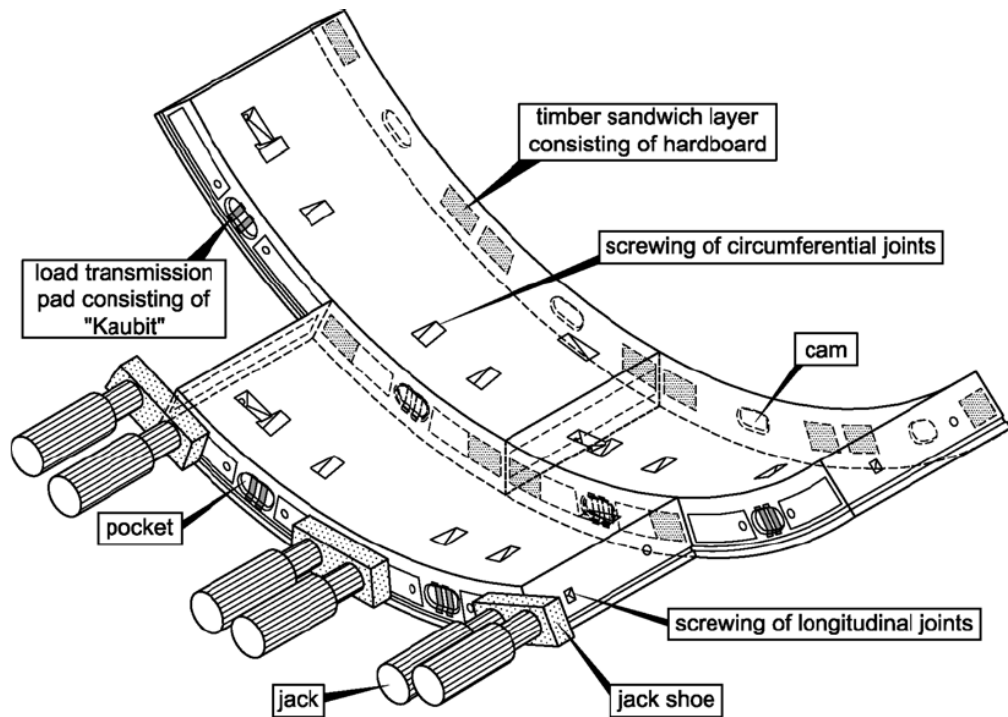


Figure 2.20. Installation of segments and transmission of thrust forces into the segmental linings [14]

Before the installation of key segment, it should be checked if there is enough space between the counter segments for mounting the keystone. If there is not enough space, the ring should be dismantled and erected again. The key segment is installed with the erector far enough to create the required prestressing of gaskets in the circumferential joints. The jacks of the adjacent segments are slightly retracted to avoid restraints in order to install the keystone completely. Afterwards, the thrust cylinders are only pushed again when the screws in the longitudinal joints are completely fixed [14].

As mentioned above, circumferential and longitudinal connections are mostly fixed with bolts for the installation of segmental ring and to secure the geometry. Generally, the screw connections are removed after imbedding the

ring in the grout. Then, a bolted connection is no longer necessary, because the longitudinal joints are pressed into place by the ground pressure and water pressure; and pre-loads are present in the ring joints created by resetting forces of the sealing section [22].

CHAPTER 3

LITERATURE REVIEW

In this chapter, a brief literature review of TBM segmental lining analysis methods is provided along with recent published literature. Selected analysis methods (elastic equation method and beam – spring method) which will be evaluated in this project are explained and discussed in more detail.

3.1. Analysis Types

Structural methods used to analyze TBM segmental linings must be able to indicate loads and deformations in accordance with the geologic and construction conditions and also represent the ground – lining interaction. There are various structural methods that satisfy these criteria. They include estimations based on empirical evidence, analytical solutions, and numerical simulations. General tendency for calculating the member forces of the TBM segmental lining is to perform numerical simulation. However, analytical methods are also commonly used to provide a collective check on the results. According to ITA – WG2 [23], the member forces should be computed by using belowmentioned methods:

- Elastic Equation Method
- Schulze and Duddeck Model
- Muir Wood Model
- Beam – Spring Method
- Finite Element Method

There is no unique solution in tunnel engineering. All of these methods have strengths and weaknesses. Also, each method mentioned above has some limitations that restrict the usage of them. For that reason, strengths, weaknesses, and limitations of the methods should be investigated in detail before selecting the proper method to be used in design.

This thesis study mainly focuses on beam – spring method, but elastic equation method is also examined as an analytical approach. Therefore, this chapter particularly describes elastic equation method and beam – spring method in detail. Also, other methods are briefly mentioned.

3.1.1. Elastic Equation Method

The elastic equation method, also called as usual calculation method, is a simple method for calculating member forces of circular tunnels without a computer. This method is proposed by *Japanese Standard for Shield Tunnelling* [24] and has been widely used in Japan. Key points of this method are provided in this section.

Load distribution model used for this method is shown in Figure 3.1. In the figure, P_0 is overload (surcharge); R_0 is the external radius of shield lining; R_c is the radius of middle line of shield lining; g is gravity of lining; P_{e1} and P_{w1} are, respectively, the vertical earth pressure and water pressure acted on the up side of shield lining. The lateral earth pressure and water pressure vary linearly and act on both sides of the shield lining. They are equal to q_{e1} and q_{w1} at the top of the shield lining, and q_{e2} and q_{w2} at the bottom of shield lining; P_{e2} and P_{w2} are respectively the vertical earth pressure and water pressure acted on the bottom side of shield lining; P_g is the vertical resistance of lining weight acted on the bottom side of shield lining.

For sandy clay, the earth pressure and water pressure are assumed to act on the lining separately. If the overburden thickness is two times larger than the

external diameter D of shield lining ($h_0 \geq 2D$), an effective overburden thickness h_0 should be used and it can be determined by Terzaghi's formula described in Chapter 4.3.4.

The distribution of horizontal earth resistance has a triangular shape and its application range is shown in Figure 3.1.

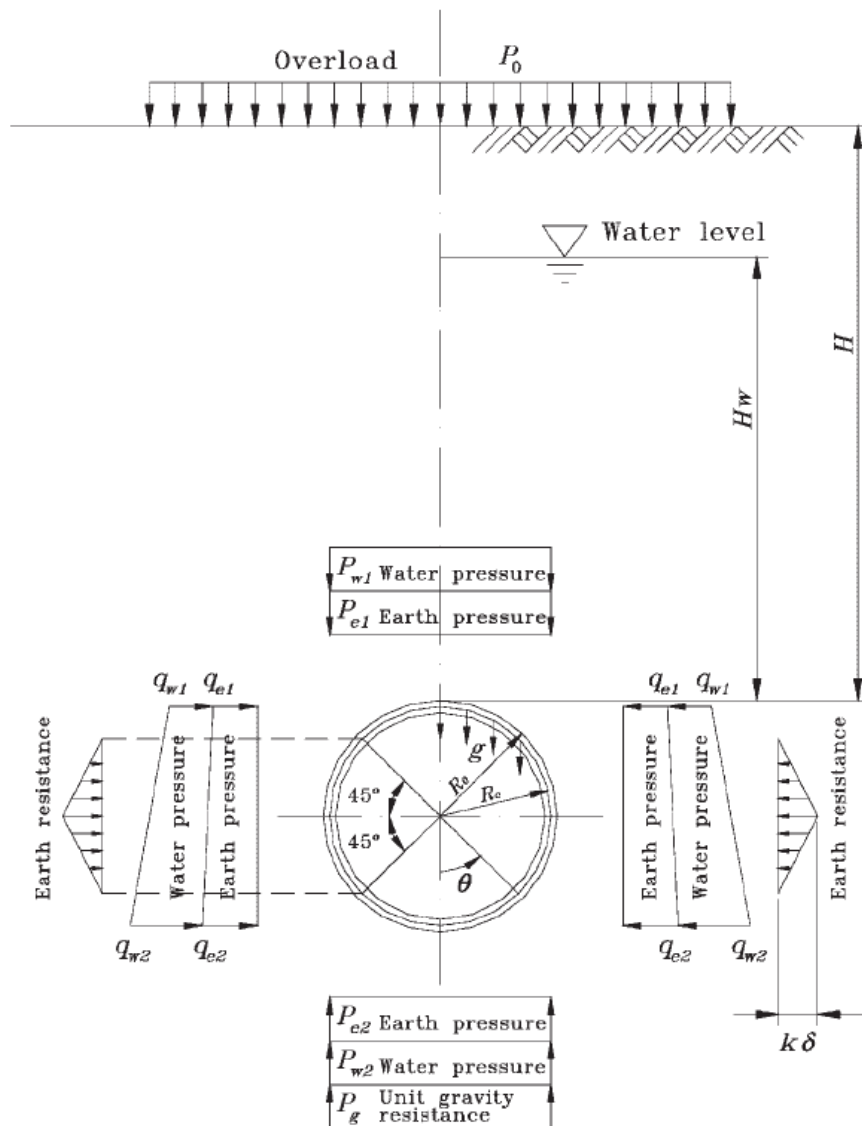


Figure 3.1. Load condition of Elastic Equation Method [24]

After having all parameters determined, the internal forces of the segmental lining can easily be computed. Elastic formulas for the calculation of member forces are given in Table 3.1.

Table 3.1. Equations of member forces for Elastic Equation Method [24]

| Load | Bending Moment | Axial Force | Shear Force |
|---|---|--|---|
| Vertical Load ($P = p_{e1} + p_{w1}$) | $(1-2S2)*P*R_c^2/4$ | $S2*R_c*P$ | $-SC*R_c*P$ |
| Horizontal Load ($Q = q_{e1} + q_{w1}$) | $(1-2C2)*Q*R_c^2/4$ | $C2*R_c*Q$ | $-SC*R_c*Q$ |
| Horizontal Triangular Load ($Q' = q_{e2} + q_{w2} - q_{e1} - q_{w1}$) | $(6-3C-12C2+4C3)*Q'*R_c^2/48$ | $(C+8C2-4C3)*Q'*R_c/16$ | $(S+8SC-4SC2)*Q'*R_c/16$ |
| Soil Reaction ($P_k = k \cdot \delta_h$) | $0 \leq \theta \leq \pi/4$ $(0.2346-0.3536C)*R_c^2*k\delta$ $\pi/4 \leq \theta \leq \pi$ $(-0.3487+0.5S2+0.2357C3)*R_c^2*k\delta$ | $0 \leq \theta \leq \pi/4$ $0.3536C*R_c*k\delta$ $\pi/4 \leq \theta \leq \pi$ $(-0.7071C+C2+0.7071S2C)*R_c*k\delta$ | $0 \leq \theta \leq \pi/4$ $0.3536S*R_c*k\delta$ $\pi/4 \leq \theta \leq \pi$ $(SC-0.7071C2S)*R_c*k\delta$ |
| Dead Load ($P_g = \pi \cdot g$) | $0 \leq \theta \leq \pi/2$ $(3/8\pi-\theta*S-5/6C)*R_c^2*g$ $\pi/2 \leq \theta \leq \pi$ $[-\pi/8+(\pi-\theta)S-5/6C-1/2\pi*S2]*R_c^2*g$ | $0 \leq \theta \leq \pi/2$ $(\theta*S-1/6C)*R_c*g$ $\pi/2 \leq \theta \leq \pi$ $(-\pi*S+\theta*S+\pi*S2-1/6C)*R_c*g$ | $0 \leq \theta \leq \pi/2$ $(\theta*C-1/6S)*R_c*g$ $\pi/2 \leq \theta \leq \pi$ $[-(\pi-\theta)*C+\theta*S+\pi*SC-1/6S]*R_c*g$ |
| Horizontal Deformation at Spring Line (δ_h) | $\delta_h = [(2P-Q')+\pi*g]*R_c^4/[24*(EI/h+0.045k*R_c^4)]$ | | |

$\theta =$ angle from crown, $S = \sin \theta$, $S2 = \sin^2 \theta$, $S3 = \sin^3 \theta$, $C = \cos \theta$, $C2 = \cos^2 \theta$, $C3 = \cos^3 \theta$

Segmental ring is composed of several segments which are connected by bolts or dowels. The deformation at these connection joints is larger than the one in a ring with uniform rigidity, because the rigidity of joints is less than the rigidity of segment section. Furthermore, the connections at the segment joints are generally staggered. However, this method assumes the segmental ring with uniform bending rigidity and can not represent the staggered geometry [24]. Nevertheless, the solutions obtained by this method can be very practical and helpful for checking the results obtained by numerical methods [2]. Also, this method is mostly used in preliminary design and cost estimation for a new tunnel project.

This method is more advantageous than other closed form solutions, because elastic equation method has a capability of calculating bending moment, axial force, and shear force of any point on the lining. However, other closed form solutions can only determine the bending moments and hoop forces at the point where relative maximum values occur.

3.1.2. Schulze and Duddeck Method

The thrust and bending moment in circular linings surrounded by an elastic medium can be determined by several closed form solutions such as Schulze and Duddeck Method. These closed form solutions deal only with tunneling models for soft ground and the some basic assumptions are applied to derive a model such that the cross-section is circular, the material behavior of ground and lining is elastic, the active soil pressures on the lining are taken as equal to the primary stresses in the undisturbed ground, and there exists a bond between the lining and the ground for radial and tangential deformations [25].

The complete and closed solutions for the model (Figure 3.2) intended for shallow tunnels ($H \leq 6R$) limited overburden is published by Schulze and Duddeck [26] in 1964. Surrounding ground is represented by ground springs.

Since tension springs may cause load reduction, bedding at the crown is omitted. The results of this study is given as direct design diagrams for bending moments, hoop forces, and radial displacements for those three points of the lining where relative maximum values occur. In this method, modulus of subgrade reaction (K_r) is a free parameter and the tangential stresses may be included in or omitted from the load parameters [25].

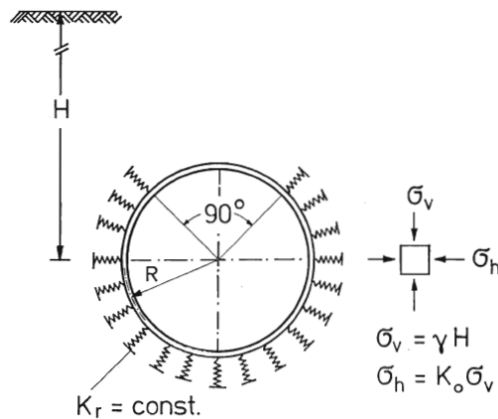


Figure 3.2. Bedded ring model without crown bedding [25]

3.1.3. Muir Wood Method

Muir Wood Method is another closed form solution used to determine hoop forces, bending moments, and radial displacements. Like most closed form solutions, this model is based on the assumption that the ground is an infinite, elastic, homogeneous, and isotropic medium. Also, the basic assumptions for closed form solutions determined in the previous section are valid for this method.

Muir Wood model [27] is based on plain strain continuum model shown in Figure 3.3. This method assumes that the circular lining deforms into an elliptical mode. The tangential ground stresses are included, but radial

deformations due to the tangential stresses are omitted. Muir Wood proposed to take only 50% of the initial ground stresses into consideration that allows for some pre-decompression of the ground around the opening before the lining is placed. By reducing the lining stiffness by an amount equivalent to the effect of less rigid joints, the moments can be reduced [25].

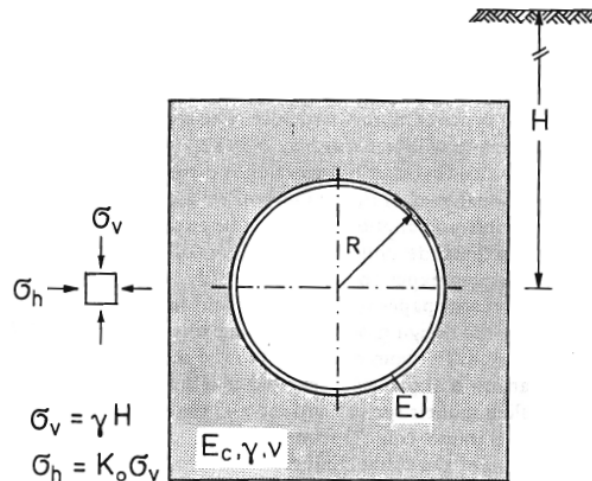


Figure 3.3. Plain strain continuum model [25]

3.1.4. Beam – Spring Method

The Beam – Spring Method, also called as “Coefficient of Subgrade Reaction Method”, is illustrated in Figure 3.4. In this method, the lining is generally represented by an arc, reduced to a polygon with fixed angles. Each piece of lining is supported by springs whose elasticity represents the ground reaction. In other words, the lining and ground are represented by a series of beams and springs respectively. It is assumed that the ground reaction is generated from the displacement of the lining proportionally to the deformation of ground. This assumption allows the consideration of the interaction between the segments and the surrounding ground [28].

In the applications of this method, the ground springs are commonly assumed to be effective in radial direction, but there are also exceptional examples assuming that the ground springs are also effective in the tangential direction [24]. In order to produce conservative (safe) results, soil springs that act only in radial direction are used to represent the surrounding ground. This assumption means that frictionless sliding of the lining against the ground occurs.

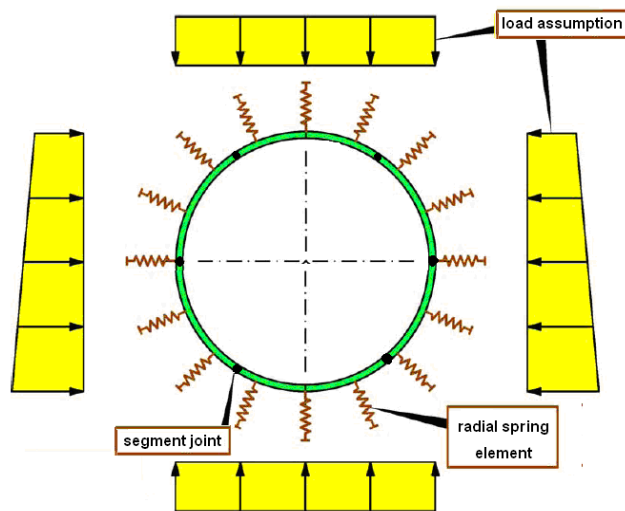


Figure 3.4. Model of Beam – Spring Method

Structural analysis with Beam – Spring Method is also based on the assumption that soil reaction forces are activated when the tunnel expands outward, but they are not activated when the tunnel contracts inward. For that reason, non-tension ground springs are used to represent the interaction between the lining and surrounding ground.

Segmental rings are generated by assembling several segments with bolts or dowels. These connection joints between the segments have a lower rigidity

than main section of the segment. Therefore, the deformation of a segmental ring tends to be larger than a ring with uniform bending rigidity. At this point, evaluation of the decrease of rigidity at joints has an importance for calculating the member forces [24]. For this purpose, various 2D approaches have been developed in order to evaluate the segment joints. In this sense, there exists several design models that assume the segmental ring as a solid ring with fully bending rigidity, solid ring with reduced bending rigidity, ring with multiple hinged joints, ring with rotational springs, and etc. These approaches are explained and discussed in Chapter 3.6.

The segments are assembled in a staggered pattern to compensate the decrease in the bending rigidity of the ring joint. Although 2D models are able to evaluate lining – ground interaction and the reduction of bending rigidity due to segment joints, they can not represent ring joints and the staggered arrangement of segments in adjoining rings. Unlike 2D models, the coupling of the adjacent rings and staggered arrangement of segments can be evaluated by 3D BSMs as illustrated in Figure 3.5.

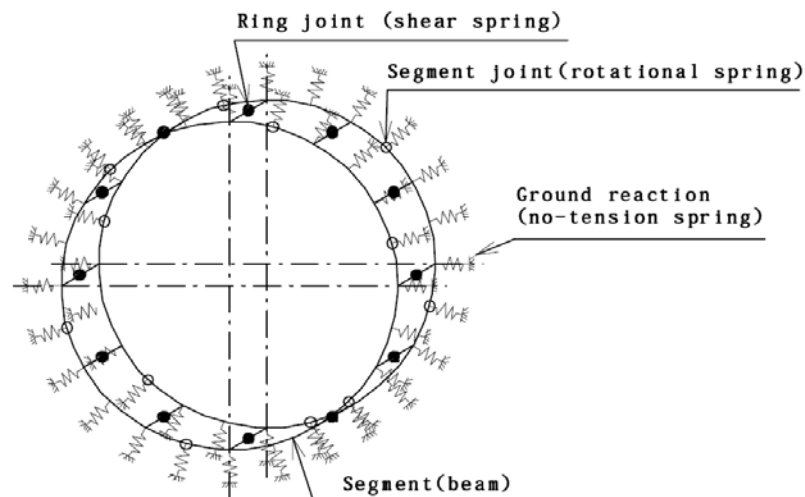


Figure 3.5. 3D Beam – Spring Model [29]

As shown in Figure 3.5, this 3D model has an ability to evaluate the reduction of bending rigidity and splice effects of staggered geometry by using a model in which a segment is considered as a curved or straight beam, a segment joint as a rotational spring, and a ring joint as a shear spring. Like 2D model, ground reaction is represented by non-tension springs. In addition, minimum two or more rings are used in the 3D analysis in order to evaluate the coupling of rings, the effect of joint locations and combinations, and shear stresses on a ring joint [24].

Design procedure, design stages, loading types and conditions, and structural calculation used in the design of segmental linings are briefly discussed in Chapter 4.

3.1.5. Finite Element Method

Finite Element Method (FEM) which is illustrated in Figure 3.6 is one of the most widely used numerical methods in geomechanics. It is a continuum model but discontinuities can also be modeled individually. In FEM, the hosting ground is discretized into a limited number of smaller elements. These elements are connected at nodal points. The stress, strain, and deformation to be analyzed are caused by changing the original subsurface conditions. For instance, such change might be induced by tunneling process. The stresses and strains generated in one element effects the interconnected elements, and so forth [6].

The stress-strain relationships of the elements are modeled mathematically by creating a global stiffness matrix which relates the unknown quantities with known quantities. Then, this matrix is solved using standard matrix reduction techniques and the results are obtained. The equations to be solved are highly complicated, and as the number of the elements in the model increase, the calculation time and the storage capacity increase dramatically.

By means of FEM, complex underground conditions and tunnel characteristics can be analyzed. Furthermore, this method enables the simulation of complex constitutive laws, non-homogeneities, and the impact of advance and time dependent characteristics of the construction methods.

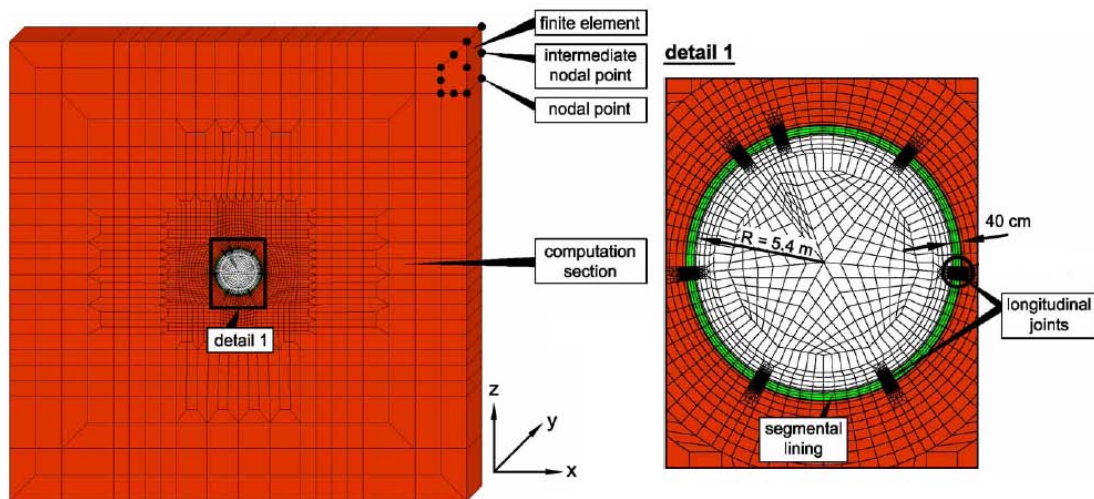


Figure 3.6. Finite element method for tunnel engineering

On the other hand, most FEM programs require more knowledge on program and computer than other methods do. Typically the output of the analysis is also complex and it becomes difficult to assess the results. Therefore, a post-processor may be utilized in order to overcome this difficulty [6].

3.2. Theoretical Approaches on Beam – Spring Method

Since Beam – Spring Method is the most effective and practical tool for the calculation of member forces of TBM segmental linings, several theoretical approaches have been developed in this field. The main determinant criteria in BSMs are the ground lining interaction and connection joints. For ground lining interaction, most approaches employ non-tension elastic ground

springs. However, these approaches have different methods to evaluate connection joints. Therefore, these theoretical approaches can be classified by joint evaluations.

Selecting the proper structural model in order to calculate the member forces of TBM segmental linings should be done carefully, because it depends on several conditions, such as usage of tunnel, design loads, geometry and arrangement of segments, ground conditions, and required accuracy of analysis. Schematic drawings of structural models outlined by JSCE [24] are illustrated in Figure 3.7.

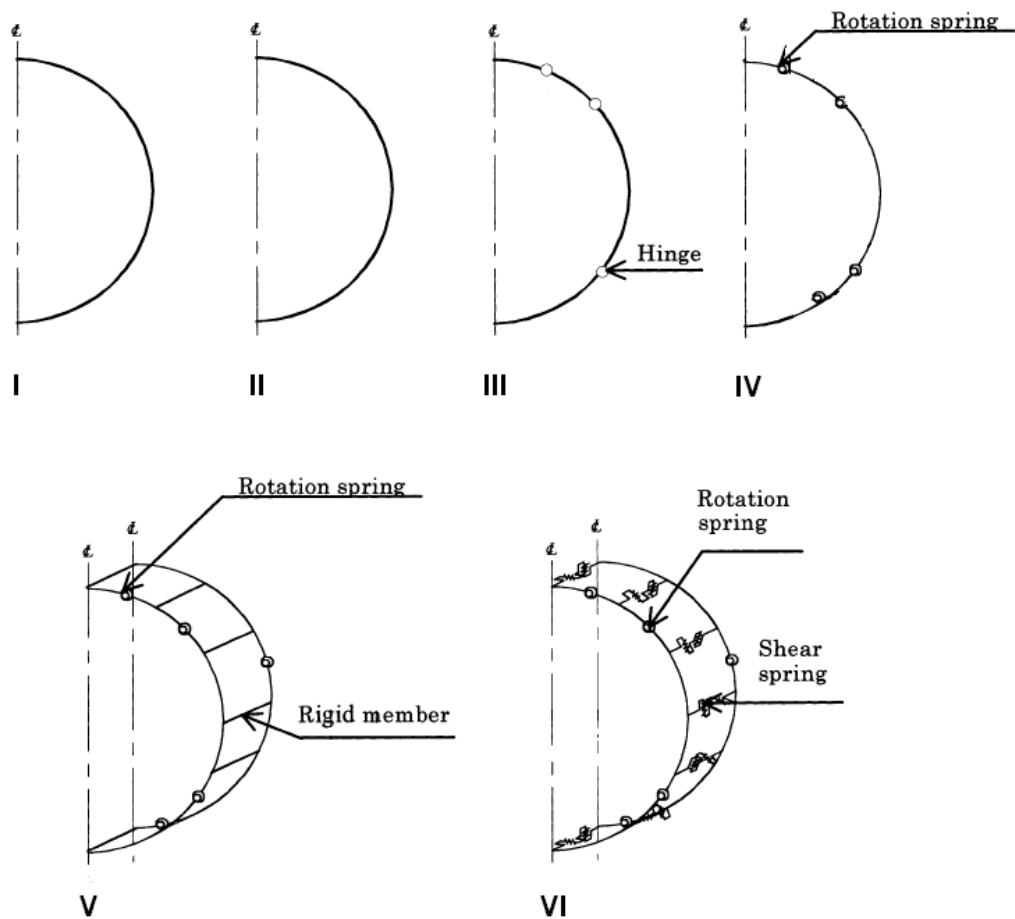


Figure 3.7. Structural design models for TBM segmental linings

Available structural models in the literature are summarized in Figure 3.7. 2D models (I-IV) are able to represent only segment joints by using reduced rigidity, hinges, or rotational springs. However, 3D models (V-VI) can simulate both segment joints and ring joints. In 3D models, segment joints are represented by rotational springs, and ring joints are modeled as rigid members or shear springs.

The common part of these BSMs is the ground – lining interaction. It is simulated by non-tension elastic ground springs in radial direction as shown in Figure 3.4 and Figure 3.5. The soil spring constant is calculated using the following theoretical formulas proposed by Muir Wood, in accordance with AFTES – WG7 Appendix 1 [28].

$$k = \frac{E}{(1 + \nu) \cdot R} \quad (3.1)$$

where, k : Modulus of subgrade reaction of the ground in the radial direction (kN/m³),
 E : Modulus of deformation of ground (kN/m²),
 ν : Poisson's ratio,
 R : Outer radius of segment (m).

$$k_r = k \cdot A_t = k \cdot l_s \cdot w \quad (3.2)$$

where, k_r : Soil spring constant in the radial direction (kN/m),
 k : Modulus of subgrade reaction of the ground in the radial direction (kN/m³),
 A_t : Tributary area (m²),
 l_s : Distance between soil springs (m),
 w : Width of segment (m).

Structural models given in Figure 3.5 are sorted from the simplest one to the most complicated one, and also show the development of the approaches. After the conditions of tunnel project are denoted, structural calculations of segmental linings can be performed by a single model. In order to decide on the proper model, all models should be investigated.

In **Model I**, the segmental ring is assumed to be a ring with uniform bending rigidity. The decrease of rigidity at segment joints is ignored and a segmental ring is treated as a ring with uniform bending stiffness EI as a main section of a segment [24]. In other words, this model can be named as “solid ring with fully bending rigidity”. This is the simplest 2D model and can not evaluate the connection joints. Therefore, this model gives more conservative results than the others.

In **Model II**, the segmental ring is again assumed to be a ring with uniform bending rigidity, but bending rigidity is reduced in order to simulate the effects of segment joints. There are different approaches for the reduction of bending rigidity.

Bickel, Kuesel, and King [30] have proposed a 2D model that simulates the segment joints by using reduced stiffness parameters. This model assumes that the stiffness (effective modulus of elasticity) of a segmental ring is half that of a monolithic ring and the moment of inertia of practical coffered precast segments ranges from 60 to 80% of that of solid sections with the same thickness. Due to reduced stiffness, this model is more flexible than Model I and expected to give less values for bending moment and hoop forces.

Furthermore, Koyama and Nishimura [31] have recommended a model in a similar manner with the former model proposed by Bickel, Kuesel, and King. According to these Japanese researchers, the tunnel lining is assumed to be

a continuous ring with a discounted rigidity by applying a reduction factor, η , to the bending rigidity (EI) of the tunnel lining. Koyama and Nishimura [31] suggested determining η by full ring structural testing. If experimental data are not available, the value of η can be assumed to be in the range of 0.6 – 1.0 for preliminary design analysis. For instance, a continuous monolithic ring beam having a constant effective rigidity ratio of $\eta= 0.8$ was used in the design of the Trans-Tokyo Bay Highway tunnel lining (Uchida 1992). The value of η adopted in the tunnel project was later verified by tests on a full-scale prototype segmental lining [32].

Muir wood [27] investigated the effects of joints between the segments and proposed an easy to use empirical formula to estimate the effects of the longitudinal joints of rings in a calculation with a homogeneous rigid ring by reducing the bending stiffness of the lining. The effective moment of inertia, I_e , for a segmental tunnel ring with a number of equal segments can be expressed as follows.

$$I_e = I_j + \left(\frac{4}{n}\right)^2 \cdot I \quad I_e \leq I, n > 4 \quad (3.3)$$

where, I_e : The effective moment of inertia,
 I_j : The moment of inertia at the force transmission zone between the joints,
 I : The moment of inertia of the lining section,
 N : Number of segments (key segment not counted).

Muir Wood [27] suggested that the existence of segment joints would not affect the rigidity of the lining for four or fewer lining segments. The earth pressure acting around a tunnel is assumed to be in an elliptical shape in this model. In order to obtain this elliptical shape for initial loading, sufficient overburden thickness is required. Therefore, Muir Wood model is more

convenient for deep tunnels. This assumption may not be valid for shallow tunnels.

First two approaches given for **Model II** make some assumptions for the effect of segment joints. However, the effects of the number of segments are not considered. Although Muir Wood model takes into consideration the number of segments, it can not simulate joint orientation. According to numerical studies done by Hefny, Tan, and Macalevey [33], the values of moments induced in the lining are reduced by 8 times by orientating the joints with an angle of 45°. This shows that in addition to the number of segment joints, the orientation of joints also affects the member forces considerably. Since these effects may lead to large reduction in costs, they should be conceived.

Model III assumes the segmental ring as a ring having several hinges. This model is used in United Kingdom and Russia, where ground conditions are relatively good i.e. hard rock. In this model, segment joints are modeled as unfixed hinges. Afterwards, deformation is calculated and checked for safety. This model gives considerably less bending moments and leads to more economical design for the grounds in good condition. Since this method fairly depends on ground conditions, adequate study should be done in order to determine whether the model is suitable for the existing ground or not [24].

Model IV simulates not only the number of segment joints but also the joint orientation. Segment joints are modeled as rotational springs as illustrated in Figure 3.8a. The crucial point for this model is the calculation of rotational spring constant. For the behavior of rotational stiffness of longitudinal joints, worldwide accepted formulas proposed by Janssen [34] based on the investigation of Leonhardt and Reimann [35] for the resistance against rotation and bending of concrete hinges are used.

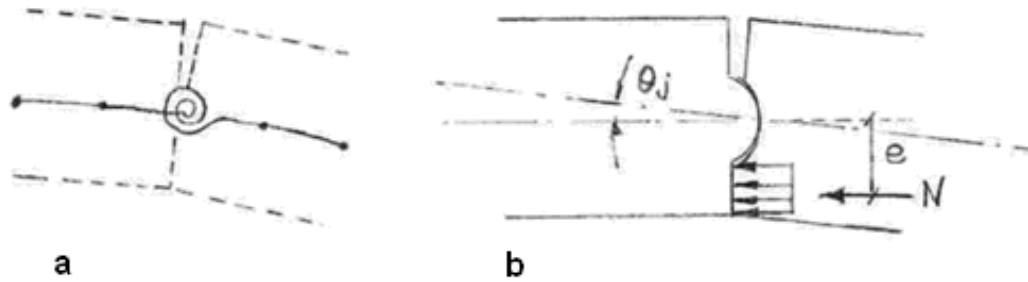


Figure 3.8. a) Rotational spring model, b) Stress distribution at the segment joint [37]

While developing the theoretical formula of Leonhardt and Reimann concerning concrete joints, the following assumptions are made on the basis of fundamental experimental results and observations concerning concrete joints.

- Tensile stress is not transmitted at joints.
- Compression stress has linear distribution.
- The deformation coefficient is constant, having the magnitude of E_0 , the initial connection elasticity coefficient in $\sigma = \varepsilon = 0$.
- The scope of deformation in the acting direction of axial force is centered on the joint surface, and limited to the same scope as the width of the convex portion of the joint. Strain is distributed uniformly.

The theoretical formulas based on the above assumptions and the geometric relationships are developed as follows and shown in Figure 3.9.

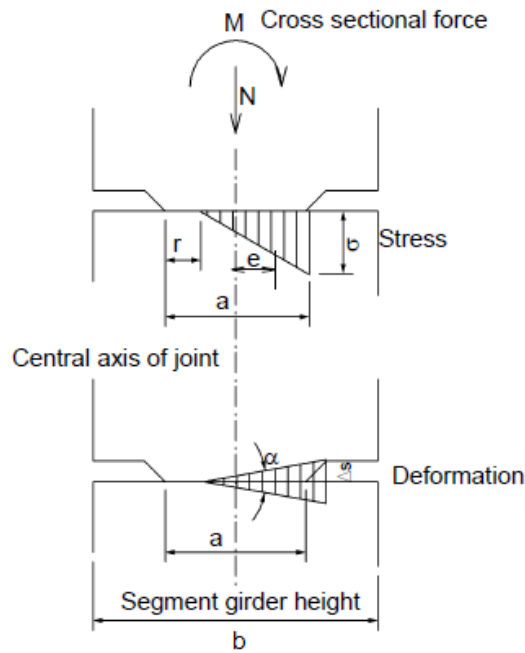


Figure 3.9. Stress and deformation in mortised portions

As long as the joint is fully compressed, the rotational stiffness is constant and could be described by the belowmentioned formula.

$$k_{\theta} = b \cdot \frac{E \cdot a^2}{12} \quad (3.4)$$

It depends only on the young's modulus E , the width of contact zone a , and the height of the segment b . If this bending moment exceeds the boundary bending moment ($M_{bou} < N \cdot b/6$), the joint is gaping like a bird's mouth as shown in Figure 3.8b. From this point, the rotational stiffness depends on the normal forces N and the bending moment M . It can be determined by the following formula.

$$k_{\theta} = M / \alpha = \left(9 \cdot \frac{b \cdot a^2 \cdot E}{8} \right) \cdot m \cdot (1 - 2 \cdot m)^2 \quad (3.5)$$

where

- k_{θ} : Rotational spring constant of joint (kN.m/rad)
- α : Rotational angle (rad)
- M : Bending moment (kN.m)
- M : Load eccentricity rate, $m = e/a = M / (N.a)$
- N : Axial force (kN)
- B : Contact zone (mortise) length (m)
- A : Contact zone (mortise) width (m)
- E : Young's modulus of concrete (kN/m²)

In order to employ this behavior, the above mentioned relationship between bending moment and rotational stiffness should be performed by non-linear rotational springs. Since rotational springs become extremely soft if the moment increases to more than about 80 % of the maximum moment, it is not necessary to define a yielding moment. Therefore, if only a linear rotational spring with the definition of a yielding moment is modeled, the simulation of behavior of segment joint seems to be very poor [36].

Model V, a 3D beam – spring model, is proposed by Koyama [38]. This model simulates the segment joints as rotational spring like model IV and supposes a rigid connection between the rings by using rigid members. It is assumed that the displacement of the ring beam is equal to that of the neighboring ring beam at the joint. Therefore, no gap occurs due to the shear stress. However, relative displacement between the two neighboring rings occurs in the longitudinal direction, and is concentrated at the centerline of the segmental rings [39].

Model VI, also proposed by Koyama [38], is an advanced version of model V. Differently from Model V, connection between the rings is modeled as shear springs. Calculation of shear spring constant is a complex issue because it depends on many factors such as type of ring joint (flat, cam-and-pocket, tongue-and-groove), type of connectors (bolt, dowel), number, and

orientation of connectors, loading on the ring, etc. Therefore, a general formula for determining the shear spring constant is not available. For that purpose, the compression characteristics of the shear strip are determined according to the relationship between the load and the displacement of materials used. This relation can be obtained by laboratory tests using actual joints. Figure 3.10 shows the relationship between deformation and the force acting on the shear strip during the application of shear force on the ring joint. Based on the figure, the shear spring constant (k_s) is calculated geometrically as follows:

$$k_s = \frac{F}{\delta} = \frac{F_n / \cos \theta}{\delta_n / \cos \theta} = \frac{F_n}{\delta_n} \quad (3.6)$$

where k_s : Shear spring constant in radial direction (kN/m),
 F : Shear force acting on the joint (kN),
 F_n : Vertical component of force on shear strip (kN),
 δ : Total displacement of shear strip (m),
 δ_n : Vertical component of compression displacement of the shear strip (m).

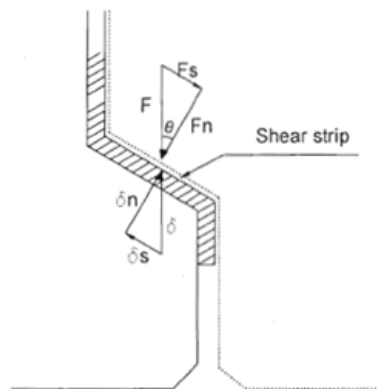


Figure 3.10. Forces acting on the ring joints and joint displacements

For the 3D analysis of segmental rings, the shear spring constant is generally obtained by laboratory tests or by experience of other comparable projects. However, if flat (plate) ring joints with plywood hardboards are used, the following formula for the shear stiffness of plywood can be used to determine shear spring constant [36].

$$k_s = \frac{G \cdot A}{d} \quad (3.7)$$

where k_s : Shear spring constant in radial direction (kN/m),
 G : Shear modulus of plywood (kN/m²),
 A : Area of hardboard (m²),
 D : Thickness of hardboard (m).

Among the models in scope, this model is the unique one that can simulate the interaction between adjacent rings. If spring constants are calculated properly, the most realistic results can be obtained with this model.

3.3. 2D and 3D Analysis of TBM Segmental Linings

Tunneling is a 3D problem where structural behavior of tunnel in the longitudinal direction and the analysis of loads during and after the construction may play an important role in the design of tunnels. Numerical methods in tunnel engineering have been widely used with a steady growth since the early applications in the mid 1960's. This is most probably due to the fact that numerical methods are capable of simulating the excavation, construction, and service steps. In contrast with analytical solutions, these are the distinctive advantages for numerical methods [40].

Although 3D numerical analysis of tunnels can simulate the structural behavior of tunnel in the longitudinal direction and construction process, 2D numerical studies in tunneling are much more popular than the 3D analysis.

2D analyses assume plane-strain conditions for the lining and ground. This leads to avoiding three-dimensional effects. This type of simplifications made by performing 2D numerical analysis make the calculations easier and less time consuming, but they are not able to simulate 3D effects. In other words, 2D numerical methods are suitable for some cases, but they are not as accurate as 3D models. For that reason, it is crucial to identify which situations are convenient for 2D or 3D analysis. Consequently, the aim of this study is to evaluate available analysis methods (analytical, 2D and 3D numerical) for TBM segmental lining and propose suitable type of analysis for certain situations.

Blom et al. [41] investigated the stresses due to tunnel excavation by implementing 3D finite element model analyses for shield-driven Green Heart Tunnel. They have also compared the results obtained by 3D finite element analyses with analytical method (Schulze and Duddeck Model) and on-site measurements. This study showed that the results of 3D finite element model were so consistent with values obtained by on-site measurements, and 3D analysis simulated the stress distribution realistically. However, sectional forces predicted by analytical model did not fit well to on-site measurements. It can be concluded that 3D finite element models simulate the stresses and structural behavior of tunnels much more realistically than conventional methods.

Klappers et al. [36] made a comparison between 3D Beam – Spring Method and 3D FEM analysis with shell elements. This comparison showed that the calculated sectional forces of both models were more or less the same, and also only deformations differed slightly. This means that 3D FEM calculations are not necessary for normal loading conditions. For special cases like openings in the lining, different loads on the rings or varying bedding conditions, 3D FEM modeling is needed to calculate internal forces and deformations.

Mashimo and Ishumura [29] investigated loads acting on the shield tunnel lining by using 3D BSM. This study also revealed that 3D BSM gives realistic results if loading conditions and spring constants are calculated accurately.

Previous studies showed that 3D Beam – Spring Method is a useful tool in order to obtain sectional forces of TBM segmental linings. In this thesis study, an analytical method (elastic equation method), 2D beam – spring methods with different approaches and 3D beam – spring method will be evaluated and validity of methods for certain situations will be determined.

CHAPTER 4

TBM SEGMENTAL LINING DESIGN

Segmental linings are commonly used form of lining particularly for relatively long tunnels where using a TBM is advantageous in terms of economy. Design of a segmental linings not only requires structural analysis for the ground loads and the TBM ram loads applied to segments, but it also requires the designer to consider the total process of manufacture, storage, delivery, handling, and erection as well as the stresses caused by sealing systems and bolts.

Tunneling as an engineering discipline is unique. It has relied mainly on experience and most segmental lining designers came from a structural engineering background. The general approach for the design of segmental lining is to estimate, as accurately as, the magnitude and distributions of loads applied to tunnel support system and then detail the lining to carry the loads [42]. A proper design can be performed by following a progressive procedure taking into consideration all conditions of the problem.

This chapter typically indicates the design procedure, loading conditions, and structural calculation procedure used in the design of segmental tunnel linings. In the scope of this study, all structural analysis models are performed in accordance with these procedures.

4.1. Design Procedure

It is essential to state that there is no unique design for a segmental lining. There exist various competent design methods for shield tunnel linings, and the aim of this study is to investigate and compare different analysis methods used in the design. Today, the design and dimensioning of a reinforced concrete segmental ring are still carried out under consideration of its ultimate state. Limit states analysis allows checking of both the structure's factor of safety with respect to failure and its satisfactory behavior with respect to serviceability. The main characteristics of the two limit states are recalled in the following table.

Table 4.1. Limit states for the design of segmental lining [17]

| Ultimate Limit States (ULS) | Serviceability Limit States (SLS) |
|--|---|
| Failure of a section due to crushing of concrete | Excessive opening of cracks (infiltration, corrosion) |
| Excessive deformation of steel | Excessive compression of concrete causing microcracking |
| Instability of shape (buckling, bulging) | Excessive ring deformation |
| Loss of static equilibrium at ring erection | |

4.1.1. Design for the Ultimate Limit States

The design for the ultimate limit states takes into consideration the load combination factors and is performed for four loading conditions: basic combined actions (permanent loads), basic variable action (railway live load), loads applied during construction, and accidental combined actions (earthquakes, explosions, fires, and train derailment).

4.1.2. Design for the Serviceability Limit States

The design for the serviceability limit states takes into consideration the load combination factors and loading conditions for basic combined actions (permanent loads).

4.1.3. Design Stages

The design of a shield tunnel lining often follows the planning works, according to a sequence given below [23]:

- 1. Adherence to specification, code or standard:** The tunnel should be designed according to the appropriate specification, code or standards, which are decided by the people in charge of the project and the designers.
- 2. Decision on inner dimension of tunnel:** The inner diameter of the tunnel should be decided considering of the space that is demanded by the functions of the tunnel.
- 3. Determination of load condition:** The designer should select the load cases critical to the lining design such as earth pressure, water pressure, dead load, reaction, and surcharge, etc.
- 4. Determination of lining conditions:** The designer should decide on the lining conditions, such as dimension of the lining (thickness), strength of material, and arrangement of reinforcement, etc.
- 5. Computation of member forces:** By using appropriate models and design methods, the designer should compute the member forces such as bending moment, axial force, and shear force.

6. **Safety check:** The designer should check the safety of the lining against the computed member forces. Safety measures to be checked for both limit states are:
 - For Serviceability Limit State
 - Check cracking
 - Check deformation
 - Check compressive stress
 - For Ultimate Limit State
 - Check ultimate strength
7. **Review:** If the designed lining is not safe against design loads, or safe but not economical, the designer should change the lining conditions and redesign the lining.
8. **Approval of the design:** After the designer judges that the designed lining is safe, economical, and optimally designed, a document of design should be approved by the responsible authority.

The flow chart given in the Figure 4.1 summarizes these steps to be followed in the design of tunnel linings.

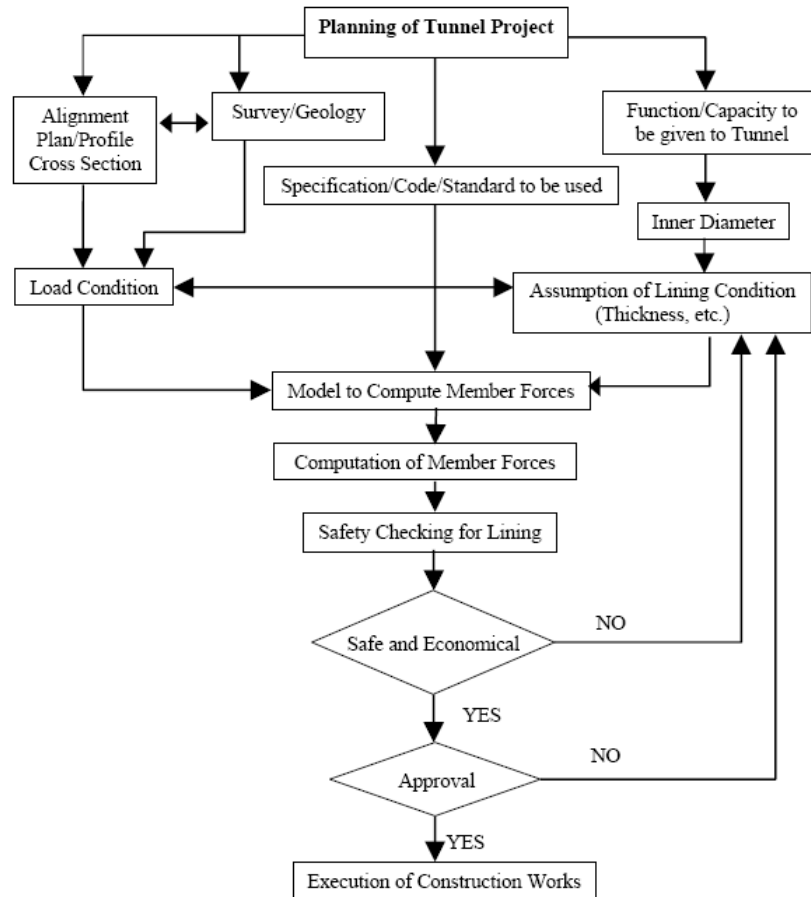


Figure 4.1. Flow chart of shield tunnel lining design [23]

4.2. Loading Conditions

The tunnel lining behind the TBM must be capable of withstanding all loads and combined actions without excessive deformation, especially during ring erection and advance. In addition, it should also keep durability against external effects during its service life. Therefore, reinforced concrete segmental rings behind the TBM are designed to fulfill those demands.

There are several loading cases that should be considered in the design and construction of segmental linings. This chapter gives general information about these loading cases.

According to Japanese Standard for Shield Tunneling [24], following load cases shall normally be considered in designing the lining of the shield tunnels,

1. Vertical and horizontal earth pressure
2. Water pressure
3. Dead weight
4. Effects of surcharge
5. Soil reaction
6. Internal loads
7. Construction loads
8. Effects of earthquakes
9. Effects of two or more shield tunnels construction
10. Effects of working in the vicinity
11. Effects of ground subsidence

Among these load cases, several load combinations can be composed according to the purpose of the tunnel usage. A generally accepted load classification from the design point of view is given in Table 4.2.

Table 4.2. Classification of the loads for shield tunneling [24]

| | |
|------------------------|---|
| Primary Loads | <ol style="list-style-type: none"> 1. Ground Pressure 2. Water Pressure 3. Dead Load 4. Surcharge 5. Soil Reaction |
| Secondary Loads | <ol style="list-style-type: none"> 6. Internal Loads 7. Construction Loads 8. Effects of Earthquakes |
| Special Loads | <ol style="list-style-type: none"> 9. Effects of Adjacent Tunnels 10. Effects of Working in the Vicinity 11. Effects of Ground Subsidence 12. Other Loads |

Primary loads are the basic loads that should always be considered in the design of linings. Secondary loads are the loads acting during construction or after completion of the tunnel. These loads should be taken into account according to the objective, the conditions of construction, and location of the tunnel. On the other hand, the special loads are the loads specifically considered according to the conditions of the ground and the tunnel usage.

The notations used for the structural calculation of lining are defined as follows: bending moment (M), axial force (N), and shear force (Q) (for member forces, the directions indicated in Figure 4.2 are assumed to be positive).



Figure 4.2. Notations of bending moment, axial force, and shear force

4.2.1. Primary Loads

a) Earth Pressure: A section of tunnel and surrounding ground are shown in Figure 4.3. The ground pressure should be calculated in accordance with suitable analysis. For instance, the ground pressure should act radially on the lining or be divided into the vertical ground pressure and the horizontal ground pressure. Generally, the ground pressure is determined by dividing it into horizontal and vertical components in order to simplify the calculations [24].

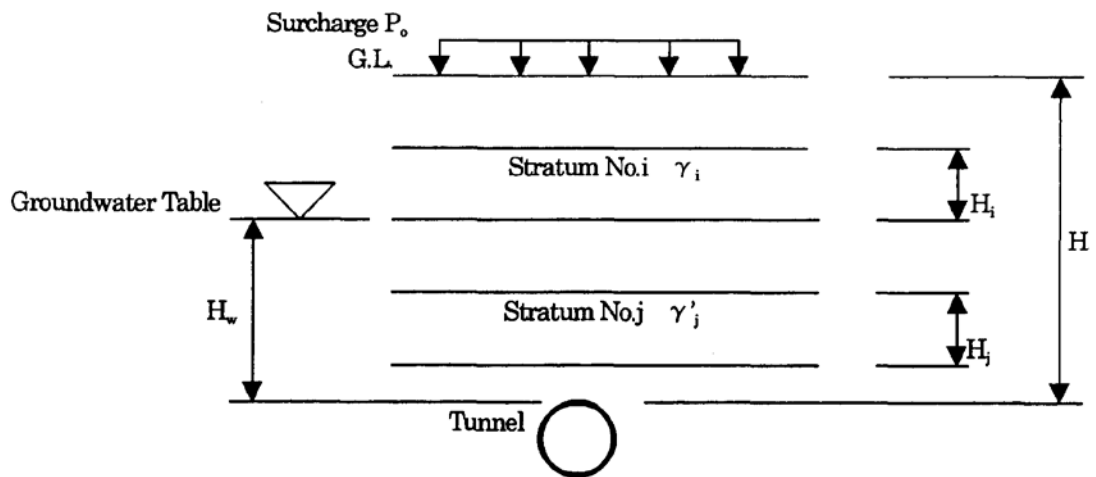


Figure 4.3. Section of tunnel and surrounding ground [23]

i) Vertical Earth Pressure: The vertical ground pressure at the tunnel crown should be a uniform load and should be equal to the overburden pressure as a rule if the designed tunnel is a shallow tunnel. In other words, it is preferable not to expect the effect of arch action at the soil for the tunnel of which overburden (H) is less than the width of loosened soil (B). However, if it is a deep tunnel, the effect of arch action occurs and reduced earth pressure can be adopted in accordance with Terzaghi's formula (4.2) and Protodiaconov's formula (4.3).

Soil

For shallow tunnels ($H < B$), ground pressure is equal to total overburden pressure and can be calculated in accordance with Equation 4.1. Regarding the unit weight of soil for the calculation of earth pressure, the wet unit weight should be used for soil above the groundwater table and submerged unit weight should be used for soil below the groundwater table.

$$P_{e1} = P_0 + \sum \gamma_i H_i + \sum \gamma'_i H_i \quad (4.1)$$

where, P_{e1} : Vertical earth pressure at tunnel crown
 P_0 : Surcharge
 γ_i : Unit weight of soil stratum No. i, which is located above the groundwater table
 H_i : Thickness of stratum No. i, which is located above the groundwater table
 γ_j : Unit weight of soil stratum No. j, which is located below the groundwater table
 H_j : Thickness of stratum No. j, which is located below the groundwater table

For deep tunnels ($H > B$), ground pressure is calculated as follows using Terzaghi's formula in accordance with AFTES – WG7 Appendix 1 [28].

$$P_{e1} = \frac{B \left(\gamma - \frac{2C}{B} \right)}{2 \tan \phi} \cdot \left(1 - e^{\frac{-2H}{\beta} \tan \phi} \right) \quad (4.2)$$

When $\phi = 0$, the above formula is rewritten as follows.

$$P_{e1} = H \left(\gamma - \frac{2C}{B} \right) \quad (4.3)$$

where, P_{e1} : Loosening ground load acting on the top of a ring (kN/m^2)
 B : Width of loosened soil at the top of a ring (m)
 G : Weight of soil per unit volume (kN/m^3)
 C : Cohesion of soil (kN/m^2)
 ϕ : Internal friction angle of soil (deg)
 H : Overburden depth (m)
 R : Mean tunnel radius (m)

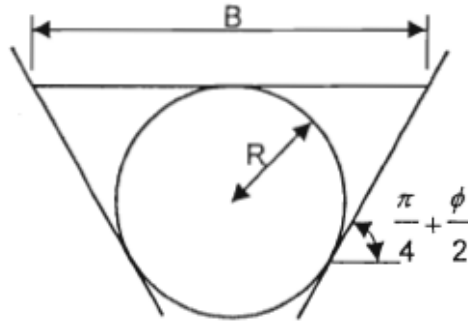


Figure 4.4. Calculation of loosening ground load

The width of loosened soil is calculated by the following equation.

$$B = 2R \cdot \tan\left(\frac{3\pi}{8} - \frac{\phi}{4}\right) \quad (4.4)$$

The minimum overburden thickness used to calculate the section force of a segment is treated as follows:

| | |
|----------------|----------------------|
| $H < B$ | Whole Overburden |
| $B < H < 2.5B$ | Minimum Overburden B |
| $H > 2.5B$ | Minimum Overburden B |

Rock

For tunnels to be bored in rock, the ground pressure is calculated by Protodiakonov's formula in accordance with AFTES-WG7 Appendix 1 [28].

$$P_{e1} = \frac{B}{0.10\sigma'} \quad (4.5)$$

where, B : Width of ground between slip planes, level with crown
 σ' : Uniaxial compressive strength

ii) Horizontal Earth Pressure: The horizontal ground pressure should be the uniformly varying load acting on the centroid of lining from the crown to bottom. Its magnitude is determined as the vertical load pressure multiplied by the coefficient of lateral earth pressure.

Soil

For tunnels to be bored in soil, the horizontal ground pressure is calculated by the following equations, in accordance with AFTES-WG7 Appendix 1 [28].

$$q_e = \lambda \cdot P_e \quad (4.6)$$

$$\lambda = 1 - \sin \phi \quad (4.7)$$

where,

- q_e : Horizontal ground pressure
- P_e : Vertical ground pressure
- λ : Coefficient of lateral ground pressure
- ϕ : Internal friction angle of soil

Rock

The horizontal ground pressure acting on a tunnel section surrounded by rock is calculated by the following equations, in accordance with AFTES-WG7 Appendix 1 [28].

$$q_e = \lambda \cdot P_e \quad (4.8)$$

$$\lambda = \frac{\nu}{1 - \nu} \quad (4.9)$$

where,

- q_e : Horizontal ground pressure
- P_e : Vertical ground pressure
- λ : Coefficient of lateral ground pressure
- ν : Poisson's ratio

Vertical and horizontal ground pressures are illustrated in Figure 4.5.

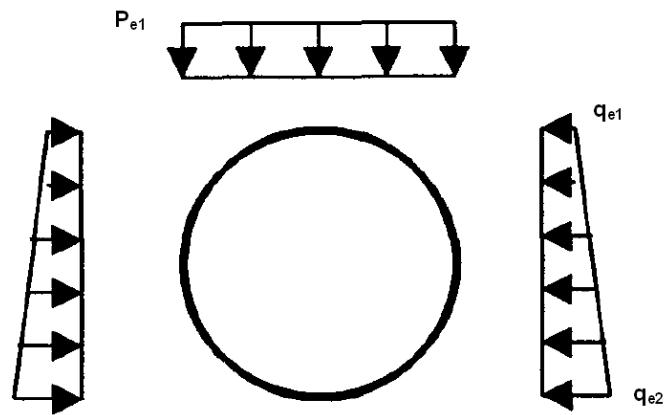


Figure 4.5. Ground pressures acting on lining

b) Water Pressure: The water pressure acting on the lining should be the hydrostatic pressure (see Figure 4.6). The resultant water pressure acting on the lining is the buoyancy. The hydrostatic pressure in the ground is usually calculated along the mean fiber of the lining in the radial direction. The magnitude of water pressure is proportional to the depth measured from the tunnel crown.

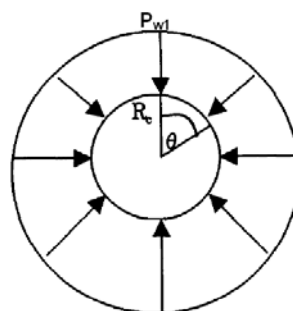


Figure 4.6. Hydrostatic pressure

$$P_w = P_{w1} + \gamma_w \cdot R_c (1 - \cos \theta) \quad (4.10)$$

$$P_{w1} = \gamma_w \cdot H_w \quad (4.11)$$

where,

- P_w : Water pressure
- P_{w1} : Water pressure at tunnel crown
- γ_w : Unit weight of water
- R_c : Radius of a circle of the centroidal line of segments
- θ : Angle from tunnel crown (clockwise)
- H_w : Depth of water at tunnel crown

c) Dead Load: The dead weight of the segments per unit length is calculated as a vertical load distributed along the centroid of the lining. It is calculated in accordance with Equation 4.9.

$$g_1 = \frac{W_1}{2\pi \cdot R_c} \quad (4.12)$$

where,

- g_1 : Dead weight of the segments per unit length
- W_1 : Weight of one ring of segments
- R_c : Radius of a circle of the centroidal line of segments

d) Surcharge: The effect of surcharge acting on the tunnel is determined by taking into consideration the distribution of the stress in the ground. It increases earth pressure acting on the lining. The following loads are considered as surcharge in design:

- Road traffic load
- Railway traffic load
- Weight of buildings
- All future expected loads

e) Soil Reaction: Among all the loads acting on the lining, soil reaction is the generic name of the design ground reaction, which is distinguished from the imposed loads determined independently. Considerations on soil reactions are different depending on the design calculation method employed [24].

In the usual calculation method, the vertical soil reaction caused by the imposed loads is irrelevant to the ground deformation and it is the uniform reaction equilibrating to these imposed loads. On the other hand, horizontal soil reaction acting on the tunnel can be defined as the generated reaction by the displacement of the lining towards the ground and it has a triangular distribution with the peak intensity at the spring line spreading within the range of the central angle of $\pm 45^\circ$ from the spring line.

Contrary to usual calculation method, soil reaction is the uniform reaction balancing the vertical ground pressure at the bottom of the tunnel in BSMs. Especially, in case of large diameter tunnels, the dead weight of segments can be taken into consideration in BSMs.

4.2.2. Secondary Loads

a) Internal Loads: The internal load is a load which acts inside the lining after completing the tunnel and is determined according to the actual condition. The railway vehicle load acting on the bottom of the lining is considered as internal load. In addition, internal water pressure should be taken into consideration in conveyance tunnels as an internal load [23].

b) Construction Loads: The design of segments takes into consideration the construction conditions and following loads [24].

i) Thrust Force of Jacks: The thrust force of jacks is a temporary load that is applied to the segment rings when advancing the shield machine. It is

the most influential force among the loads acting on the segments during construction.

ii) Backfill Grouting Pressure: Where backfill grout is injected in a well-controlled manner, the exterior surface of the segment ring is subjected to a force similar to fluid pressure. The backfill grout pressure acting on the segments varies depending on the grouting method and the grout conditions. In actual construction, the segments can be subjected to locally large pressures. Therefore, it is necessary to consider these pressures in the design. In normal cases, it is acceptable to use the value 100 kN/m^2 for grouting pressure.

iii) Load from Erector Operation: The load from erector operation is one of the loads acting on the segments. The load from erector operation is taken into account when designing the segment hangers and when evaluating the effect of load on the segments during their erection.

iv) Superimposing: The superimposing load is the other one under the condition where segments are superimposed during their storage and transportation. The impact during storage and transportation is taken into consideration by multiplying the load by the impact coefficient.

v) Other Loads: In addition to loads mentioned above, other construction loads such as dead weight of the trailing gear, jack load of the tunnel shape retainer, the cutter rotation force, and the loads being determined by the shield type, etc. are considered if needed.

c) Effects of Earthquakes: If the tunnel is driven through relatively uniform soils and has a large overburden, the effects of earthquakes are considered to be small since the tunnel behaves in a way similar to that of the surrounding soils. However, if the tunnel is subjected to any of the following

conditions, it could be greatly affected by the behavior of the surrounding soils, and the effects of earthquakes are determined by considering the dynamic interaction between the tunnels and surrounding soil [24]:

- When the lining structure changes suddenly.
- When the tunnel is in soft ground.
- When the ground conditions such as geology, overburden and bedrock depth change suddenly.
- When the alignment includes sharp curves.
- When the tunnel is in loose saturated sand and there is a possibility of liquefaction.

4.2.3. Special Loads

a) Effects of Adjacent Tunnels: Where two or more tunnels are constructed near each other, the preceding tunnel could be affected by the succeeding tunnel and their interaction creates earth pressures and soil reactions different from those cases where only one tunnel is driven. Moreover, such an interaction could cause long-term adverse effects on the tunnels.

Where two tunnels are driven near each other, the succeeding tunnel is bored through soils supporting the soil mass above the preceding tunnel. This redistributes the stresses in the ground and increases the vertical pressure acting on the preceding tunnel. The vertical pressure acting on the succeeding tunnel is smaller than that acting on the preceding tunnel and differs from the vertical pressure acting on a single tunnel when no other tunnel is near by.

It is necessary to perform analyses by properly modeling the ground conditions and by taking into consideration such factors as the relative location of the tunnels, and their outer diameters and conditions during

construction in order to develop a design method that can perfectly solve this type of problems [24].

b) Effects of Working in the Vicinity: When it is anticipated that other structures are to be constructed in close proximity during or after a shield tunneling, an assessment should be made if any bad effect may exert.

If any of the following four conditions exists, there should be made an appropriate evaluation of loads with considering a rational calculation method. Moreover, when evaluating a secondary lining as a structural member for future load fluctuation, an appropriate model for structural calculation should be considered [24].

- When a new structure is constructed directly above or is excavated resulting in a great change in the surcharge.
- When the soil directly above or below a tunnel is excavated resulting in a great change in the condition of vertical or horizontal earth pressure and ground characteristics such as the coefficient of soil reaction.
- When the ground at the side of the tunnel is disturbed resulting in a great change in the lateral or resistance earth pressure.
- When there is a great change in the water pressure working on the tunnel.

c) Effects of Ground Subsidence: When constructing a tunnel in soft ground, attention should be paid to how the soil characteristics affect ground settlement apart from those caused by the tunnel construction process. It is necessary to consider the effects of ground settlement on the tunnel and the joints between the tunnel and the shaft. The effects of ground settlement on the tunnel can be studied in two ways:

- Study of the effect of consolidation settlement on the tunnel in the transverse direction.
- Study of the effect of unequal settlement on the tunnel in the longitudinal direction.

Moreover, relative displacement tends to occur at the joint between the tunnel and the shafts because different types of structures are connected at these positions. Therefore, it is desirable to prevent stress concentrations by applying the flexible joints where necessary or to reduce the effect of relative settlement by making the foundation of the shaft a floating foundation [24].

d) Other Loads: Apart from abovementioned special loads, specific cases such as fire, explosion, train derailment, and temperature changes, etc. can be considered depending on the conditions of the tunnel project.

4.3. Structural Calculation Procedure

In order to perform structural calculations for design, the first four steps of design procedure given in Chapter 4.1.3 should be implemented. In other words, specifications and codes to be used, inner dimensions of tunnel, load and lining conditions should be decided before this stage.

4.3.1. Critical Sections

After determining the lining and loading conditions, the design calculation of the tunnel cross-section should be done for the following critical sections.

- Section with deepest and shallowest overburden
- Section with highest and lowest ground water table
- Section in the case of rapid change in the ground
- Section with large surcharge
- Section with eccentric loads

- Section with unlevel surface
- Section with adjacent tunnel at present or to be done in future

4.3.2. Computation of Member Forces

For the design of segmental lining sections, member forces (M, N, S) can be calculated by using several structural models. Structural analysis methods used to determine member forces are determined in Chapter 3 in detail. All of these methods have strengths and weaknesses. For that reason, proper analysis method may change depending on the conditions of the project.

Among the structural analysis methods expressed in Chapter 2, beam-spring method that simulates the interaction between the lining and surrounding ground realistically is the most widely used method due to its effectiveness. In spite of being a simple and limited method type, analytical methods, i.e. elastic equation method, are also utilized in order to compare and evaluate the results obtained by more sophisticated methods. Accordingly, the evaluation of elastic equation method and beam-spring methods is implemented in Chapter 5.

4.3.3. Safety of Section

After the calculation of member forces with a selected analysis method, the safety of critical sections should be checked using the limit state design method or the allowable stress design method. Sections to be checked are as follows [23]:

- Section with maximum moment
- Section with maximum axial force
- Section with maximum shear force

4.3.4. Limit State Design Method

The interaction diagram as shown in Figure 4.7 describes the relationship between the design axial capacity and the design flexural capacity of member cross-sections subjected to axial load and flexural moment. If the point (M_d, N_d) is located inside the (M_{ud}, N'_{ud}) curve at the side of the origin, the section is safe against the design loads according to limit state design method.

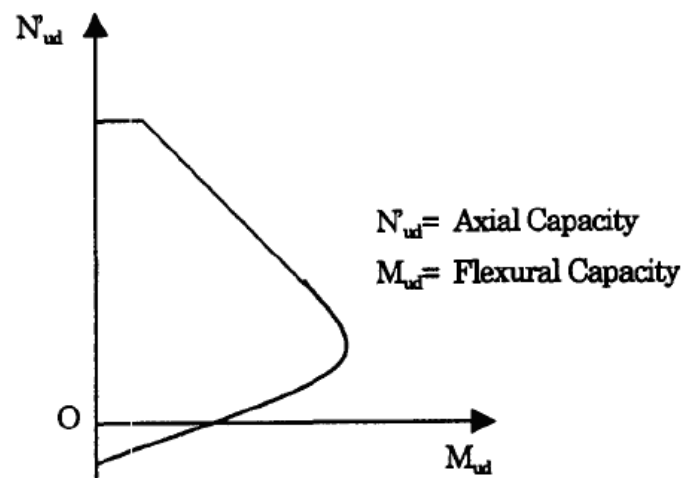


Figure 4.7. Interaction diagram [23]

4.3.5. Allowable Stress Design Method

If the extreme fiber stress of concrete and the stress of reinforcement are less than their allowable stresses, the section is safe against the design loads according to allowable stress design method (see (4.13) and (4.14)).

$$\sigma_c \leq \sigma_{ca} = f_{ck} / F_c \quad (4.13)$$

$$\sigma_s \leq \sigma_{sa} = f_{yd} / F_s \quad (4.14)$$

where,

- σ_c : Extreme fiber stress of concrete
- σ_{ca} : Allowable stress of concrete
- f_{ck} : Characteristic compressive strength of concrete
- F_c : Safety factor of concrete
- σ_s : Stress of reinforcement
- σ_{sa} : Allowable stress of steel
- f_{yd} : Yield stress of steel
- F_s : Safety factor of steel

4.3.6. Safety of Joints

The flexural rigidity of segmental lining at the joint is smaller than the flexural rigidity of the segment. Also, if the segments are staggered, the moment at the joint is smaller than the moment of the adjacent segment. The actual effect of the joint should be evaluated in the design. Accordingly, the safety of joints can be checked by the same method with sections as determined in Chapter 4.3.3 by considering the effect mentioned above.

CHAPTER 5

METHODS OF ANALYSES

There are several analysis methods recommended for the design of TBM segmental linings as described in Chapter 3. Each method has its typical assumptions and approaches differently. For that reason, it is necessary to compare these methods for certain situations in order to determine the efficiencies of each method. In this chapter, selected analytical and numerical methods are implemented for a typical railway tunnel, and the sensitivities of methods are compared under certain situations.

For the evaluation, elastic equation method and Beam – Spring Method are carried out as analytical and numerical methods, respectively. As described in Chapter 3, elastic equation method based on simple assumptions is a practical way for the analysis of circular tunnels. Besides, Beam – Spring Method is the most widely used numerical method that is able to simulate the structural behavior of segmental rings. Also, there exist many different approaches for 2D and 3D BSMs. In this chapter, various structural models including elastic equation method, 2D and 3D BSMs with different approaches are employed for a rational comparison.

Literature review of TBM segmental lining analysis methods provided along with recent published studies shows that 3D BSM gives reasonable results compatible with finite element models, laboratory tests, and on-site measurements. This study investigates the sensitivity of elastic equation method and 2D BSMs by comparing 3D BSM. As a result of this comparison,

the applicability of methods is introduced. Also, the effects of mesh coarseness, shear stiffness between the ring connections, arrangement of key segments, rapid change in surcharge, and sharp alteration in soil stiffness are investigated and the competence of 2D and 3D models for these effects is indicated. The situations described above are examined in terms of the changes in the forces, moments, and deflections of the lining.

A multipurpose structural analysis and design software, “LARSA 4D”, has been utilized in order to carry out beam – spring analyses. Structural applications require advanced models for the simulation of the non-linear, time-dependent, and inelastic behavior of structural elements. The LARSA 4D is equipped with special features to deal with the numerous aspects of complex structural elements. Moreover, it has functional modeling tools including meshing, generation, templates, and advanced drawing and it is especially suitable for BSM analyses, because it has specific elements such as non-tension ground springs for ground – tunnel interaction, two-node spring elements for ring joints, one-node rotational spring elements for segment joints, member end releases for simulating segments connected with hinges, and etc.

5.1. The Geometry of the Problem

The tunnel cross-section and geometry of the problem are given in Figure 5.1 and Figure 5.2, respectively. As it is shown in Figure 5.1, the typical TBM segmental ring having a circular shape consists of four ordinary segments (A1, A2, A3, and A4), two counter segments (B1 and B2), and one key segment (K1). Key segment is located at 43.2° from the crown and has a degree of 14.4° which is the quadrant of the other segments. The thickness and width of the linings are estimated as 320 mm and 1500 mm respectively according to the ranges summarized in Table 2.2. The outer and inner diameters of the ring are 7680 mm and 7040 mm, respectively. Also, 25 cam-and-pocket type ring joints regularly located are shown in the Figure 5.1.

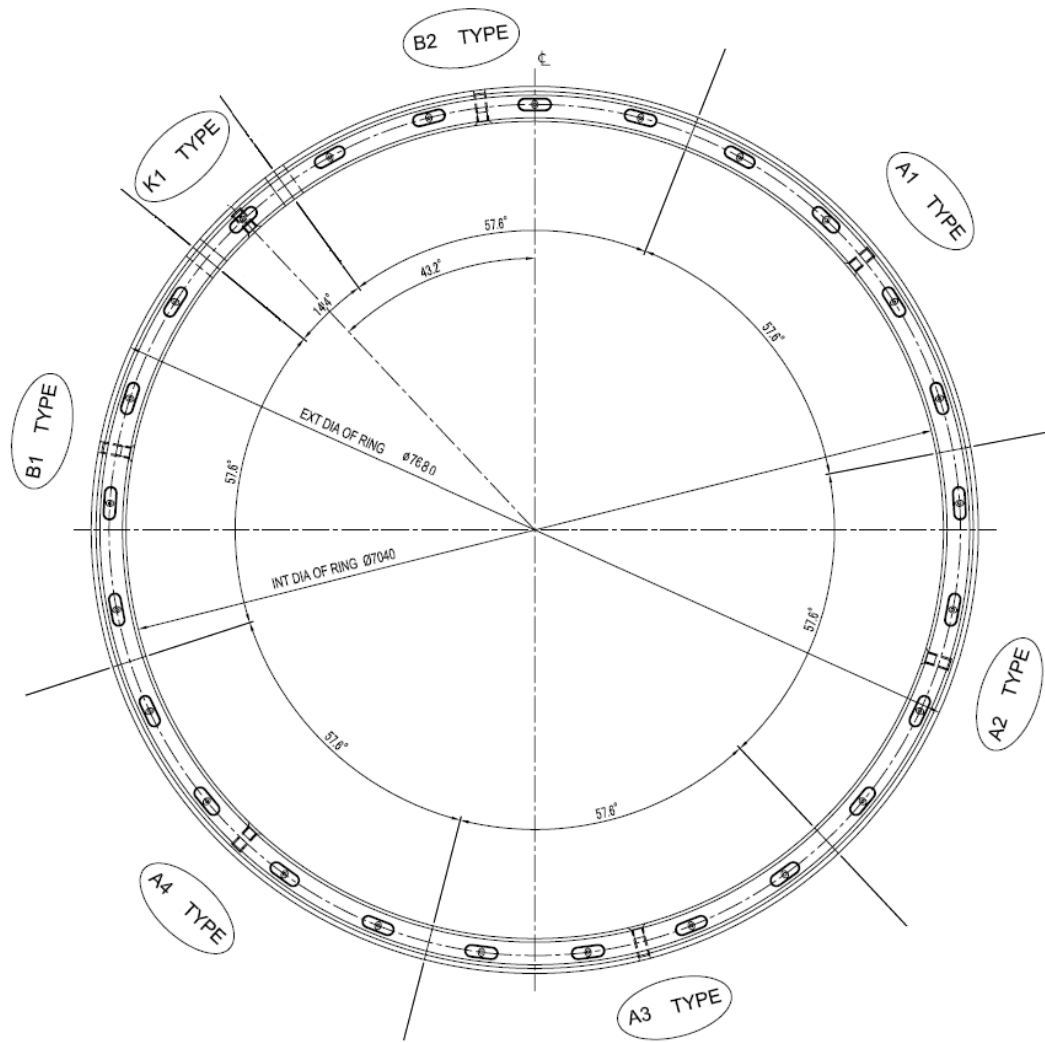


Figure 5.1. Tunnel cross-section

General properties of ring used in the analyses are summarized as follows:

| | |
|------------------------|-------------------------------|
| Type of tunnel | : TBM Tunnel |
| Type of segment | : Reinforced concrete segment |
| Type of segment joint | : Flat type joints |
| Type of ring joint | : Cam-and-pocket |
| Outer diameter of ring | : 7680 mm |

Inner diameter of ring : 7040 mm
 Width of segment : 1500 mm
 Thickness of segment : 320 mm
 Partitions : 4 ordinary + 2 counter + K segment
 Type of key segment : Axially inserted type

The excavation and loading geometries of the problem are in a range which is common in civil engineering practice. The cover depth of the tunnel is 15402 mm as shown in Figure 5.2. Also, the groundwater level is situated 5994 mm above the tunnel crown.

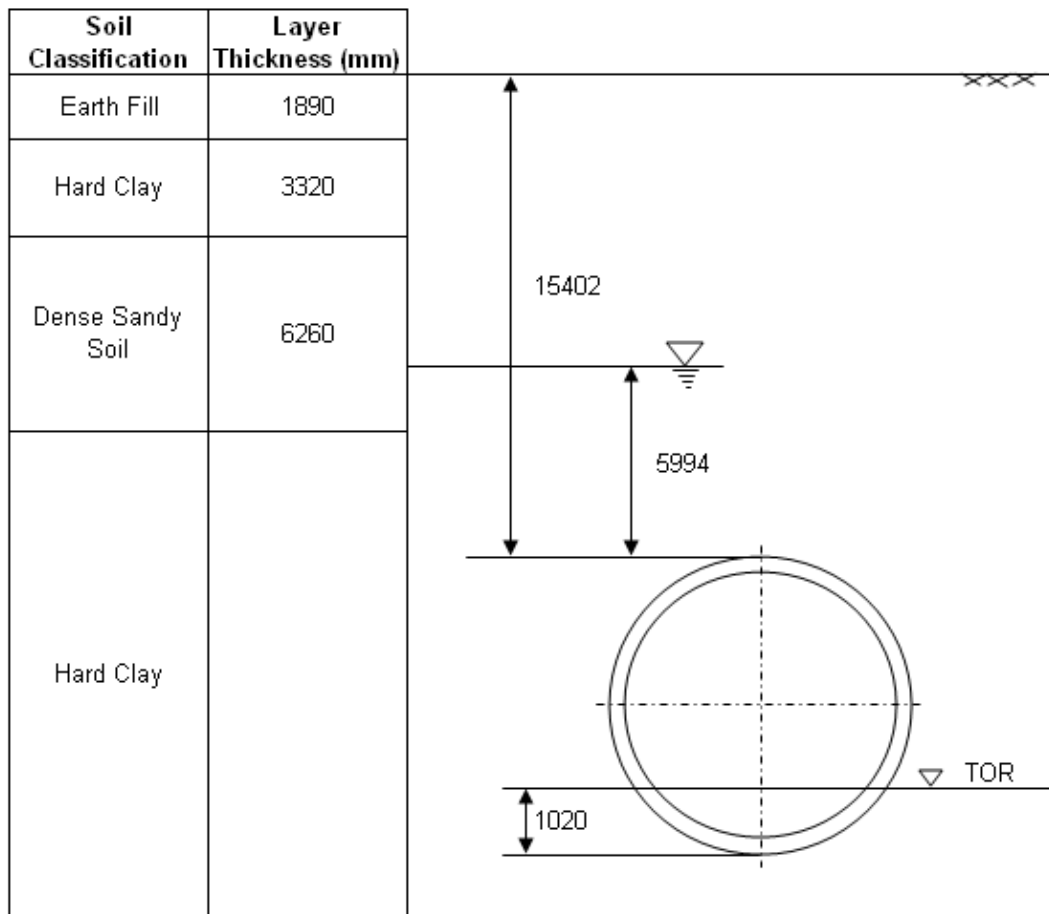


Figure 5.2. Geometry of the problem (not to scale)

5.2. Geotechnical and Material Parameters

The tunnel is surrounded by relatively hard clay. Also, earth fill, hard clay, and dense sandy soil layers exist above the tunnel. Geotechnical properties of these layers are given in Table 5.1.

Table 5.1. Geotechnical parameters of the soil layers

| Parameters | Earth Fill | Hard Clay | Dense Sandy Soil |
|---|------------|-----------|------------------|
| Average SPT N Value | 8 | 29 | 33 |
| Saturated Unit Weight (kN/m ³) | 19 | 19 | 20 |
| Internal Friction Angle (°) | 27 | - | 40 |
| Cohesion (kN/m ²) | - | 170 | - |
| Poisson's Ratio | 0.35 | 0.40 | 0.40 |
| Modulus of Elasticity (kN/m ²) | 22400 | 81200 | 92400 |

Mechanical properties of precast reinforced concrete segments and steel reinforcement bars used as supporting elements are listed below:

| | | | |
|---|------------|--------|--------------------|
| Compressive strength of concrete: | f_{ck} | = 50 | N/mm ² |
| Tensile strength of concrete: | f_{ct} | = 4.1 | N/mm ² |
| Modulus of elasticity of concrete: | E_c | = 37 | kN/mm ² |
| Poisson's ratio of concrete: | ν | = 0.20 | |
| Unit weight of concrete: | γ_c | = 26 | kN/m ³ |
| Yield strength of steel reinforcement bars: | f_y | = 420 | N/mm ² |
| Modulus of elasticity of steel: | E_s | = 200 | kN/mm ² |

5.3. Analytical Analysis with Elastic Equation Method

As an analytical approach, elastic equation method is used to analyze the segmental lining in this study. As discussed in Chapter 3, this method is a practical and most widely used analytical tool for the analysis of segmental linings. Due to its limitations mentioned in Section 3.1.1, this method is not used for the final design calculations, but it might be quiet useful to get a first idea of the forces in the lining.

In order to calculate member forces with this method, working sheets are developed by using Microsoft Excel 2003 and Macro Visual Basic applications. Input sheet, load condition sheets, and member forces sheet are given in Appendix A (Figure A1-A4). Input sheet includes geometrical, material, and geotechnical properties of the problem. Calculations of loads and member forces are also provided in load conditions sheet and member forces sheet, respectively.

For the vertical earth pressure, the depth of tunnel is not adequate for arching action. Therefore, total overburden governs the vertical earth pressure. Calculations performed for other loads are also given in the Appendix A.

Member forces for any location on the ring can be obtained by this method. The sheet is generated to obtain the most critical member forces occurred on the ring. However, calculations to obtain member forces are performed for a segmental ring with unit width. Therefore, the results of this analysis are multiplied by 1.5 in order to obtain member forces for the segmental ring with a width of 1.5 m.

The evaluation and comparison of results obtained by elastic equation method and 2D and 3D Beam – Spring Methods are mentioned in the next chapter.

5.4. Numerical Analyses

In order to evaluate analysis methods, the tunnel section of which geometrical and material properties are described in the former chapters is analyzed by performing different approaches mentioned in the literature review. Before explaining the models one by one, it is necessary to determine common features for 2D and 3D models. The segmental ring is simulated by a series of beams and ground – lining interaction is represented by radial ground springs in all models. In this study, different mesh densities are used by dividing the segmental ring into 50, 150, and 250 beams in order to evaluate the effect of mesh densities on member forces. Typical 2D and 3D computer models divided into 50 pieces are illustrated in Figure 5.3 and Figure 5.4, respectively.

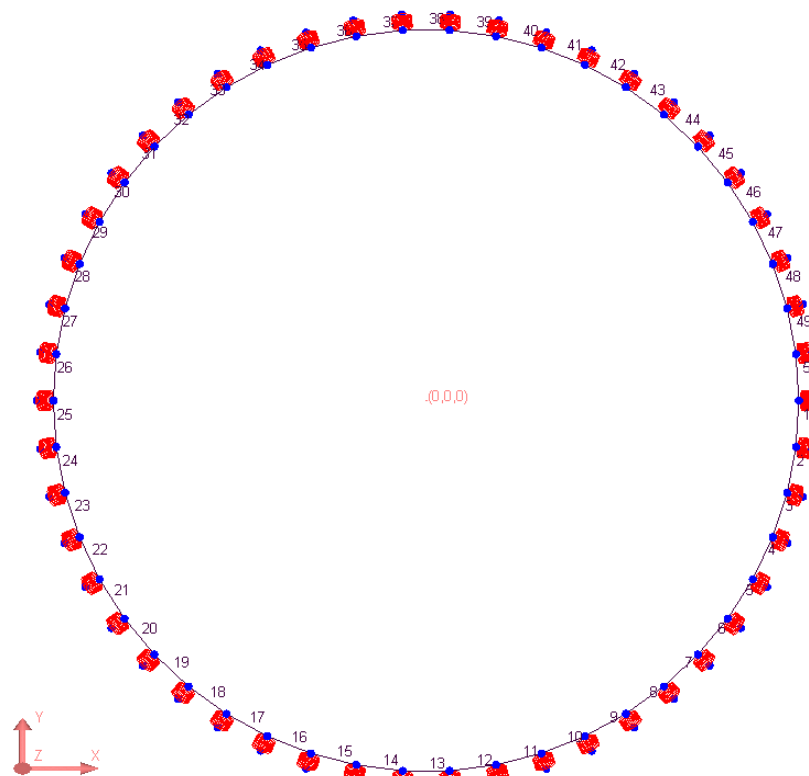


Figure 5.3. Typical 2D beam – spring model composed of 50 members

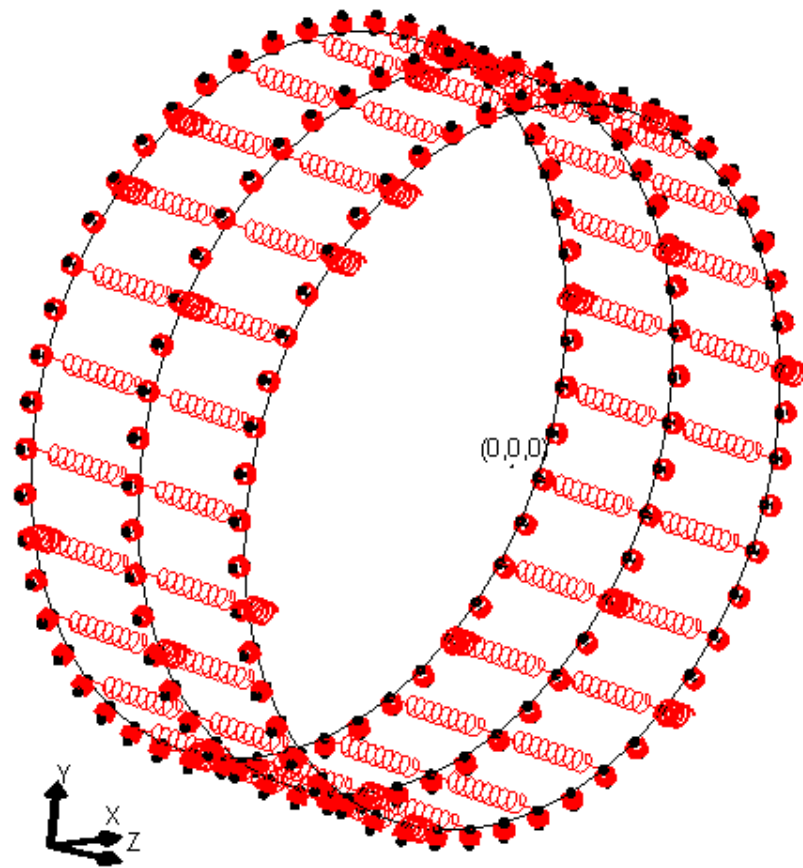


Figure 5.4. Typical 3D beam – spring model composed of 50 members

The ground-lining interaction is modeled as linear elastic springs of which constants are calculated by the equation proposed by Muir Wood, in accordance with AFTES – WG7 Appendix 1 [28]. It is assumed that ground reaction forces are activated when the tunnel expands outward, but they are not activated when the tunnel contracts inward. Therefore, non-tension (compression only) springs are used in the analysis. The graph showing the constants of non-tension ground springs for 3 different mesh densities is given in Figure 5.5. As shown in figure, ground springs are assumed to have a linear elastic behavior. Ground spring constants are obtained by multiplying coefficient of subgrade reaction with the tributary area of springs.

Ground springs are placed at each member joint in radial direction and so the number of ground springs is equal to the number of beam members. The ground behavior in tangential direction is generally ignored in BSMs. Although this leads to frictionless sliding of the lining against the ground, it has a negligible effect on member forces. For that reason, ground springs are only considered in radial direction.

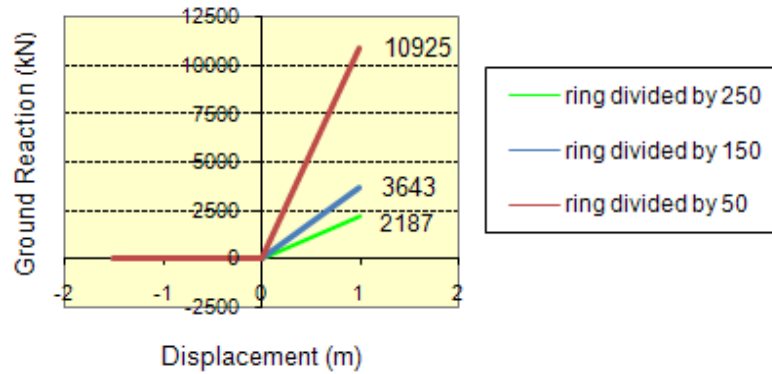


Figure 5.5. Ground spring constants

Contrary to elastic equation method, there is no need to multiply the results of computer models, because the calculations of computer models are done for a ring with a width of 1.5 m. Therefore, the cross-sectional area of lining (A) and moment of inertia of lining (I) per ring are calculated as follows:

$$A = 1.5 \times 0.32 = 0.48m^2 \text{ (segment width} = 1.5m, \text{thickness} = 0.32m)$$

$$I = \frac{1}{12} \times 1.5 \times 0.32^3 = 4.096 \cdot 10^{-3} m^4$$

Abovementioned features of sections to be analyzed constitute the input parameters of computer models. These input parameters of models with different mesh densities are listed in Table 5.2.

Table 5.2. General features of beam - spring models

| Features | Model with 50 beams | Model with 150 beams | Model with 250 beams |
|---|--------------------------------|---------------------------------|---------------------------------|
| # of Members | 50 | 150 | 250 |
| # of Ground Springs | 50 | 150 | 250 |
| # of Nodes | 100 | 300 | 500 |
| Length of Members (l_b) | 462mm | 154mm | 92.5mm |
| Radius of Ring (R_c) | 3,680mm | 3,680mm | 3,680mm |
| Width of Segments (w) | 1,500mm | 1,500mm | 1,500mm |
| Thickness of Segments (t) | 320mm | 320mm | 320mm |
| Moment of Inertia of Segments (I) | 4.096 E-03m ⁴ | 4.096 E-03m ⁴ | 4.096 E-03m ⁴ |
| Cross-sectional Area of Segments (A) | 0.48m ² | 0.48m ² | 0.48m ² |
| Modulus of Elasticity (E) | 81,200kN/m ² | 81,200kN/m ² | 81,200kN/m ² |
| Coefficient of Lateral Earth Pressure $\left(\lambda = \frac{\nu}{1-\nu}, \nu = 0.4 \right)$ | 0.67 | 0.67 | 0.67 |
| Coefficient of Subgrade Reaction $\left(k = \frac{E}{(1+\nu) \cdot R_c} \right)$ | 15,760kN/m ³ | 15,760kN/m ³ | 15,760kN/m ³ |
| Ground Spring Constant $\left(k_r = k \cdot l_b \cdot w \right)$ | 10,925kN/m | 3,643kN/m | 2,187kN/m |

5.4.1. 2D Structural Models

Theoretical approaches on BSMs have been discussed in Chapter 3. The important point in beam – spring method is the modeling of connections. Since 2D models are unable to simulate the ring joints, the difference between these 2D models is the modeling of segment joints. In this study, all 2D approaches mentioned in Chapter 3 are performed by computer models. Totally, four different 2D approaches are analyzed and evaluated and the descriptions of these models can be summarized as follows.

a) Model A (Rigid Ring): This is the simplest 2D model that assumes the ring having a uniform bending stiffness (EI). In other words, segment joints are assumed to be fully rigid connections. Due to this assumption, reduction of rigidity at the segment joints is ignored. In this model, the stiffness parameters (E and I) of segment section are also used for segment joints in order to obtain fully rigid ring.

b) Model B (Muir Wood): This model also assumes the ring having a uniform bending stiffness. However, a reduced bending stiffness is used in order to simulate the effect of segment joints. The reduction in the bending stiffness can be calculated according to several approaches mentioned in Chapter 3. In this study, the approach proposed by Muir Wood [27] is utilized. The effective moment of inertia can be calculated by using the following formula (Formula 3.3) which depends on the section at the force transmission zone and number of segments.

$$I_{eff} = I_j + \left(\frac{4}{n}\right)^2 \cdot I = \frac{1}{12} \cdot 1,5 \cdot 0,160^3 + \left(\frac{4}{6}\right)^2 \cdot 4.096 \cdot 10^{-3} = 2.332 \cdot 10^{-3} m^4$$

The stiffness of the lining section is reduced by using this effective moment of inertia for the entire section. Since the structure in this model is more flexible,

it gives lower sectional forces and bending moments. Therefore, this approach leads to more economical results for the design.

c) Model C (Multiple Hinges): In this model, segment joints are modeled as unfixed hinges. Figure 5.6 illustrates the configuration of segment joints at which the hinges are located. Not only the number of segment joints, but also the segment orientation is considered by means of these hinges. However, a ring with multiple hinged joints is an unstable structure. Therefore, the model may encounter convergence problems. In order to prevent convergence problems, 90 % of bending moments at segment joints is released and 10 % of moments occurred at the segment joints is kept. Normally, uniform bending stiffness is used in this method.

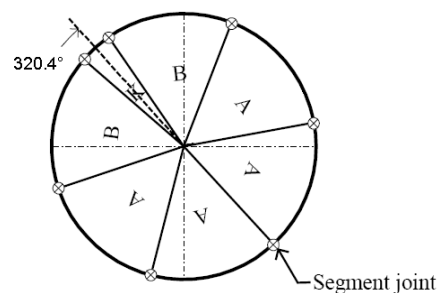


Figure 5.6. Configuration of segment joints in 2D models

d) Model D (Rotational Springs): This model simulates the segment joints as rotational springs. This enables the model to consider both the number and orientation of segments. The configuration of segment joints at which the rotational springs are located is shown in Figure 5.6. Linear and non-linear approaches are available for rotational spring constants. If only a linear rotational spring with the definition of a yielding moment is performed, the simulation of behavior of the joints seems to be too rough. In order to have

more sensitive simulation, the non-linear rotational spring approach is utilized in this model. Rotational spring constants are calculated according to following theoretical formulas (Formula 3.4, Formula 3.5) proposed by Janssen [34].

- I. A constant rotational stiffness until $M > N \cdot a / 6$:

$$k_{\theta} = b \cdot \frac{E \cdot a^2}{12} = 1,5 \cdot \frac{37 \cdot 10^6 \cdot 0,16^2}{12} = 118.400 \text{ kN.m/rad}$$

- II. The rotational stiffness is non-linear if bending moment exceeds the boundary bending moment, $M_{\text{bou}} < N \cdot a / 6$:

$$k_{\theta} = M / \alpha = \left(9 \cdot \frac{b \cdot a^2 \cdot E}{8} \right) \cdot m \cdot (1 - 2 \cdot m)^2, \quad m = \frac{M}{N \cdot a}$$

Considering the above indicated formulation, the relationship between the M/N ratio and joint rotational stiffness k_{θ} can be shown in the following figure.

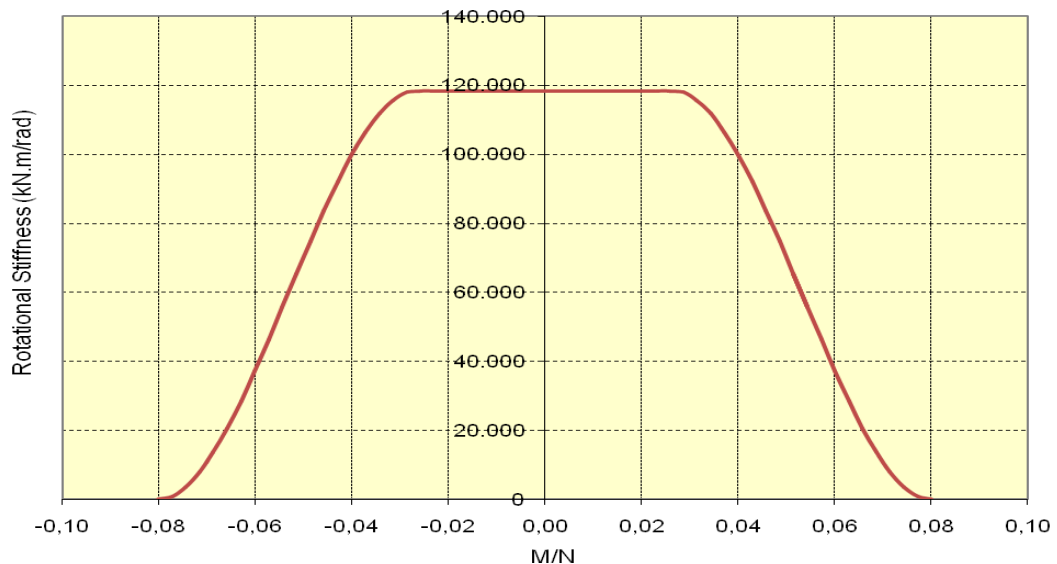


Figure 5.7. The relationship between the M/N ratio and joint rotational stiffness k_{θ} (for reference purpose only)

Janssen formulation allows taking into account the decrease in rotational joint stiffness due to the joint rotation. In order to do this, an iterative procedure has been carried out on the basis of the results of Larsa4D computation. Several iterations have been carried out to match the actual joint rotational stiffness (rigidity) which is the input parameter of the Larsa4D program with the M/N ratio calculated from formulation. Different joint stiffness and behavior have been considered depending from the applied moment, and axial force for each rotational spring.

In detail, each iteration has been carried out as follows:

- A tentative joint rotational rigidity (*118.400 kN.m/rad*) has been taken as input value in BSMS for each joint.
- The numerical model has been run and the maximum M/N value computed at the joints has been plotted on the chart given in Figure 5.7.

If the value corresponding to the input rigidity and the resulting M/N ratio does not correspond to a valid point on the Janssen curve, the steps indicated above are repeated. After the first iteration, bending moment and axial force acting on the joints are used as an input for Janssen computation and a new rotational stiffness is calculated for each joint. This procedure is performed until the match is found.

The example of iteration process carried out to match the input rigidity with the output M/N ratio is given in Figure 5.8. Red dots indicate the results of last (n^{th}) iteration that fully match with the Janssen curve. As shown from figure, some of green dots that indicate the $(n-1)^{\text{th}}$ iteration results do not fit on the Janssen curve and one more iteration is needed. Figure 5.8 also shows the range $-a/6 < M/N < a/6$ where rotational stiffness is constant. As

the absolute value of M/N out of this range increases, the rotational stiffness of the joint decreases and this leads to increase in rotational deformation.

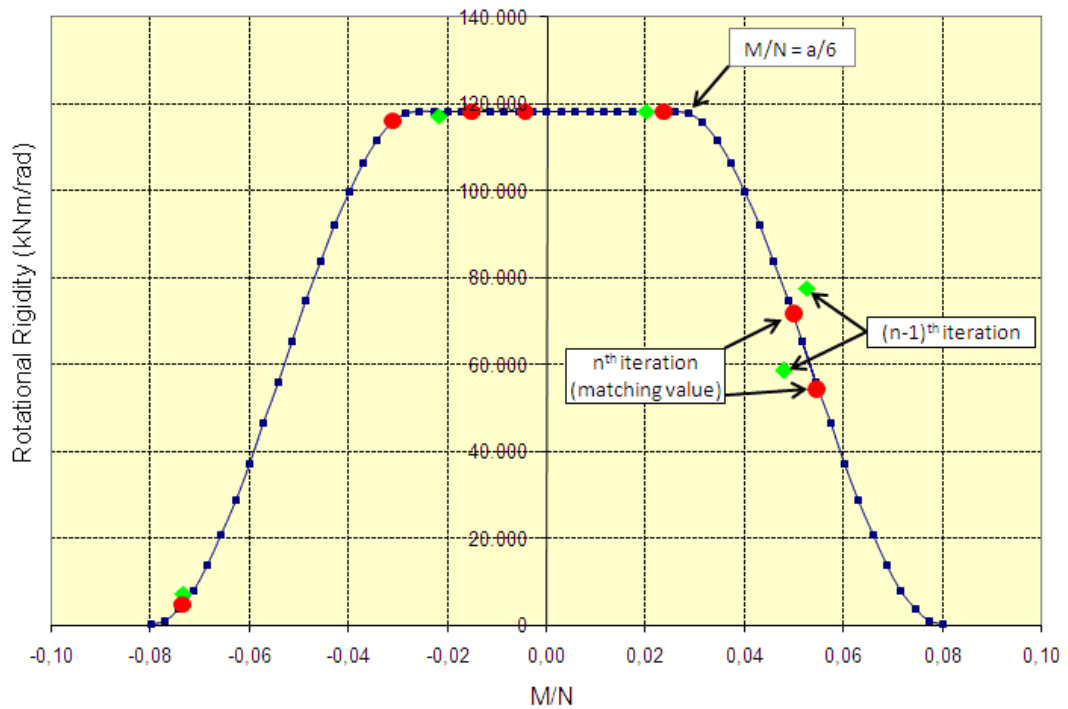


Figure 5.8. The iteration process for the computation of joint rotational stiffness

Iteration processes of all rotational springs used in 2D and 3D BSMs are enclosed in Appendix B.

5.4.2. 3D Structural Model

3D BSMs are able to simulate the segment and ring joints for sequential rings. In this study, 3D BSM proposed by Koyama [38] is performed. Model VI described in Section 3.2 is used as a reference in order to constitute the 3D model.

The configuration of 3D BSM for three adjacent rings is shown in Figure 5.4. It consists of several beams forming the segments, rotational springs between the segment joints, shear springs between the adjacent rings, and ground springs representing the ground – lining interaction. The modeling of rotational and ground springs is the same with 2D models. Therefore, Figure 5.5 and Figure 5.7 that show the ground and rotational spring constants respectively are also valid for this model.

The major difference of this 3D model from 2D models is the shear springs at ring joints that enable 3D models to simulate interaction between adjacent rings. Furthermore, 3D models are able to represent the staggered geometry of sequential rings. In order to represent the staggered geometry, three sequential rings are modeled and connected to each other by shear springs. The configuration and staggered geometry of segment joints are illustrated in Figure 5.9.

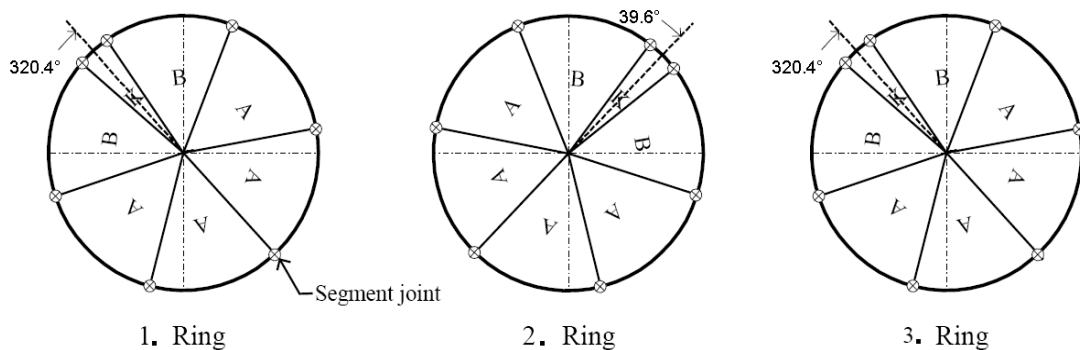


Figure 5.9. Configuration of segment joints in 3D models

The shear springs are located at each ring joint which is distributed around the ring uniformly. The configuration of 25 ring joints can be seen in Figure 5.1. As discussed in Section 3.2, the calculation for a shear spring constant is

a complex issue, and there is no general formula available in the literature for determining the shear spring constant. In this study, the shear spring constant is assumed to be 20.000 kN/m in radial direction. This is a reasonable value for a segmental ring with segment thickness of 320 mm and shear strip width of 50 mm. Since a shear strip is placed on both end of each segment, the shear spring constant between two adjacent rings is calculated as follows:

$$k_s = 20.000 \times 2 = 40.000 \text{ kN} / \text{m}$$

The shear spring constant is selected by considering comparable studies performed by BSMs. The graph showing the shear spring constant used in 3D models is given in Figure 5.10.

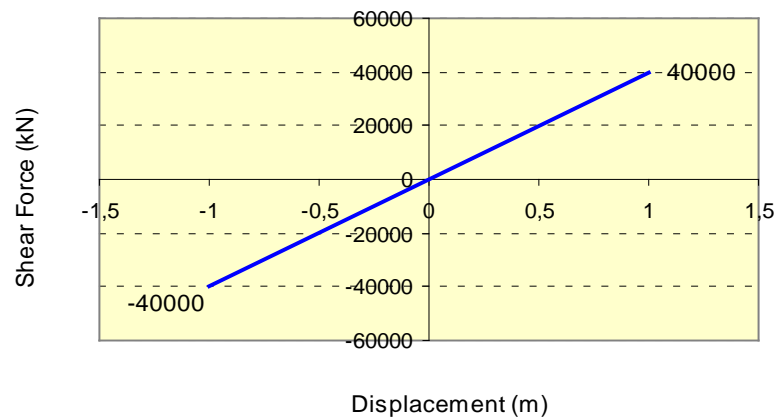


Figure 5.10. Shear spring constant

5.5. Loading Conditions

Loading conditions for a tunnel differ from others depending on soil profile, soil and material properties, longitudinal profile of the route, geometry, type and usage area of tunnel, and etc. In this study, primary load cases are

analyzed to investigate different analysis methods. As primary load cases, vertical earth pressure, horizontal earth pressure, water pressure, dead weight, soil reaction, and effect of surcharge are taken into consideration in the analyses. The calculation of these load cases are comprehensively expressed in Section 4.2. Calculations are made according to these expressions and summary of load conditions is given in Table 5.3.

Table 5.3. Summary of load conditions

| Load Conditions | Abbreviation | Units | Values |
|---|-----------------|-------|--------|
| Overburden | H | m | 15.50 |
| Groundwater level | H _w | m | 5.99 |
| Vertical earth pressure | P _{vc} | kN/m | 358.44 |
| Lateral earth pressure at tunnel crown | q _{e1} | kN/m | 240.15 |
| Lateral earth pressure at tunnel bottom | q _{e2} | kN/m | 306.64 |
| Water pressure at tunnel crown | P _{w1} | kN/m | 89.91 |
| Water pressure at spring line | P _{ws} | kN/m | 144.96 |
| Water pressure at tunnel bottom | P _{w2} | kN/m | 200.16 |
| Soil reaction | P _r | kN/m | 370.92 |
| Dead weight | g | kN/m | 12.48 |
| Coefficient of lateral earth pressure | λ | - | 0.67 |

* The values given in the table are loads acting on one ring (longitudinal length: 1.5m).

* The earth pressure includes surcharge.

* The overburden and groundwater level are measured from the centroid of the segment.

Load combination used in the analyses is selected by considering serviceability limit state (SLS). Basic load combination for SLS proposed by AFTES [43] is given in Table 5.4.

Table 5.4. Combination of loads

| Loads | Basic Load Combination (SLS) |
|------------------------|------------------------------|
| Vertical Ground Load | 1.0 |
| Horizontal Ground Load | 1.0 |
| Hydrostatic Loads | 1.0 |
| Dead Load | 1.0 |
| Surcharge | 1.0 |
| Soil Reaction | 1.0 |

5.6. Flowchart of Calculation

Analysis of TBM segmental linings is investigated both with analytical and numerical methods. Also, variations in input parameters and conditions of the problem are examined in order to evaluate 2D and 3D BSMs.

The studies carried out for the given tunnel cross-section can be summarized as follows:

CASE 1: The analyses of given tunnel section are performed by using analytical (elastic equation method) and numerical (2D and 3D BSMs) methods of which definitions are previously given. The comparison of

analysis methods is carried out by evaluating the results of models performed.

Firstly, 2D analytical and numerical methods are compared between each other. Then, results obtained from 2D analytical and numerical methods are compared together with 3D BSM. By means of this comparison; the sensitivities of analysis methods are assessed.

CASE 2: Comparison of 2D and 3D BSMs is also carried out for the tunnels passing through a transition zone having relatively different soil stiffness. Tunnel with a length of 9 m is modeled by 6 sequential rings. It is assumed that there is a sharp transition from stiff soil to soft soil in the middle of the model. Soil profile of the tunnel route is given in Figure 5.11.

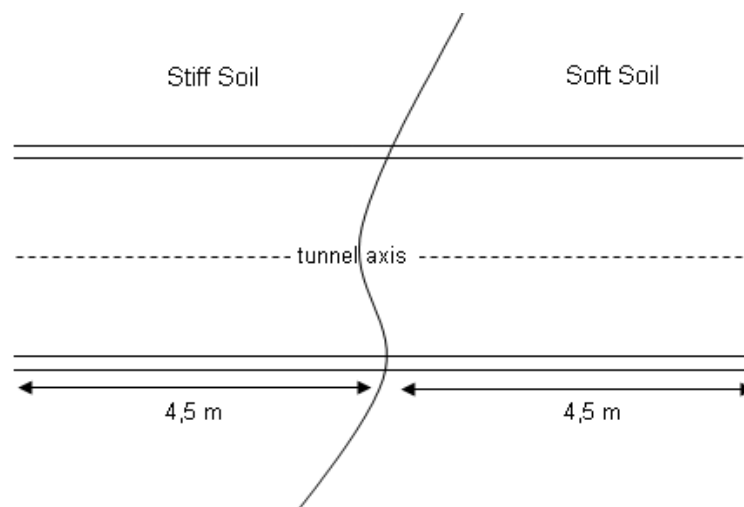


Figure 5.11. Soil profile of the tunnel route

Three different transition zones having different soil stiffness are selected for the evaluation. The moduli of elasticity of stiff and soft soils in these transition zones to be analyzed are given in Table 5.5. Difference in soil stiffness is

directly proportion to subgrade reactions in the analysis models. Except for soil stiffness, all other conditions of the problem are the same with the first model of which load conditions are given in Table 5.3.

Table 5.5. Soil stiffness for transition zones

| Transition Zone | Stiff Soil Stiffness (kN/m ²) | Soft Soil Stiffness) (kN/m ²) |
|-----------------|---|---|
| I | 80000 | 40000 |
| II | 80000 | 20000 |
| III | 80000 | 10000 |

The rotational spring constant calculated by the Formula 3.5 shows nonlinearity and changes according to the M/N ratio. For that reason, the calculation for rotational springs requires an iteration process. Since six sequential rings having totally 42 rotational springs are considered in this case, it is a difficult and long process to execute this iteration process for rotational spring constants. Therefore, in order to simplify the calculation for Case 2, rotational spring constants are modeled in three stages as shown in Figure 5.12. As a result, rotational spring constants for Case 2 are taken as follows:

- for $IM/NI < 0.035$, $k_{\theta} = 110000$ kN.m/rad
- for $0.035 < IM/NI < 0.055$, $k_{\theta} = 55000$ kN.m/rad
- for $0.55 < IM/NI$, $k_{\theta} = 0$ kN.m/rad

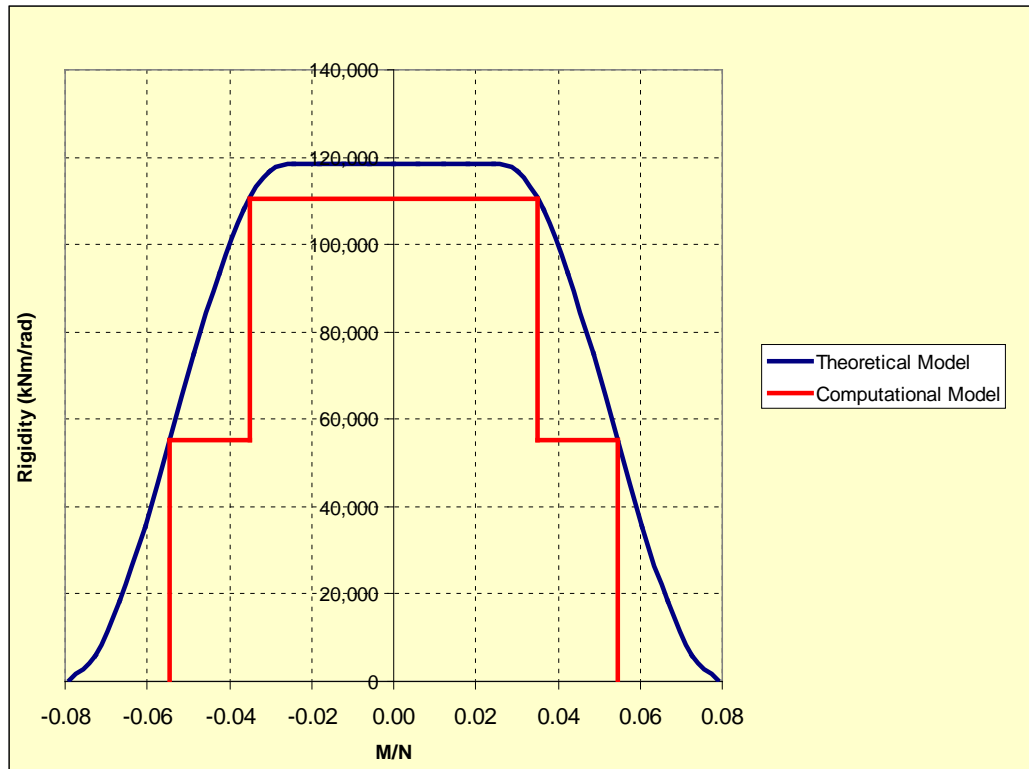


Figure 5.12. Theoretical and computational models of the rotational spring constant

The calculation is made with 2D BSMs for the tunnel section both in stiff and soft soil individually. The calculation is also performed by 3D BSM for the entire profile and the results of 2D and 3D models are compared for the evaluation.

CASE 3: A shallow tunnel passing under an existing structure is also analyzed in order to compare 2D and 3D BSMs simulating the effect of sudden change in loading conditions. A surcharge pressure of 100 kN/m^2 is assumed to occur along 9 m in the longitudinal direction. The Figure 5.13 shows the longitudinal profile of tunnel under surcharge pressure.

Existing surcharge pressure of 100 kN/m^2 on the ground is distributed to tunnel lining with a slope of 1H:2V. Equivalent surcharge pressure acting on the tunnel lining is calculated as 60 kN/m^2 along 15 m in the longitudinal direction. Therefore, the surcharge load is taken as 90 kN/m for a ring with length of 1.5 m .

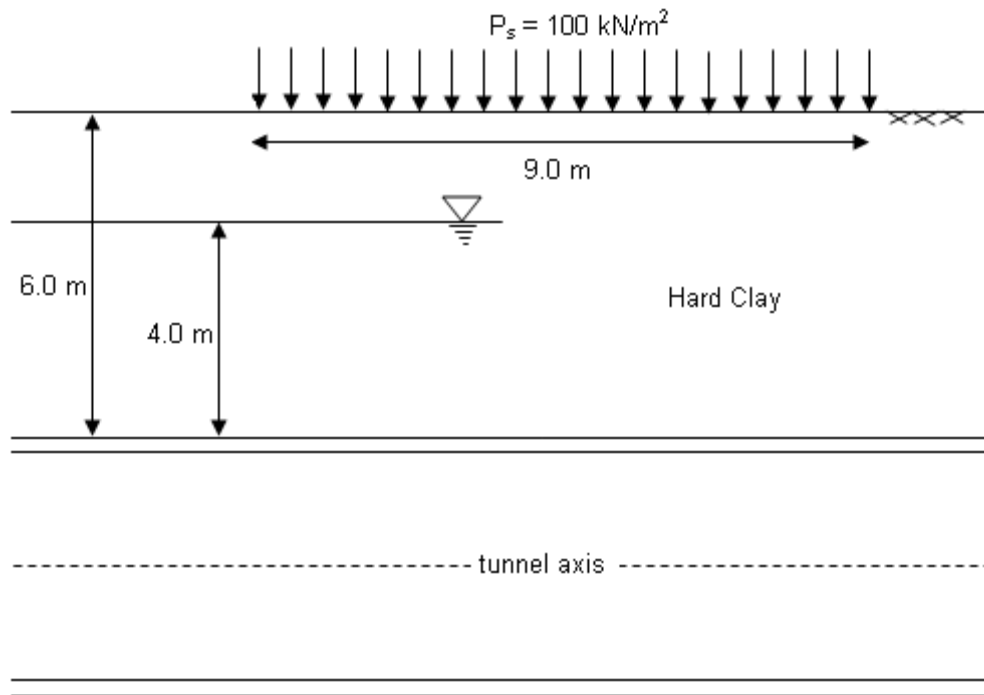


Figure 5.13. Longitudinal profile of the tunnel under surcharge pressure

The tunnel is modeled for 30 m length and composed of 21 sequential rings. The first 15 m of the tunnel is not exposed to surcharge load, although the rest is under the surcharge load. The tunnel is assumed to be surrounded by hard clay of which geotechnical properties are given in Table 5.1. In addition, the loads acting on the lining are calculated as expressed in Section 4.2. The summary of loads for this model is given in Table 5.6.

21 sequential rings having totally 147 rotational springs are examined for this case. Therefore, it is also a difficult and long process to execute iteration process for rotational spring constants. For that reason, in order to simplify the calculation for Case 3, rotational spring constants are also modeled in three stages as shown in Figure 5.12.

Table 5.6. Summary of load conditions for Case 3

| Load Conditions | Abbreviation | Units | Values |
|---|--------------|-------|--------|
| Vertical earth pressure | P_{vc} | kN/m | 111.00 |
| Lateral earth pressure at tunnel crown | q_{e1} | kN/m | 74.00 |
| Lateral earth pressure at tunnel bottom | q_{e2} | kN/m | 93.37 |
| Water pressure at tunnel crown | P_{w1} | kN/m | 40.00 |
| Water pressure at spring line | P_{ws} | kN/m | 76.70 |
| Water pressure at tunnel bottom | P_{w2} | kN/m | 113.40 |
| Surcharge pressure on the lining | P_s | kN/m | 90.0 |
| Soil reaction | P_r | kN/m | 123.48 |
| Dead weight | g | kN/m | 12.48 |
| Coefficient of lateral earth pressure | λ | - | 0.67 |

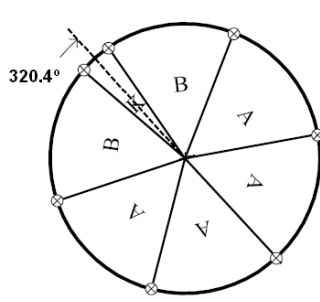
The calculation is made with 2D BSMs for tunnel sections in and out of surcharge impact area. Also, 3D BSM is performed for the entire region and the results of 2D and 3D analyses are compared. By this way, the necessity of 3D models for the analysis of tunnels under the surcharge effect is checked.

CASE 4: Selecting a proper mesh density is an important subject in numerical analyses. For that reason, in order to evaluate the effect of mesh coarseness in 2D and 3D BSMs, the analyses are performed by dividing the segmental ring into 50, 150, and 250 beam elements. Then, sectional forces and crown deformation obtained from 2D and 3D BSMs having different mesh densities are compared.

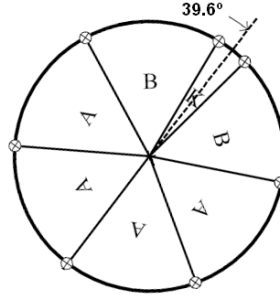
CASE 5: In addition to mesh coarseness, another variable in 3D Beam – Spring Method is the shear spring constant. For the ring section examined in this study, the shear spring constant is selected as an average value of 20000 kN/m by considering previous studies. As mentioned in Section 3.2, the shear spring constant varies by material used in ring joints and its properties, such as shear modulus, area, and thickness. For that reason, in order to evaluate the effect of shear spring constant in 3D Beam – Spring Method, three different analysis models having a shear spring constant of 15000 kN/m, 20000 kN/m, and 25000 kN/m are examined, respectively. Consequently, the sensitivity of shear spring constant is determined by comparing the obtained results.

CASE 6: As a whole, key segments are placed in a staggered layout typically having an equal angle about the vertical axis. In this sense, the arrangement of key segments can be determined in various positions. In order to investigate the effect of segment layout on the results obtained from 3D Beam – Spring Method, four different segment arrangements are implemented as shown in Figure 5.14. Rings having these different key segment arrangements are analyzed with 3D BSMs and the results of models are compared for the evaluation.

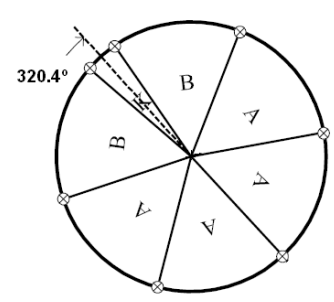
LAYOUT 1



1. Ring

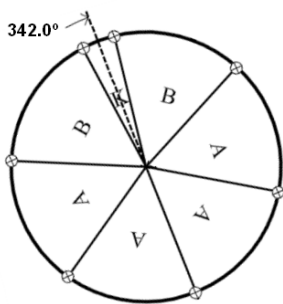


2. Ring

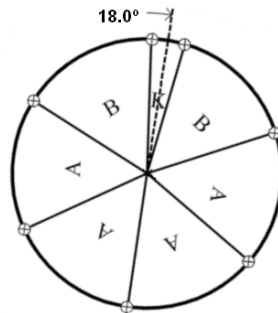


3. Ring

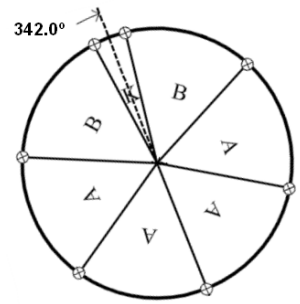
LAYOUT 2



1. Ring

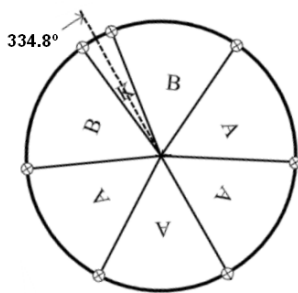


2. Ring

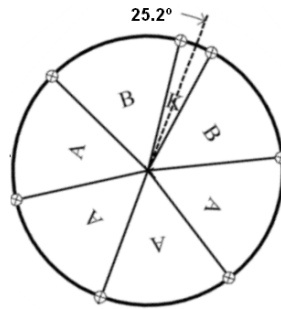


3. Ring

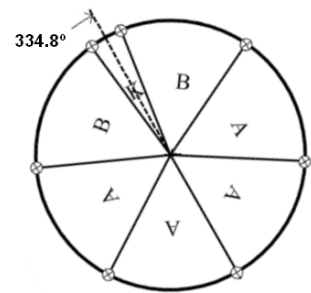
LAYOUT 3



1. Ring

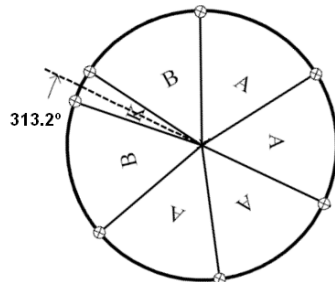


2. Ring

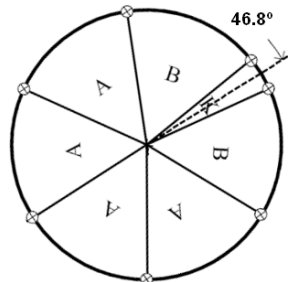


3. Ring

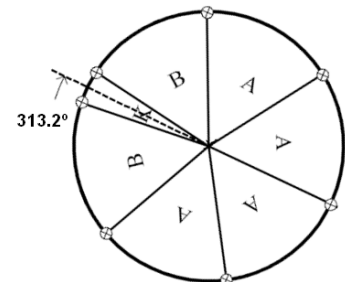
LAYOUT 4



1. Ring



2. Ring



3. Ring

Figure 5.14. Segment configurations for 4 different layouts

The summary of abovementioned analysis cases is given in Table 5.7.

Table 5.7. Summary of analysis cases

| Analysis Cases | Analysis Cases | | | | | |
|---|------------------------------|-------------------------|------------------|------------------------------|-------------------------|----------------------------------|
| | Case 1 | Case 2 | Case 3 | Case 4 | Case 5 | Case 6 |
| Method of Calculation | EEM 2D BSM 3D BSM | 2D BSM 3D BSM | 2D BSM 3D BSM | 2D BSM 3D BSM | 3D BSM | 3D BSM |
| Reduced Bending Stiffness (EI)_{eff} | Only Model B | X | X | Only Model B | X | X |
| Simulation of Segment Joint | Model C Model D 3D BSM | √ | √ | Model C Model D 3D BSM | √ | √ |
| Simulation of Ring Joint | Only 3D BSM | Only 3D BSM | Only 3D BSM | Only 3D BSM | √ | √ |
| Type of Soil | Stiff Soil | Stiff Soil Soft Soil | Stiff Soil | Stiff Soil | Stiff Soil | Stiff Soil |
| Mesh Coarseness (ring divided by) | 50 | 50 | 50 | 50 150 250 | 50 | 50 |
| Shear Spring Constant (kN/m) | 20000 | 20000 | 20000 | 20000 | 15000 20000 25000 | 20000 |
| Key Segment Configuration (angle from crown) | 39.6° | 39.6° | 39.6° | 39.6° | 39.6° | 39.6° 18.0° 25.2° 46.8° |

* EEM: Elastic Equation Method

CHAPTER 6

RESULTS AND DISCUSSION

The results of the analyses and their interpretations are presented in this chapter. The results are given in tabular form. In this chapter, axial forces, shear forces, bending moments, and maximum crown deformations obtained from analytical and numerical (2D & 3D BSMs) analysis cases are summarized in Table 6.1 through Table 6.7.

6.1. Evaluation of Analysis Methods

In the scope of this study, a typical TBM segmental lining section is examined by the elastic equation method and 2D & 3D beam – spring methods under certain conditions. The main aim of this study is to evaluate analysis methods and parameters affecting the forces in the tunnel lining. This is achieved by comparing and evaluating the results obtained from several analysis approaches.

Firstly, 2D analytical and numerical methods are compared between each other. By this way, maximum sectional forces (bending moment and corresponding axial force, axial force, and shear force) and maximum crown deformations obtained from elastic equation method and 2D beam – spring methods, such as Model A (rigid ring), Model B (Muir Wood), Model C (multiple hinges) and Model D (rotational spring) are summarized in Table 6.1 for the comparison.

Table 6.1. Analysis results obtained from elastic equation method and 2D beam – spring methods

| Structural System | Member Forces | | | | Max Crown Deformation |
|------------------------------------|---------------------|-----------------|-------------------|-------------------|------------------------|
| | Max Bending Moment | | Max Axial Force | Max Shear Force | |
| | M_{max} (kN.m) | N (kN) | N_{max} (kN) | V_{max} (kN) | δ_{max} (mm) |
| Elastic Equation Method | 152.7 100 % | 1459.7 100 % | 1722.5 100 % | 91.5 100 % | - - |
| Model A (Rigid Ring) | 170.8 112 % | 1441.9 99 % | 1890.9 110 % | 105.8 116 % | 5.9 100 % |
| Model B (Muir Wood) | 157.1 103 % | 1453.7 100 % | 1893.6 110 % | 100.0 109 % | 8.7 147 % |
| Model C (Multiple Hinges) | 162.6 106 % | 1453.7 100 % | 1892.8 110 % | 101.5 111 % | 7.3 124 % |
| Model D (Rotational Spring) | 134.0 88 % | 1734.8 119 % | 1918.9 111 % | 123.5 135 % | 4.2 70 % |

For the sectional forces, results obtained from elastic equation method are used as a base and they are accepted as 100 %, so sectional forces and deformation become easy to be compared. Since elastic equation method is not able to calculate maximum crown deformation, Model A (Rigid Ring) is used as a base and accepted as 100 % only for maximum crown deformation.

Table 6.1 shows that elastic equation method gives an average value for bending moment. Model A gives the maximum bending moment. Since Model A assumes a fully rigid ring and ignores the reduction of bending stiffness (EI) at segment joints, maximum bending moments occurs in this model. On the other hand, Model C presents greater bending moment than

Model B. It means that in spite of releasing 90% of bending moments occurred at segment joints, the ring at Model C is stiffer than the ring at Model B. The reason for this is that the flexural rigidity of ring at Model B is reduced to nearly half of its actual value in accordance with Muir Wood formulation. The minimum bending moment is generated by Model D which is the most complicated 2D analysis method. The nonlinear rotational springs having different stiffness according to M/N ratio at each segment joint are able to transfer axial forces, bending moments due to eccentric axial forces, and also shear forces from external and internal loading. Different-sized rotational springs transfer moments between adjacent segments according to rotations in segment joints. Owing to this function of rotational springs, a balanced moment distribution is provided in Model D. As a result of this; the maximum bending moment obtained from Model D is less than the others.

In terms of axial forces, all 2D BSMs give nearly equal values. Since elastic equation method considers subgrade reaction only in lateral directions with an angle of 90 degrees and ignores subgrade reaction in other directions, it presents 10 % less results than 2D BSMs for axial loads.

Shear forces obtained from Model A, B, and C display a similar trend and are nearly equal. Elastic equation method gives 9 % ~ 15 % less result for shear force rather than these models, because elastic equation method is not able to simulate ground – lining interaction and underestimates the shear forces. Maximum shear force at circular tunnel linings exists at the point having an angle of 45° from crown. At Model D, one of the segment joints that are modeled as rotational springs is located at the point having an angle of 46.8° from crown. This rotational spring is very close to the point where maximum shear force occurs and also it is one of the segment joints where shear force transition takes place. Due to the location of this rotational spring, Model D gives the maximum shear force at that point.

Furthermore, maximum crown deformation does not match well because each model has different assumptions. Due to the balanced moment distribution in segments, Model D gives the minimum crown deformation. Then, since Model A assumes a stiffer ring than Model B and C, it presents less crown deformations than the others. Since Model B and C substantially reduce the bending stiffness (EI) of segmental ring in accordance with the Muir Wood formulation and assumption of multiple hinges, respectively, these two models expectedly give higher crown deformations.

The abovementioned comparison of 2D analytical and numerical methods shows that although models give close results for some sectional forces and crown deformation, generally they do not display a similar trend. For that reason, a further comparison should be performed at this stage.

Previous studies show that internal forces and deformations calculated by 3D BSMs fit very well to results obtained from FEM and laboratory tests. Therefore, the results obtained from 2D analytical and numerical methods are compared with the ones calculated by 3D analyses in order to have a suggestive evaluation. This comparison is summarized in Table 6.2. For this case, the results of 3D BSM are used as a base and they are accepted as 100 % for the convenience of comparisons.

Table 6.2. Analysis results obtained from elastic equation method and 2D & 3D beam - spring methods

| Structural System | Member Forces | | | | Max Crown Deformation |
|------------------------------------|---------------------|-----------------|-------------------|-------------------|------------------------------|
| | Max Bending Moment | | Max Axial Force | Max Shear Force | |
| | M_{max} (kN.m) | N (kN) | N_{max} (kN) | V_{max} (kN) | $\bar{\delta}_{max}$ (mm) |
| 3D Beam – Spring Model | 157.2 100 % | 1784.9 100 % | 1946.4 100 % | 126.0 100 % | 4.2 100 % |
| Elastic Equation Method | 152.7 97 % | 1459.7 82 % | 1722.5 88 % | 91.5 73 % | - - |
| Model A (Rigid Ring) | 170.8 109 % | 1441.9 81 % | 1890.9 97 % | 105.8 84 % | 5.9 140 % |
| Model B (Muir Wood) | 157.1 100 % | 1453.7 81 % | 1893.6 97 % | 100.0 79 % | 8.7 206 % |
| Model C (Multiple Hinges) | 162.6 103 % | 1453.7 81 % | 1892.8 97 % | 101.5 81 % | 7.3 173 % |
| Model D (Rotational Spring) | 134.0 85 % | 1734.8 97 % | 1918.9 99 % | 123.5 98 % | 4.2 100 % |

As seen in Table 6.2, the values of bending moment obtained from elastic equation method, Model B, and Model C are nearly equal to the result calculated by 3D BSM. However, other sectional forces differ up to 27 %. Especially, Model B and C create quite higher maximum crown deformations than 3D BSM. The differences in maximum crown deformations calculated by Model B and C are respectively 106 % and 73 % in reference to 3D analysis results. On the other hand, Model A gives 9 % higher values for bending moment due to the assumption of fully rigid ring. Moreover, maximum shear force and maximum crown deformation do not fit well to the results of 3D analysis.

Model D is expected to give closest results to 3D analysis because 3D BSM is the extended version of Model D through third dimension. It is achieved by circumferential joints connecting adjacent rings. Since the relative deformation between adjacent rings having different deformation patterns is restricted by friction at the ring joints, coupling forces are created in ring joints. The coupling of rings simulated by shear springs leads to an increase in flexural stiffness of segmental linings. Furthermore, adjacent rings have different bending stiffness which causes a load transfer from less stiff segment to stiffer segment. This leads to higher bending moments at the stiffer ring. As a result of abovementioned reasons, 3D BSMs are expected to give higher bending moments than 2D BSMs simulating segment joints by rotational springs like Model D.

As it is expected, Model D presents 15 % less maximum bending moment than 3D BSM. However, other maximum sectional forces except for bending moment and maximum crown deformations are nearly equal to the ones given by 3D BSM. Also, Model D is the unique 2D model that gives crown deformation consistent with 3D model.

The comparison and evaluation of analysis methods show that although analytical and 2D BSMs give compatible results with 3D model for some sectional forces or crown deformation, none of these methods is able to present results reasonably consistent with 3D model for all sectional forces and crown deformation. Despite Model D gives 15 % less bending moments than 3D BSM, it is the unique model that gives reasonable results for all sectional forces and crown deformation. Therefore, this model might be used in the design of TBM segmental linings as an alternative to 3D BSM. In order to clarify this issue, additional analyses for certain factors such as joint stiffness, joint distribution, soil stiffness, mesh coarseness, and different load conditions have been examined with 2D (Model D) and 3D BSMs for a

comprehensive comparison. Further evaluation of these 2D and 3D BSMs are given in the next sections.

6.2. The Effect of Soil Stiffness on Beam – Spring Analysis

2D and 3D BSMs are examined for the tunnel sections passing through a soil transition zone having 3 different soil stiffness ratios. The results obtained from these analyses are summarized in Table 6.3. For a clear comparison, the results obtained from 2D BSMs for the tunnel section in softer soils are used as a base and accepted as 100 %.

As seen in Table 6.3, 2D BSMs for the tunnel sections in stiffer soil give less bending moment, shear force, and crown deformation. Subgrade reaction is directly proportional to soil stiffness. Therefore, as the stiffness of soil surrounding the tunnel increases, subgrade reaction also increases and this leads to less sectional forces and deformation in the lining. In the same manner, 2D BSMs for the tunnel sections in softer soil give higher bending moment, shear force, and crown deformation.

For the comparison of 2D and 3D BSMs, due to load transfer between rings by shear springs, 3D BSM presents higher sectional forces as expected. However, the difference between the sectional forces obtained from 3D BSM and 2D BSM for the tunnel section in softer soil differs slightly, except for shear force. This means that 2D and 3D BSMs can represent such a situation where soil stiffness suddenly changes in a same manner except for shear forces.

Table 6.3. Analysis results obtained from 2D and 3D beam - spring methods for the section passing through a soil transition zone

| Structural System | Member Forces | | | | Max Crown Deformation |
|--|---------------------|-----------------|-------------------|-------------------|------------------------------|
| | Max Bending Moment | | Max Axial Force | Max Shear Force | |
| | M_{max} (kN.m) | N (kN) | N_{max} (kN) | V_{max} (kN) | $\bar{\delta}_{max}$ (mm) |
| 2D BSM ($E_s = 40000$) | 162.3 100 % | 1751.3 100 % | 1912.5 100 % | 126.6 100 % | 5.9 100 % |
| 2D BSM ($E_s = 80000$) | 141.4 87 % | 1751.9 100 % | 1912.1 100 % | 117.3 93 % | 4.7 80 % |
| 3D BSM | 166.5 103 % | 1810.2 103 % | 1955.1 102 % | 147.9 117 % | 5.8 98 % |
| 2D BSM ($E_s = 20000$) | 165.8 100 % | 1754.0 100 % | 1912.8 100 % | 128.5 100 % | 6.2 100 % |
| 2D BSM ($E_s = 80000$) | 141.4 85 % | 1751.9 100 % | 1912.1 100 % | 117.3 91 % | 4.7 76 % |
| 3D BSM | 171.3 103 % | 1815.4 104 % | 1960.2 102 % | 149.4 116 % | 6.0 97 % |
| 2D BSM ($E_s = 10000$) | 166.8 100 % | 1754.6 100 % | 1913.0 100 % | 129.0 100 % | 6.3 100 % |
| 2D BSM ($E_s = 80000$) | 141.4 85 % | 1751.9 100 % | 1912.1 100 % | 117.3 91 % | 4.7 75 % |
| 3D BSM | 174.2 104 % | 1809.1 103 % | 1954.3 102 % | 145.0 112 % | 5.9 94 % |

6.3. The Effect of Surcharge Load on Beam – Spring Analysis

For the comparison of 2D and 3D BSMs, 3 analyses have been performed for the tunnel section subjected to surcharge load. Two 2D models are employed for the tunnel section located in and out of influence area of surcharge load. Also, a 3D model simulating both in and out of influence area of surcharge load is generated. The results obtained from these models are given in Table 6.4. In this section, the results of 2D BSM for the tunnel section subjected to surcharge load are used as a base and they are accepted as 100 % for the convenience of comparisons.

Table 6.4. Analysis results obtained from 2D and 3D beam - spring methods for the tunnel section subjected to surcharge load

| Structural System | Member Forces | | | | Max Crown Deformation |
|--------------------------|---------------------|-----------|-------------------|-------------------|------------------------|
| | Max Bending Moment | | Max Axial Force | Max Shear Force | |
| | M_{max} (kN.m) | N (kN) | N_{max} (kN) | V_{max} (kN) | δ_{max} (mm) |
| 2D BSM | 114.7 | 763.1 | 1156.5 | 104.2 | 5.1 |
| (Under Surcharge) | 100 % | 100 % | 100 % | 100 % | 100 % |
| 2D BSM | 67.0 | 867.1 | 957.7 | 112.6 | 3.7 |
| (No Surcharge) | 58 % | 114 % | 83 % | 108 % | 73 % |
| 3D BSM | 171.1 | 854.6 | 1296.3 | 136.4 | 5.2 |
| | 149 % | 112 % | 112 % | 131 % | 102 % |

As seen in Table 6.4, the results obtained from 2D BSM for the section not subjected to surcharge load gives considerably lower results than 3D BSM as expected. However, the differences between the results of 2D BSM for the

section subjected to surcharge load and 3D BSM are also quite high. 3D BSM model presents 71 % higher bending moment and 31 % higher shear force than the 2D model. Deformation patterns of tunnel sections in and out of influence area of surcharge load are very different. The load transfer between the rings increases in order to obtain a harmonized deformation pattern. As a result of this, 3D BSMs give nearly the same crown deformation and considerably higher sectional forces as compared with 2D BSMs. This means that 2D BSMs are inadequate to represent such a situation where loading conditions suddenly changes.

6.4. The Effect of Mesh Coarseness on Beam – Spring Analysis

In order to examine the effect of mesh coarseness on 2D and 3D BSMs, the segmental ring is divided into 50, 150, and 250 beam elements having a length of 0.462 m, 0.154 m, and 0.093 m, respectively. The results obtained from 2D and 3D analyses with different mesh coarseness are given in Table 6.5. Results of models having a ring divided into 50 beams are used as a base and they are accepted as 100 % for convenience in comparisons.

As seen in Table 6.5, the results obtained from 2D and 3D analyses for three different mesh coarseness do not show significant difference among each other. Maximum difference (5 % - 6 %) due to mesh coarseness is shown at axial forces for all analysis methods. Also, mesh coarseness in Model D leads to 4 % ~ 5 % lower results for bending moments. However, these differences in sectional forces and crown deformation do not affect the design of segmental linings dramatically.

Table 6.5. Analysis results obtained from 2D and 3D beam – spring methods for different mesh coarseness

| Structural System | Ring Divided By | Member Forces | | | | Max Crown Deformation |
|------------------------------------|-----------------|---------------------|-----------------|-------------------|-------------------|------------------------------|
| | | Max Bending Moment | | Max Axial Force | Max Shear Force | |
| | | M_{max} (kN.m) | N (kN) | N_{max} (kN) | V_{max} (kN) | $\bar{\delta}_{max}$ (mm) |
| 3D Beam – Spring Model | 50 | 157.2 100 % | 1784.9 100 % | 1946.4 100 % | 126.0 100 % | 4.2 100 % |
| | 150 | 159.0 101 % | 1809.0 101 % | 1875.3 96 % | 127.4 101 % | 4.3 102 % |
| | 250 | 160.3 102 % | 1811.5 101 % | 1860.6 96 % | 127.5 101 % | 4.3 102 % |
| Model A (Rigid Ring) | 50 | 170.8 100 % | 1441.9 100 % | 1890.9 100 % | 105.8 100 % | 5.9 100 % |
| | 150 | 169.0 99 % | 1444.0 100 % | 1811.8 96 % | 106.0 100 % | 5.9 100 % |
| | 250 | 168.8 99 % | 1444.2 100 % | 1794.7 95 % | 106.1 100 % | 5.9 100 % |
| Model B (Muir Wood) | 50 | 157.1 100 % | 1453.7 100 % | 1893.6 100 % | 100.0 100 % | 8.7 100 % |
| | 150 | 155.4 99 % | 1455.9 100 % | 1814.7 96 % | 100.2 100 % | 8.8 101 % |
| | 250 | 155.2 99 % | 1456.1 100 % | 1797.5 95 % | 100.2 100 % | 8.8 101 % |
| Model C (Multiple Hinges) | 50 | 162.6 100 % | 1453.7 100 % | 1892.8 100 % | 101.5 100 % | 7.3 100 % |
| | 150 | 164.6 101 % | 1448.6 100 % | 1812.7 96 % | 103.6 102 % | 7.4 101 % |
| | 250 | 165.9 102 % | 1447.1 100 % | 1795.2 95 % | 104.2 103 % | 7.4 101 % |
| Model D (Rotational Spring) | 50 | 134.0 100 % | 1734.8 100 % | 1918.9 100 % | 123.5 100 % | 4.2 100 % |
| | 150 | 128.1 96 % | 1736.1 100 % | 1831.9 95 % | 125.1 101 % | 4.2 100 % |
| | 250 | 127.7 95 % | 1736.1 100 % | 1812.9 94 % | 125.3 101 % | 4.2 100 % |

It is concluded from this comparison that mesh coarseness has not a considerable effect on beam – spring analyses. Also, feasible mesh coarseness can be provided by dividing segmental rings into a series of beam elements having a length of nearly 0.5 m in order to obtain reasonable results.

6.5. The Effect of Shear Spring Constant on Beam – Spring Analysis

In order to determine the sensitivity of shear spring constants, three 3D BSMs with different shear spring constants have been employed and the results are summarized in Table 6.6. The results obtained from 3D BSM with a shear spring constant of 15000 kN/m are used as a base and they are accepted as 100 % for a clear comparison.

Table 6.6. Analysis results obtained from 3D beam – spring methods for three different shear spring constants

| Structural System | Member Forces | | | | Max Crown Deformation |
|---|---------------------|-----------------|-------------------|-------------------|------------------------|
| | Max Bending Moment | | Max Axial Force | Max Shear Force | |
| | M_{max} (kN.m) | N (kN) | N_{max} (kN) | V_{max} (kN) | δ_{max} (mm) |
| 3D BSM ($K_s = 15000$ kN/m) | 148.7 100 % | 1759.3 100 % | 1918.9 100 % | 126.2 100 % | 4.2 100 % |
| 3D BSM ($K_s = 20000$ kN/m) | 157.2 106 % | 1784.9 101 % | 1946.4 101 % | 126.5 100 % | 4.2 100 % |
| 3D BSM ($K_s = 25000$ kN/m) | 176.0 118 % | 1857.4 106 % | 2001.3 104 % | 127.3 101 % | 4.2 100 % |

As seen in Table 6.6, 3D BSM with the highest shear spring constant gives the maximum results for bending moment, axial force, and shear force. Especially, difference in the maximum bending moment is 18 % between two models having the maximum and minimum shear spring constants. The reason is that as the shear spring constant increases, the load transfer between the adjacent rings also increases. Therefore, higher load transfer expectedly leads to increase in sectional forces. However, maximum crown deformation is not affected by shear spring constants due to the harmonized deformation pattern.

It can be concluded that shear spring constant which is a mechanical property of circumferential joints has a notable effect on sectional forces; especially on bending moment. Therefore, selecting a realistic shear spring constant is essential for 3D BSMs.

6.6. The Effect of Segment Layout on Beam – Spring Analysis

Four possible segment arrangements shown in Figure 5.13 for a segmental ring sequence are examined with 3D BSM in order to determine the effect of segment layout on sectional forces and deformation of segmental linings. The analysis results for four different segment layouts are given in Table 6.7. For a clear comparison, the results of Layout 1 is selected as a base and accepted as 100 %.

As shown in Table 6.7, maximum difference in results exists in bending moments. Layout 4 has the most unfavorable configuration in terms of bending moment and crown deformation. Since the longitudinal joint between segment A and segment B is located very close to crown, Layout 4 gives the maximum bending moment and crown deformation. Furthermore, axial forces are in similar range and shear forces differ slightly.

Table 6.7. Analysis results obtained from 3D beam – spring methods for four different segment configurations

| Structural System | Member Forces | | | | Max Crown Deformation |
|------------------------------|---------------------|-----------------|-------------------|-------------------|------------------------------|
| | Max Bending Moment | | Max Axial Force | Max Shear Force | |
| | M_{max} (kN.m) | N (kN) | N_{max} (kN) | V_{max} (kN) | $\bar{\delta}_{max}$ (mm) |
| 3D BSM for (LAYOUT 1) | 157.2 100 % | 1784.9 100 % | 1946.4 100 % | 126.0 100 % | 4.2 100 % |
| 3D BSM for (LAYOUT 2) | 147.3 94 % | 1756.0 98% | 1914.4 98 % | 111.6 89 % | 4.7 110 % |
| 3D BSM for (LAYOUT 3) | 130.7 83 % | 1754.5 98 % | 1913.1 98 % | 120.4 96 % | 4.2 100 % |
| 3D BSM for (LAYOUT 4) | 175.2 111 % | 1777.8 100 % | 1940.1 100 % | 134.5 107 % | 4.9 117 % |

The results show that segment layout in sequential rings is the other geometrical parameter that affects the sectional forces and deformation; especially bending moments. For that reason, different segment layouts for a ring should be analyzed with 3D BSMs in order to determine the most favorable segment configuration in the design of segmental linings.

CHAPTER 7

CONCLUSION

The evaluation of 2D and 3D analysis methods proposed for the design of segmental linings is performed by comparing the analysis results. The influences of several factors such as joint stiffness, joint configuration, soil stiffness, mesh coarseness, and different loading conditions are also investigated using the Larsa4D structural analysis program. Based on the evaluations given in the previous chapter, the following conclusions can be achieved from this thesis study. The conclusions given below are obtained from investigated cases for the selected tunnel section and loading conditions.

- It is found that Elastic Equation Method underestimates sectional forces up to 27 % in reference to 3D BSM for a regular load case.
- 2D BSMs are also found to underestimate sectional forces and deformations up to 21 % and 106 %, respectively in accordance with 3D BSM for a regular load case.
- Results obtained from 2D and 3D BSMs representing the change in the stiffness of surrounding soil differ up to 17 % for sectional forces.
- 2D and 3D BSMs simulating a TBM tunnel passing under a local surcharge load calculate sectional forces varying up to 49 %.

- The mesh coarseness has not a considerable effect on the results obtained from 2D and 3D BSMs. Accordingly, the length of beam elements representing segments can be selected as 0.5 m on average in order to obtain reasonable results.
- Bending moments obtained from 3D BSMs are found to be dependent on shear spring constant. Therefore, selection of a proper shear spring constant is a crucial point for the design of segmental linings.
- It can be concluded that segment configuration in sequential rings considerably affects the sectional forces and deformations up to 34 % and 17 %, respectively. Therefore, the most favorable segment configuration can be determined with 3D BSMs.
- It can be indicated as a general conclusion that mechanical, geometrical, and loading conditions to which tunnels can be exposed both in longitudinal and circumferential directions may have significant effects on the sectional forces and deformations of TBM segmental linings.

REFERENCES

- [1] Szechy K., *The Art of Tunnelling*, 2nd Ed., Akademiai Kiado, Budapest, 1973.
- [2] O'Rourke T.D., *ASCE Guidelines for Tunnel Lining Design*, ASCE Geotechnical Division, Virginia, 1984.
- [3] Guglielmetti V., Grasso P., Mahtab A., Xu S., *Mechanized Tunnelling in Urban Areas: Design Methodology and Construction Control*, Taylor & Francis Group, London, UK, 2008.
- [4] Möller S., *Tunnel Induced Settlements and Structural Forces in Linings*, PhD Thesis, Stuttgart University, 2006.
- [5] Megaw T.M., Bartlett J. V., *Tunnels: Planning, Design, Construction*, Volume 1, Ellis Horwood Limited, West Sussex, 1981.
- [6] Sinha R.S., *Underground Structures - Design and Instrumentation*, Elsevier, The Netherlands, 1989.
- [7] Maidl B., Herrenknecht M., Anheuser L., *Mechanized Shield Tunnelling*, Ernst and Sohn, Berlin, 1995.
- [8] Megaw T.M., Bartlett J. V., *Tunnels: Planning, Design, Construction*, Volume 2, Ellis Horwood Limited, West Sussex, 1981.

- [9] Kolymbas D., *Tunnelling and Tunnel Mechanics - A Rational Approach to Tunneling*, Elsevier, Amsterdam, 2005.
- [10] Sinha R.S., *Underground Structure - Design and Construction*, Elsevier, The Netherlands, 1991.
- [11] AFTES, *New Recommendations on Choosing Mechanized Tunnelling Techniques*, French Tunnelling and Underground Engineering Association, 2000.
- [12] Richardson H.W., Mayo R.S., *Practical Tunnel Driving*, Mc. Graw Hill, New York, 1947.
- [13] Maidl B., Schmid L., Herrenknecht M., *Hardrock Tunnel Boring Machines*, Ernst and Sohn, Berlin, 2008.
- [14] Wittke W., *Stability Analysis and Design for Mechanized Tunnelling*, Geotechnical Engineering in Research and Practice, WBI - Print 6, Aachen, 2007.
- [15] Girmscheid G., *Schildvorgetriebener Tunnelbau in Heterogenem Lokkergestein, ausgekleidet mit Stahlbetontübbingen*, Teil 2: Aspekte der Vortriebsmaschinen und Tragwerksplanung, Bautechnik 74, Heft 2, 1997.
- [16] ITA - WG14, *Recommendations and Guidelines for Tunnel Boring Machines (TBMs)*, International Tunnelling Association, Working Group No. 14 - Mechanized Tunnelling, 2000.
- [17] Toan N. D., *TBM and Lining – Essential Interfaces*, Post Graduate Ms. Thesis, Politecnico Di Torino, 2006.

- [18] Kovari K., Ramoni M., *Urban Tunnelling in Soft Ground Using TBM's*, Key Note Lecture at International Congress on Mechanized Tunnelling: Challenging Case Histories, Politecnico di Torino, Italy, 2004.
- [19] Herrenknecht AG, "<http://www.herrenknecht.com/products/tunnel-boring-machines.html>", last accessed on 11/01/2009.
- [20] Haack A., *Comparison Between Conventional Tunnel Driving Method and TBM Drives - Worldwide Demand of Tunnel Constructions*, Tunnel Boring Machines - Trends in Design and Construction of Mechanized Tunnelling, Hagenberg, Austria, 1995, Wagner & Schultze (eds), Balkema/Rotterdam, 1996.
- [21] Thewes M., *Segment Linings for Shield Machines*, International Course on Shield Tunneling, Delft Geo Academy, The Netherlands, 2008.
- [22] Herrenknecht M., Bappler K., *Segmental Concrete Lining Design and Installation*, Soft Ground and Hard Rock Mechanical Tunneling Technology Seminar, Colorado School of Mines, 2003.
- [23] ITA - WG2, *Guidelines for the Design of Shield Tunnel Lining*, International Tunnelling Association, Working Group No. 2 – Research, 2000.
- [24] JSCE, *Japanese Standard for Shield Tunnelling*, Japan Society of Civil Engineers, The third edition, Tokyo, 1996.
- [25] Duddeck H., Erdmann J., *Structural Design Models for Tunnels*, Universitat Braunschweig, Germany, 1982.

- [26] Schulze H., Duddeck H., *Spannungen in Schildvorgetriebenen Tunneln*, Beton Stahlbetonb, Germany, 1964.
- [27] Wood M., *The Circular Tunnel in Elastic Ground*, Geotechnique, Volume 25, No. 1, 1975.
- [28] AFTES – WG7, *Considerations on the Usual Methods of Tunnel Lining Design*, French Tunneling and Underground Engineering Association, Working Group No. 7 - Temporary Supports and Permanent Lining, 1993.
- [29] Mashimo H., Ishimura T., *Evaluation of the Load on a Shield Tunnel Lining in Gravel*, Public Works Research Institute, Independent Administrative Institution, Tsukuba, Japan, 2003.
- [30] Bickel J.O., Kuesel T.R., King E.H., *Tunnel Engineering Handbook*, Chapman & Hall, United States of America, 1996.
- [31] Koyama Y., Nishimura T., *Design of Lining Segment of Shield Tunnel Using a Beam – Spring Model*, Quarterly Report of Railway Technical Research Institute, Volume: 39(1), Japan.
- [32] Lee K.M., Ge X.W., *The Equivalence of a Jointed Shield-Driven Tunnel Lining to a Continuous Ring Structure*, Canadian Geotechnical Journal, Volume 38, No. 3, 2001.
- [33] Hefny A.M., Tan F.C., Macalevey N.F., *Numerical Study on the Behaviour of Jointed Tunnel Lining*, Journal of The Institution of Engineers, Volume 44, Issue 1, Singapore, 2004.

- [34] Janssen P., *Tragverhalten von Tunnelausbauten mit Gelenktubbings*, Report No. 83-41, University of Braunschweig, Department of Civil Engineering, Institute for Structural Analysis, 1983.
- [35] Leonhard F., Reimann H., *Betongelenke*, Der Bauingenieur, Volume 41, 1966.
- [36] Klappers C., Gruebl F., Ostermeier B., *Structural Analysis of Segmental Lining – Coupled Beam and Spring Analyses Versus 3D FEM Calculations with Shell Elements*, Tunneling and Underground Space Technology, Volume 21, Issues 3-4, 1999.
- [37] Wang J.J., *The Design Considerations for the Segmental Lining of the Hsuehshan Tunnel*, International Symposium on Design, Construction and Operation of Long Tunnels, Taiwan, 2005.
- [38] Koyama Y., *Study on the Improvement of Design Method of Segments for Shield-Driven Tunnels*, RTRI Report: Special No. 33, 2000.
- [39] Koyama Y., *Present Status and Technology of Shield Tunneling Method in Japan*, Tunneling and Underground Space Technology, Volume 18, 2003.
- [40] Gioda G., Swoboda G., *Developments and applications of the numerical analysis of tunnels in continuous media*, International Journal for Numerical and Analytical Methods in Geomechanics, Volume 23, 1999.
- [41] Blom C.B.M., Horst E.J., Jovanovic P.S., *Three-Dimensional Structural Analyses of the Shield-Driven “Green Heart” Tunnel of the High-Speed*

Line South, Tunneling and Underground Space Technology, Volume 14, No. 2, 1999.

- [42] BTS - ICE, *Tunnel Lining Design Guide*, The British Tunneling Society and Institution of Civil Engineers, Thomas Telford, London, 2004.
- [43] AFTES, *Recommendations for The Design, Sizing and Construction of Precast Concrete Segments Installed at the Rear of a Tunnel Boring Machine (TBM)*, French Tunneling and Underground Engineering Association, Version 1, 1997.

APPENDIX A

WORKING SHEETS FOR THE ANALYSIS WITH ELASTIC EQUATION METHOD

Input, load conditions, and member forces sheets developed for the analysis with Elastic Equation Method by using Microsoft Excel 2003 and Macro Visual Basic applications are given in the following pages. Input sheet includes geometrical, material, and geotechnical properties of the problem. Calculations of loads and member forces are also provided in load conditions sheets and member forces sheet, respectively.

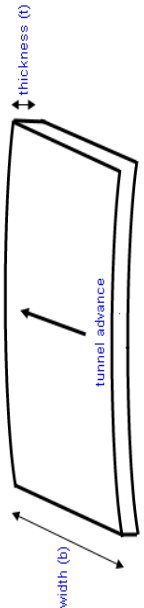
Microsoft Excel - Analytical TBM Analysis.xls [Read-Only]

File Edit View Insert Format Tools Data Window Help Adobe PDF

100% Arial

| SEGMENT PROPERTIES | | | |
|--------------------|--------------------|--------------------------|--|
| Diameter | (D ₀): | 7680mm | |
| Radius | (R _C): | 3680.0mm | |
| Width | (b): | 1000mm | |
| Thickness | (t): | 320mm | |
| Elasticity Modulus | (E _C): | 37.0E+3MPa | |
| Unit Weight of RC | (γ _c): | 26KN/m ³ | |
| Inertia of Segment | (I): | 2.73E-3m ⁴ /m | |

EI: Bending Rigidity in Unit Width



| GROUND PROPERTIES | | | |
|---------------------------------------|--------------------|---------------------------|--|
| Overburden | (H): | 15m | |
| Groundwater Table | (H _g): | 6m | |
| SPT N Value | (N): | 30 | |
| Unit Weight | (γ): | 19KN/m ³ | |
| Submerged Unit Weight | (γ'): | 9KN/m ³ | |
| Unit Weight of Water | (γ _w): | 10KN/m ³ | |
| Internal Friction Angle | (φ): | 0° | |
| Cohesion | (c): | 170KN/m ² | |
| Coefficient of Reaction | (k): | 15.8 E+3KN/m ³ | |
| Coefficient of Lateral Earth Pressure | (K): | 0.67 | |
| Surcharge | (P ₀): | 0KN | |
| Soil Type | | Hard Clay | |

if multiple layers exist:

| Layer | Y | H | Y _{sat} | H _{sat} |
|-------|------|-----|------------------|------------------|
| 1 | | | 9.0 | 3.9 |
| 2 | | | 10.0 | 2.1 |
| 3 | 20.0 | 4.2 | | |
| 4 | 19.0 | 3.3 | | |
| 5 | 19.0 | 1.9 | | |

| TUNNEL TYPE | |
|----------------------------------|---|
| <input checked="" type="radio"/> | Railway Tunnels |
| <input type="radio"/> | Drainage, Electric Power, Communication Tunnels |

Ref: JAPANESE STANDARD FOR SHIELD TUNNELLING

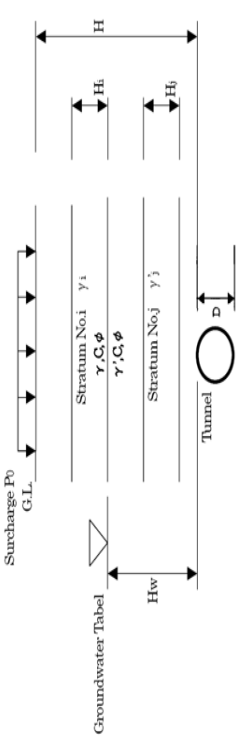


Figure A.1. Input sheet for the analysis with Elastic Equation Method

Microsoft Excel - Analytical TBM Analysis.xls [Read-Only] Type a question for help

VERTICAL EARTH PRESSURE

$\sigma_v = \frac{B_1 \cdot (\gamma - c/B_1)}{K_0 \cdot \tan \phi} \cdot (1 - e^{-K_0 \cdot \tan \phi \cdot H/B}) + P_0 \cdot e^{-K_0 \cdot \tan \phi \cdot H/B}$

$h_o = \sigma_v / \gamma$

σ_v : Terzaghi's Loosening Pressure
 h_o : Computed height of loosening soil
 K_0 : The ratio of horizontal earth pressure to vertical pressure (usually, 1.0 can be adopted as K_0)
 $\sigma_v = \#DIV/0!$
 $h_o = \#DIV/0!$

for drainage, electric power, communication tunnels for railway tunnels

$P_{e1} = 238.96 \text{ kNm}^2$

Loosening Earth Pressure.
 $B_1 = B/2 = 8.8843$

$P_{e1} = \text{MAX}(\gamma \cdot h_o, 1.5 \cdot \gamma \cdot D_o, 200)$

$P_{e1} = \#DIV/0!$

Total Overburden:

| Layer | Y | H | Y sat | H sat |
|-------|------|-----|-------|-------|
| 1 | 0.0 | 0.0 | 9.0 | 3.9 |
| 2 | 0.0 | 0.0 | 10.0 | 2.1 |
| 3 | 20.0 | 4.2 | 0.0 | 0.0 |
| 4 | 19.0 | 3.3 | 0.0 | 0.0 |
| 5 | 19.0 | 1.9 | 0.0 | 0.0 |

$P_{e1} = P_0 + \sum \gamma_i \cdot H_i + \sum \gamma'_j \cdot H'_j$

$P_{e1} = 238.96 \text{ kNm}^2$

B = width at the tunnel roof of the volume contained between slip surfaces
for a circular tunnel:
if $H < B$, whole overburden
if $H > B$, min overburden B
if $B < H < 2.5B$, min overburden B
 $B = 17.8 > H = 15$ ($B = 2B$)

Vertical Earth Pressure: Total Overburden

Figure A.2. Load conditions sheet 1 for the analysis with Elastic Equation Method

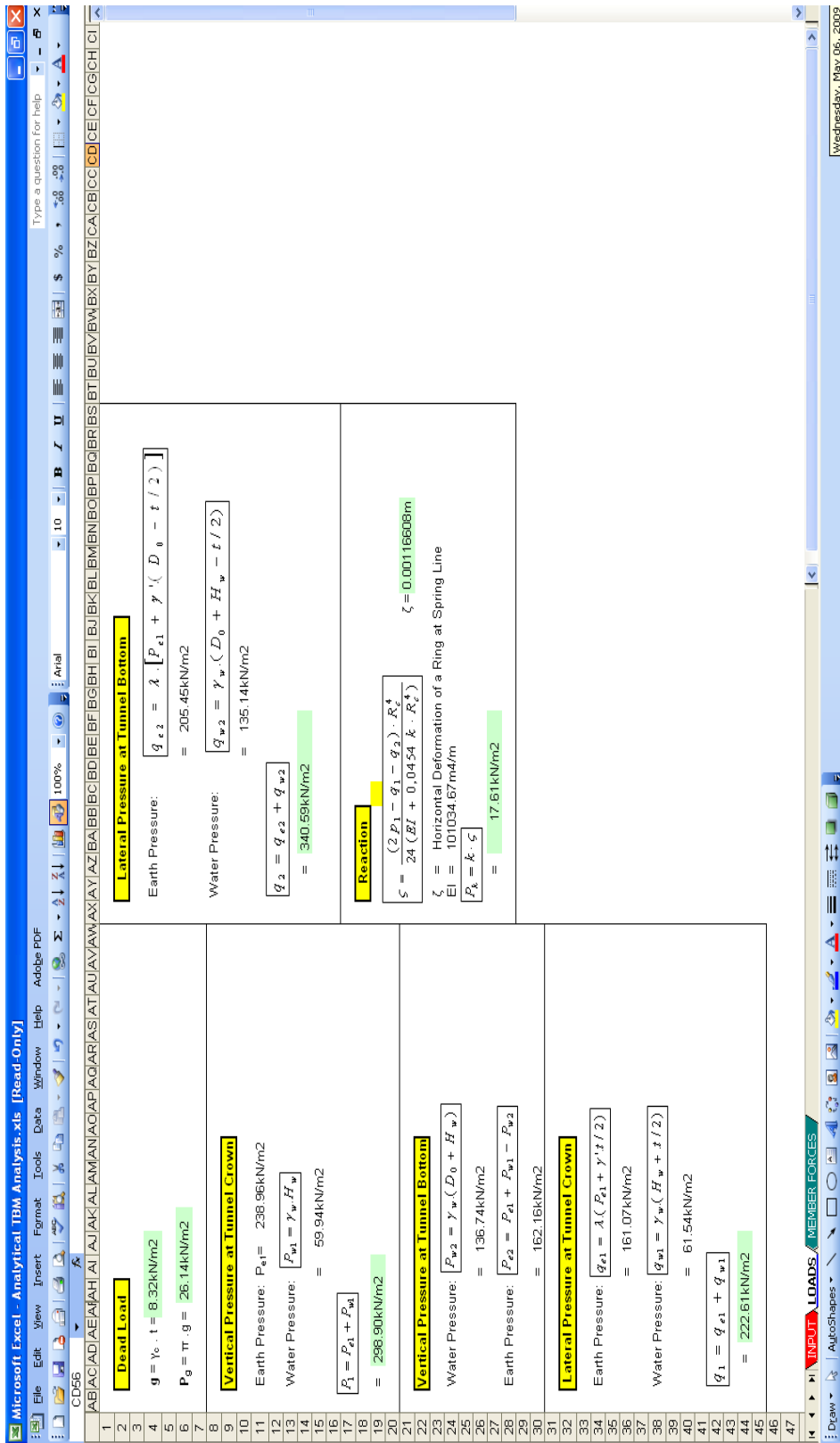


Figure A.3. Load conditions sheet 2 for the analysis with Elastic Equation Method

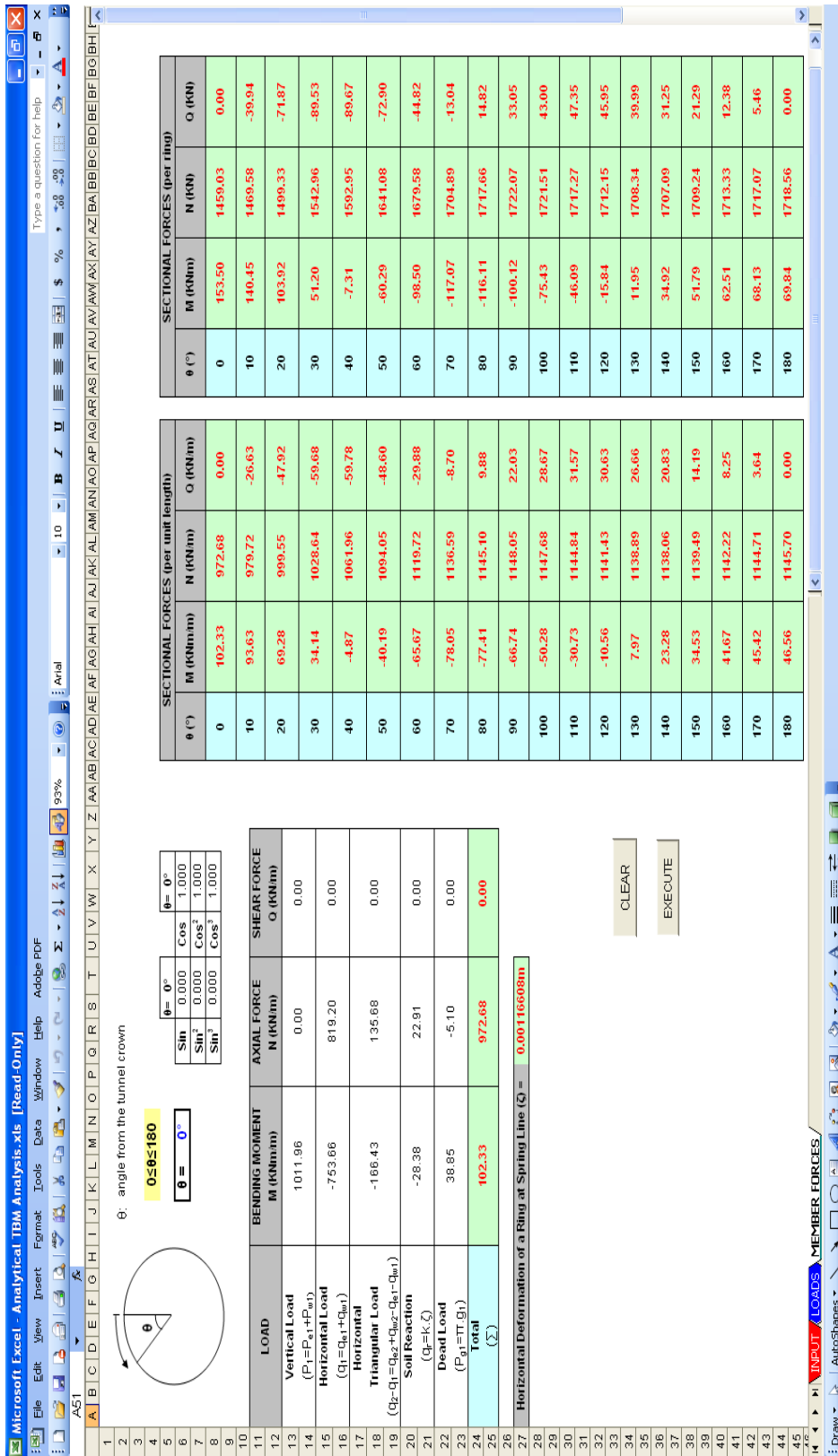


Figure A.4. Member forces sheet for the analysis with Elastic Equation Method

APPENDIX B

SHEAR SPRING CONSTANTS FOR 2D AND 3D BSMs

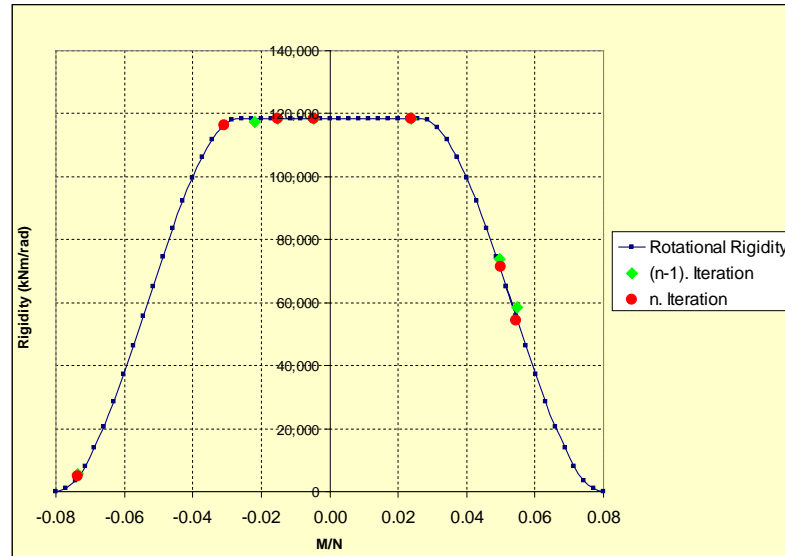


Figure B.1. Rotational Stiffness vs. M/N diagram for 2D BSM in Case 1

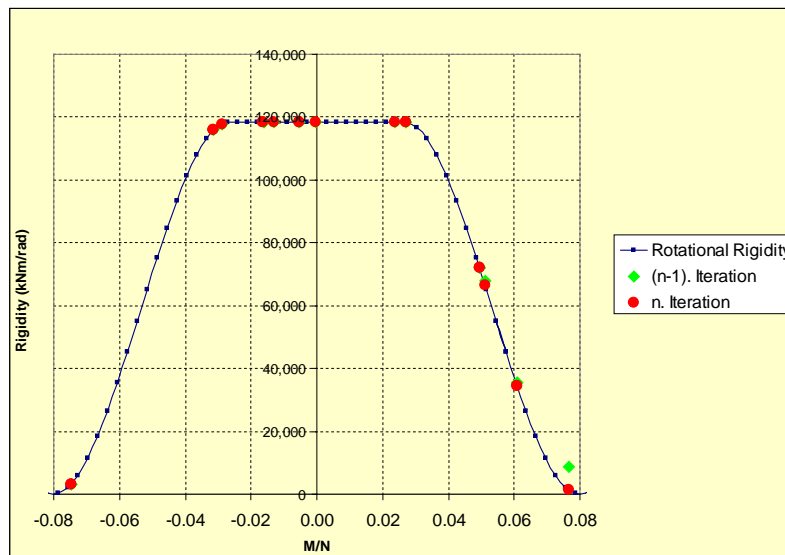


Figure B.2. Rotational Stiffness vs. M/N diagram for 3D BSM in Case 1

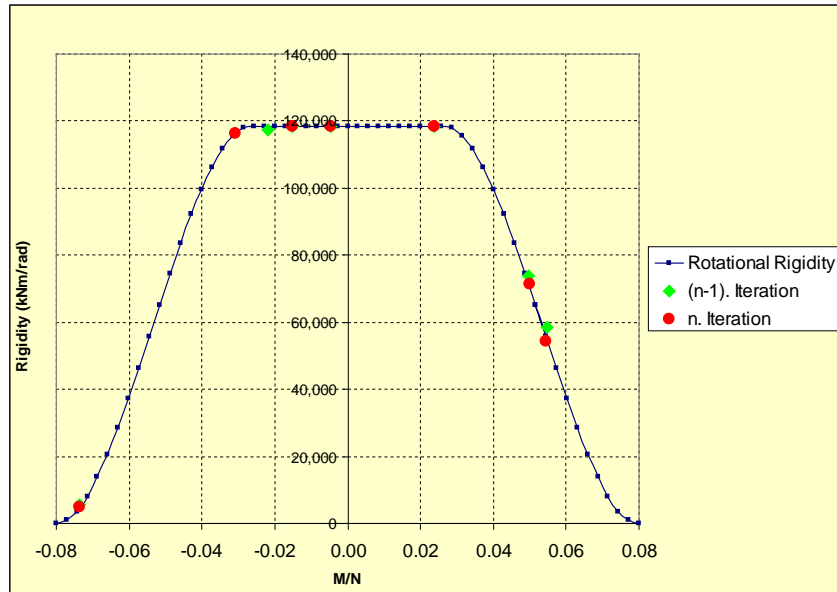


Figure B.3. Rotational Stiffness vs. M/N diagram for 2D BSM consisting of 50 beam elements in Case 4

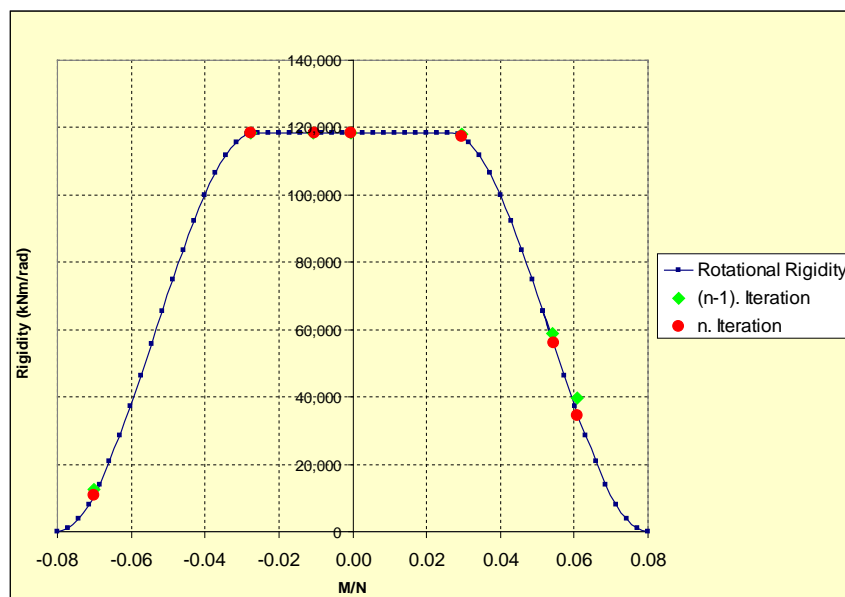


Figure B.4. Rotational Stiffness vs. M/N diagram for 2D BSM consisting of 150 beam elements in Case 4

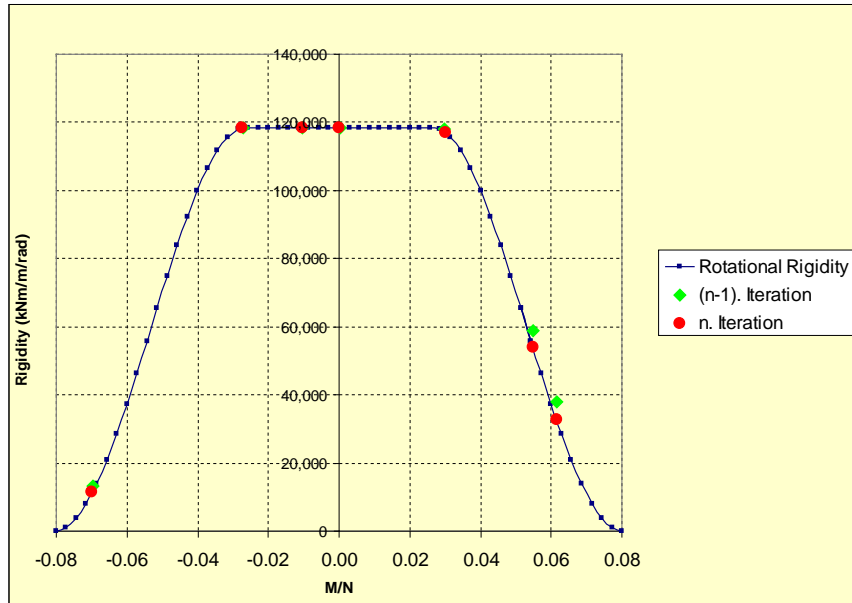


Figure B.5. Rotational Stiffness vs. M/N diagram for 2D BSM consisting of 250 beam elements in Case 4

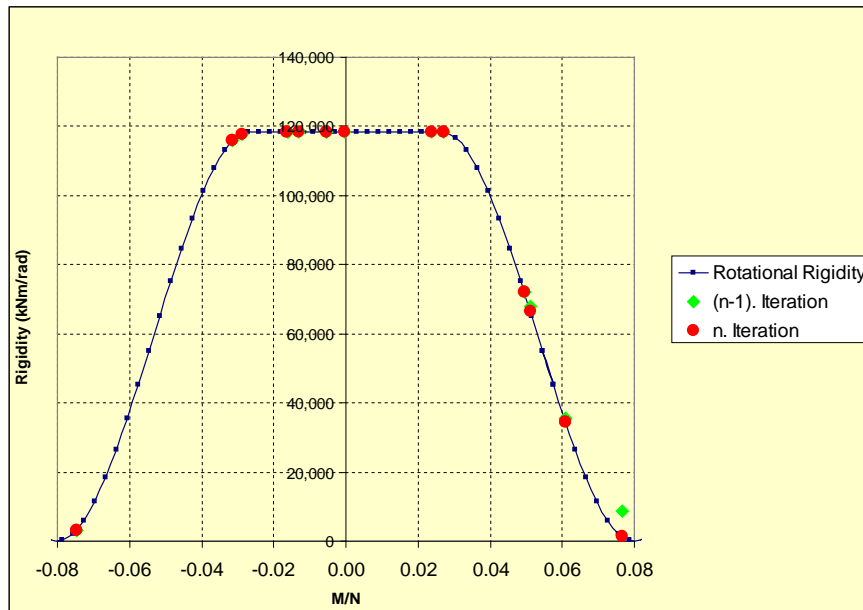


Figure B.6. Rotational Stiffness vs. M/N diagram for 3D BSM consisting of 50 beam elements in Case 4

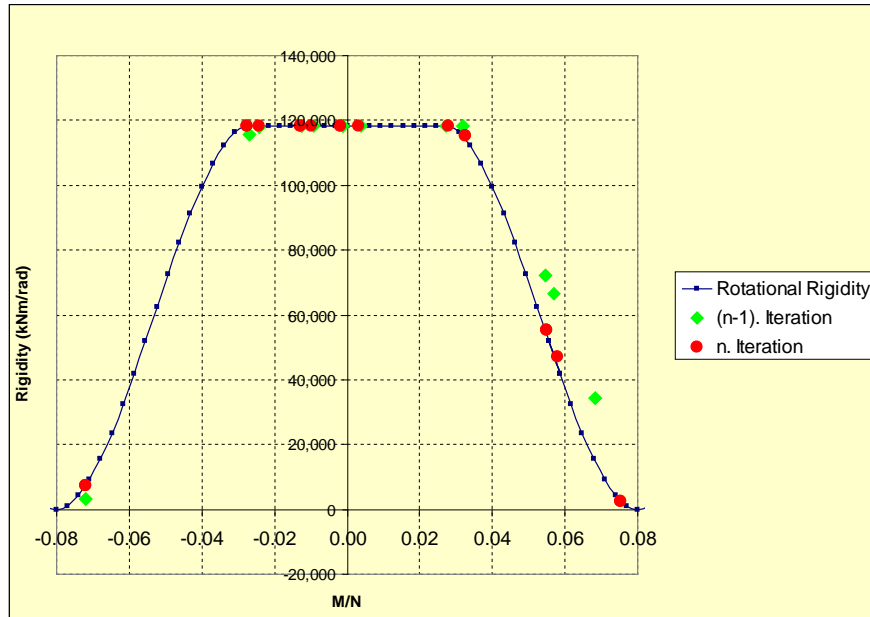


Figure B.7. Rotational Stiffness vs. M/N diagram for 3D BSM consisting of 150 beam elements in Case 4

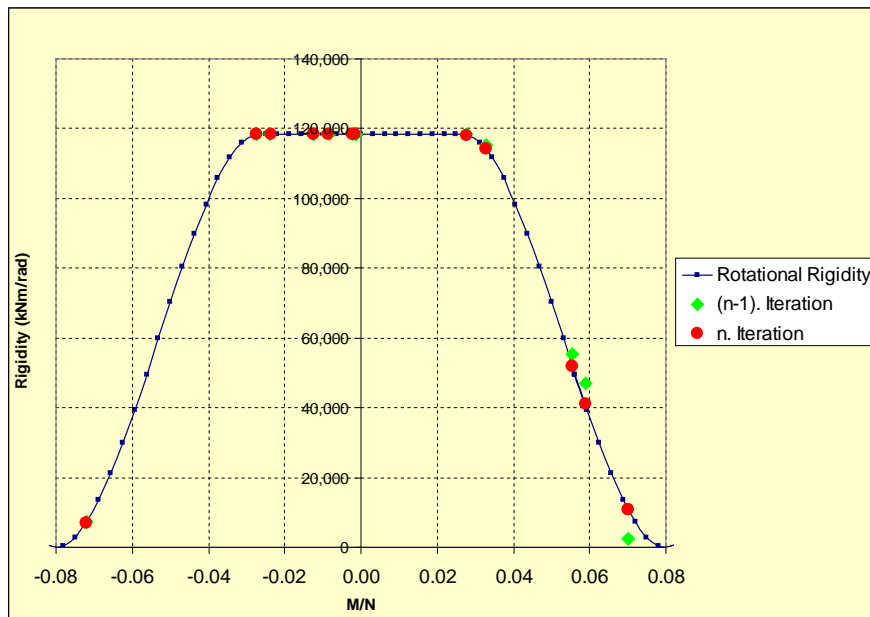


Figure B.8. Rotational Stiffness vs. M/N diagram for 3D BSM consisting of 250 beam elements in Case 4

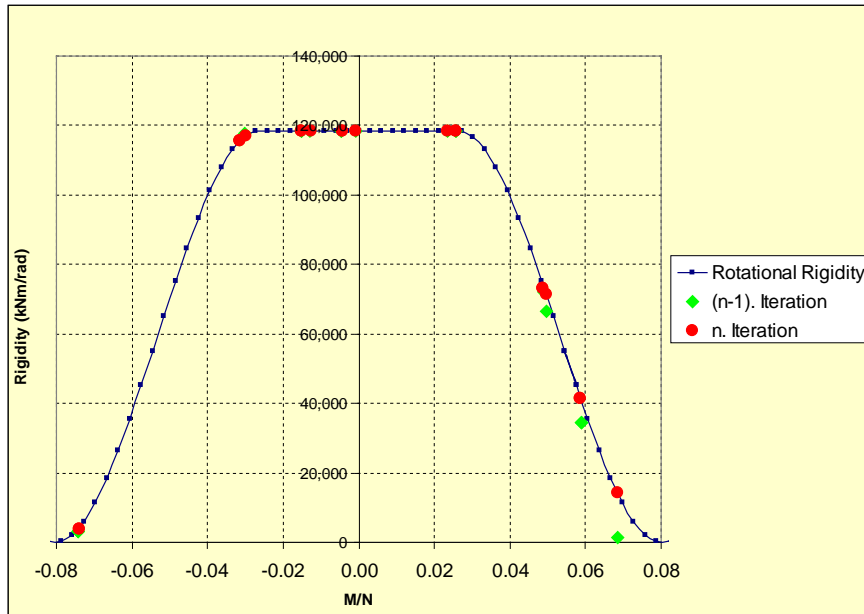


Figure B.9. Rotational Stiffness vs. M/N diagram for 3D BSM ($K_s=15000$ kN/m) in Case 5

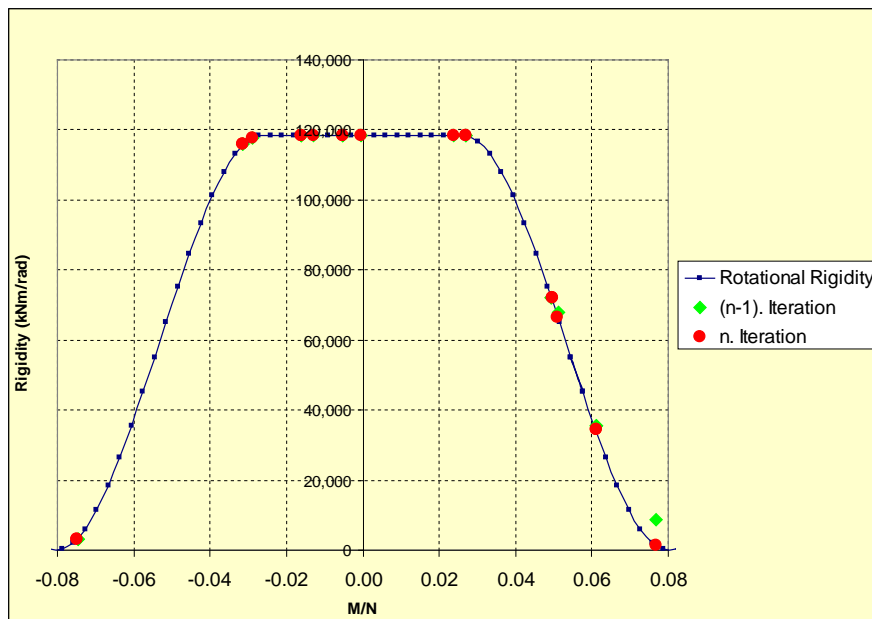


Figure B.10. Rotational Stiffness vs. M/N diagram for 3D BSM ($K_s=20000$ kN/m) in Case 5

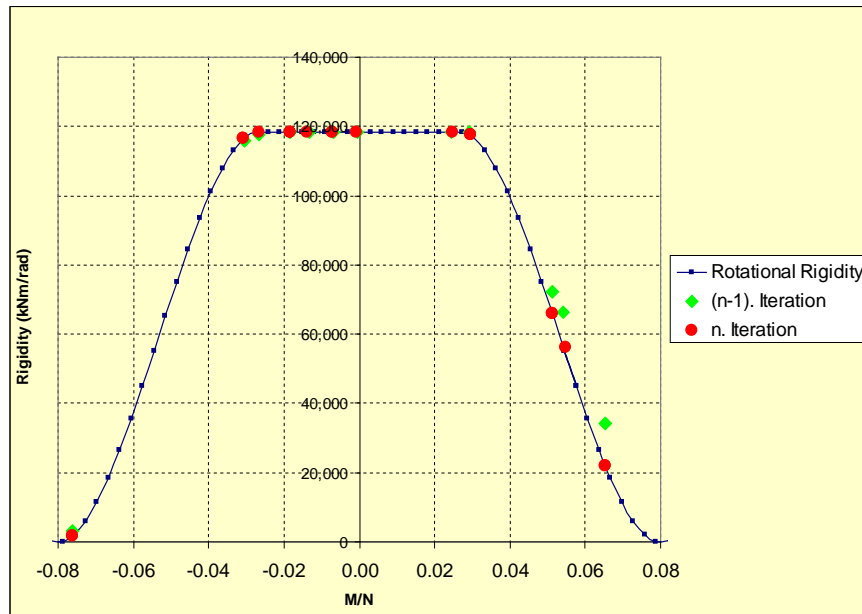


Figure B.11. Rotational Stiffness vs. M/N diagram for 3D BSM ($K_s=25000$ kN/m) in Case 5

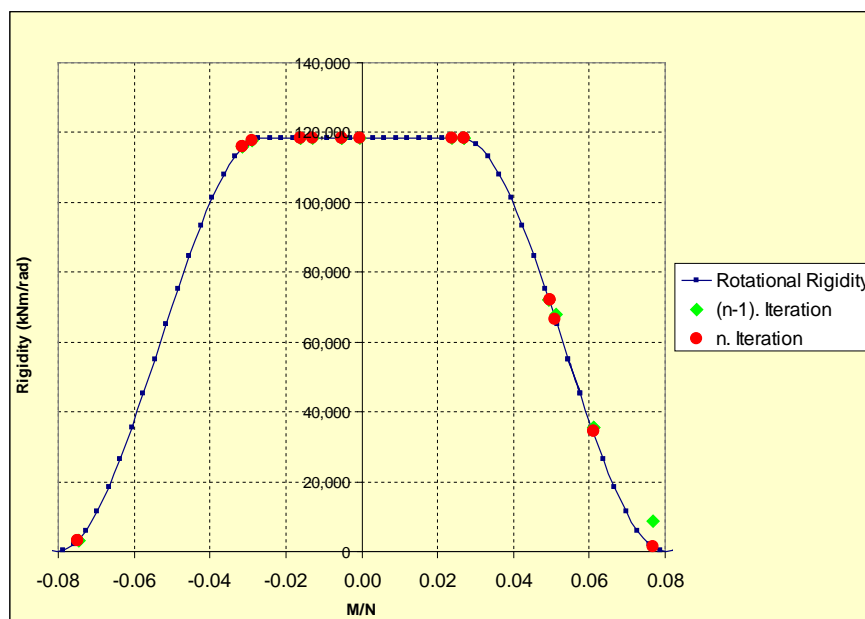


Figure B.12. Rotational Stiffness vs. M/N diagram for 3D BSM (Layout 1) in Case 6

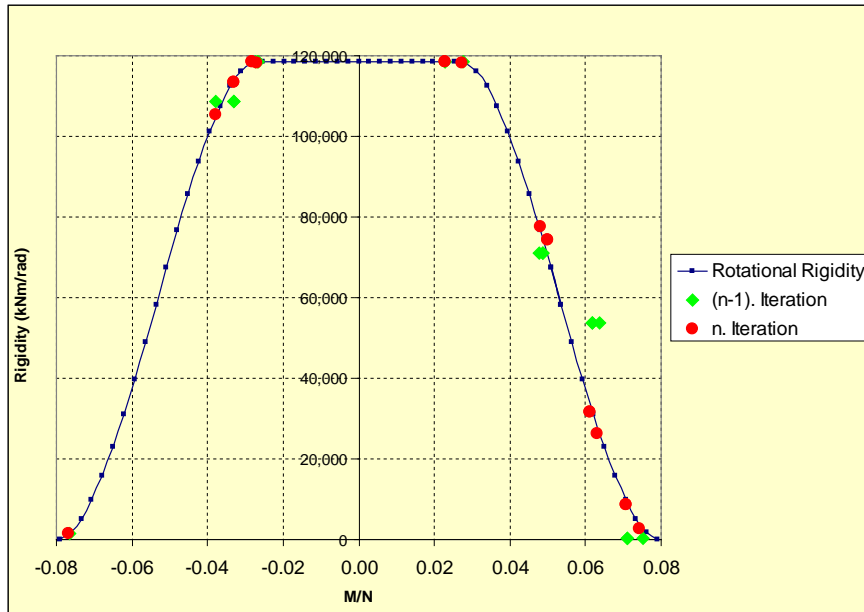


Figure B.13. Rotational Stiffness vs. M/N diagram for 3D BSM (Layout 2) in Case 6

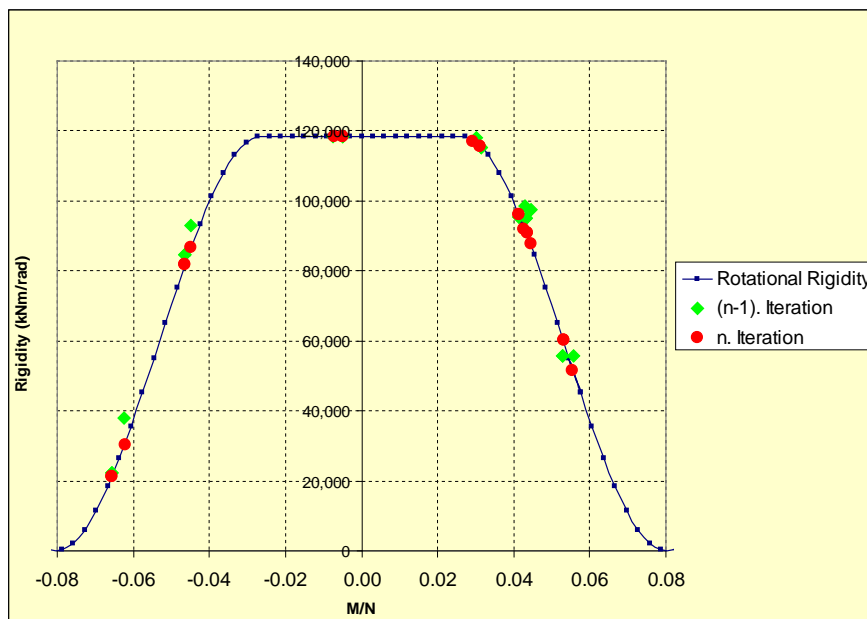


Figure B.14. Rotational Stiffness vs. M/N diagram for 3D BSM (Layout 3) in Case 6

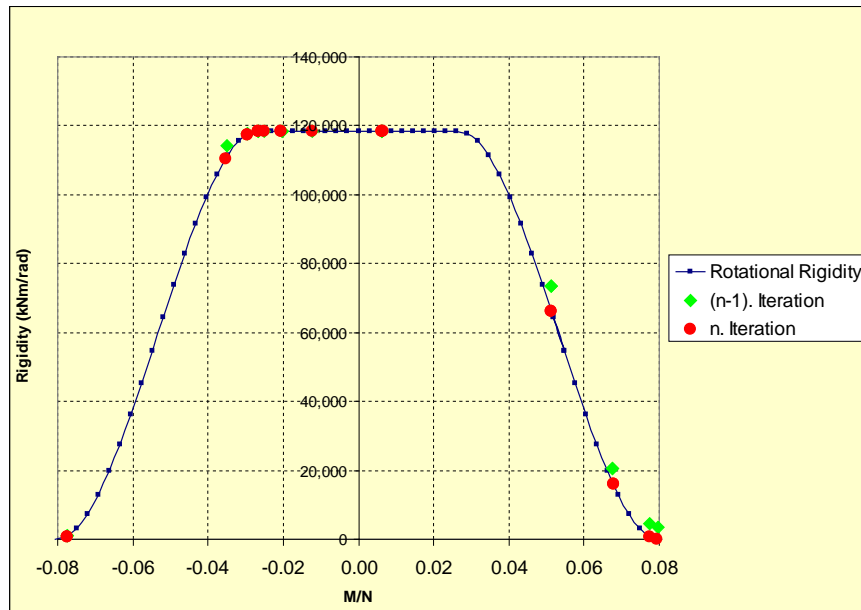


Figure B.15. Rotational Stiffness vs. M/N diagram for 3D BSM (Layout 4) in Case 6